1978

Electron transfer reactions of macrocyclic compounds of cobalt

Roger Allen Heckman
Iowa State University

Electron transfer reactions of macrocyclic compounds of cobalt

by

Roger Allen Heckman

A Dissertation Submitted to the
Graduate Faculty in Partial Fulfillment of
The Requirements for the Degree of
DOCTOR OF PHILOSOPHY

Department: Chemistry
Major: Inorganic Chemistry

Approved:

Signature was redacted for privacy.

In Charge of Major Work

Signature was redacted for privacy.

For the Major Department

Signature was redacted for privacy.

For The Graduate College

Iowa State University
Ames, Iowa

1978

TABLE OF CONTENTS

LIST OF FIGURES

LIST OF TABLES

PART I. THE HALOGEN AND HYDROGEN PEROXIDE OXIDATIONS OF MACROCYCLIC COMPOUNDS OF COBALT(II)

INTRODUCTION

Interest in macrocyclic tetraammine complexes of metal ions developed from the elucidation of the structures of Vitamin B_{12}, hemoglobin, chlorophyll, and other biological systems which contain metal ions coordinated to macrocyclic tetraaza ligands. Unusual properties of these systems such as stabilization of otherwise inaccessible oxidation states, organometallic derivatives, and electron and oxygen transport capability have provided the basis for much study of both the naturally-occurring complexes and model systems.

The very extensive work of Busch, et al. (1) has shown that much interesting chemistry remains to be explored in the area of macrocyclic tetraaza complexes of metal ions. Electrochemical studies of complexes of iron, cobalt, and nickel have shown both divalent and trivalent states, with the reduction potential for Equation I-1 dependent on the

$$M(III)(mac) + e^- \longrightarrow M(II)(mac) \qquad (I-1)$$

structure of the macrocycle. The reduction potentials for the complexes of iron and nickel span a range of nearly two volts and the complexes of cobalt, although not as extensively studied, also show a wide range of potentials (2).

Aside from electrochemical studies of most synthetic complexes and investigations of the substitution reactions of some Co(III) complexes (3), few studies have been done on the chemistry of these systems. The paucity of studies of reactions is surprising in view of the relative

ease of preparation of the complexes, the ease of handling in solution, the stability of the complexes in solution, and the wide range of steric and electronic effects available for investigation. The purpose of the research described here was to investigate the reactivities of a group of six closely related macrocyclic tetraammine complexes of cobalt(II) and to compare those reactivities to those of the Vitamin B_{12} derivative B_{12r} (Figure I-1). The macrocycles were chosen to show the effects of unsaturation in the chelate ring, peripheral substitution, and variations in the ring composition (Figure I-2).[1] The reactions studied were oxidation with H_2O_2, Br_2, and I_2. The mechanism of reduction for each oxidant will be compared to reduction mechanisms by other metal ion complexes. The subsequent sections of this introduction review the literature in this area.

The non-complementary reductions of two-electron non-metallic oxidants by divalent metal ions which are one-electron reductants has been of interest to numerous researchers. Particularly well-studied are the reactions of Cr^{2+}, Fe^{2+}, and $Co(CN)_5^{3-}$. When the oxidant is of the form

---

[1]The figures show no axial ligands but the cobalt(II) complexes are certainly at least five-coordinate and quite possibly six-coordinate in aqueous media. The coordination number has been inferred by Schneider, Phelan, and Halpern (4) to be five for $Co(dmgH)_2$ in weakly-coordinating solvents and Endicott, et al. (5) have shown several other complexes to be six-coordinate in the solid state.

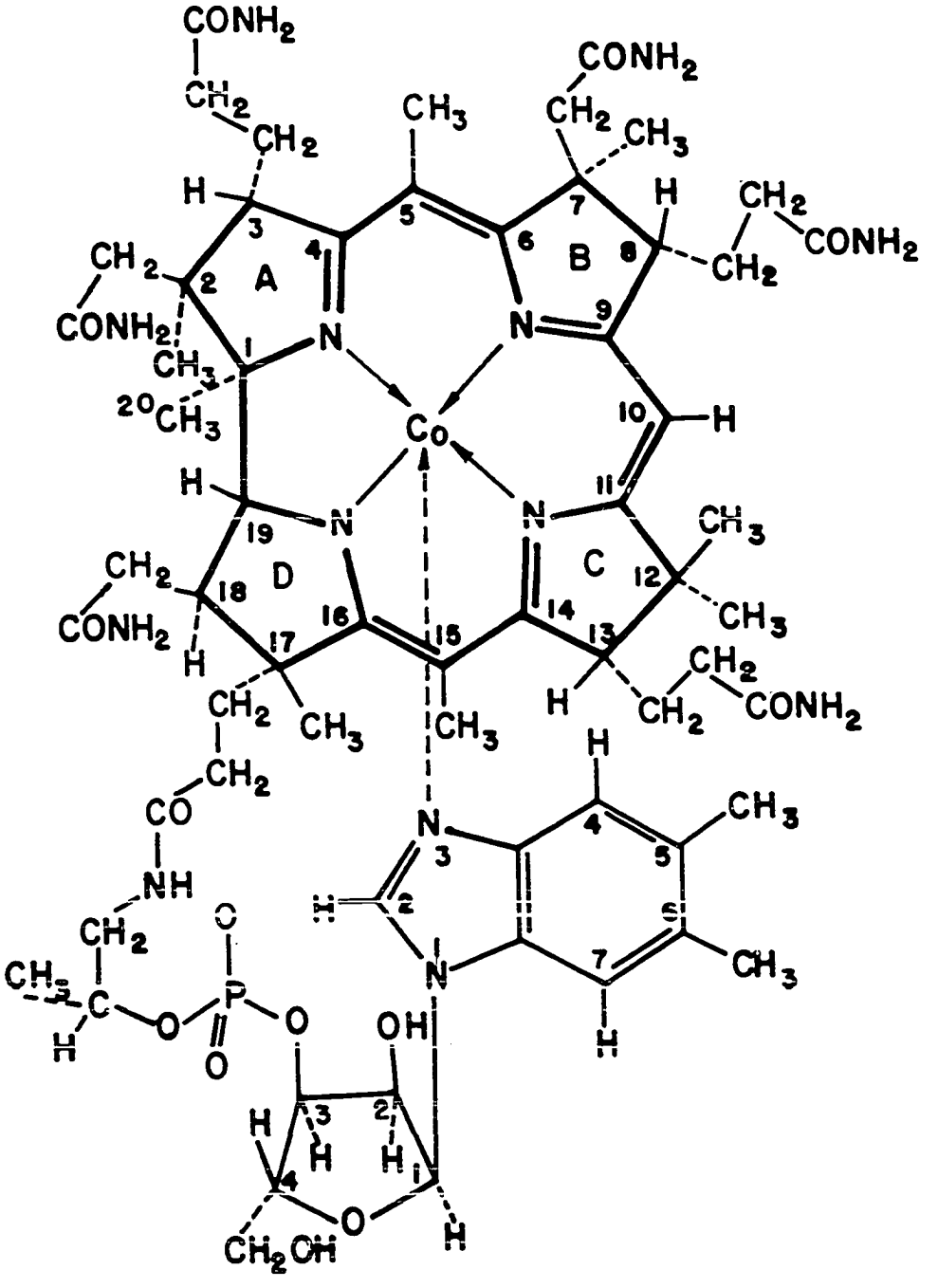

Figure I-1. The structure of B_{12r}

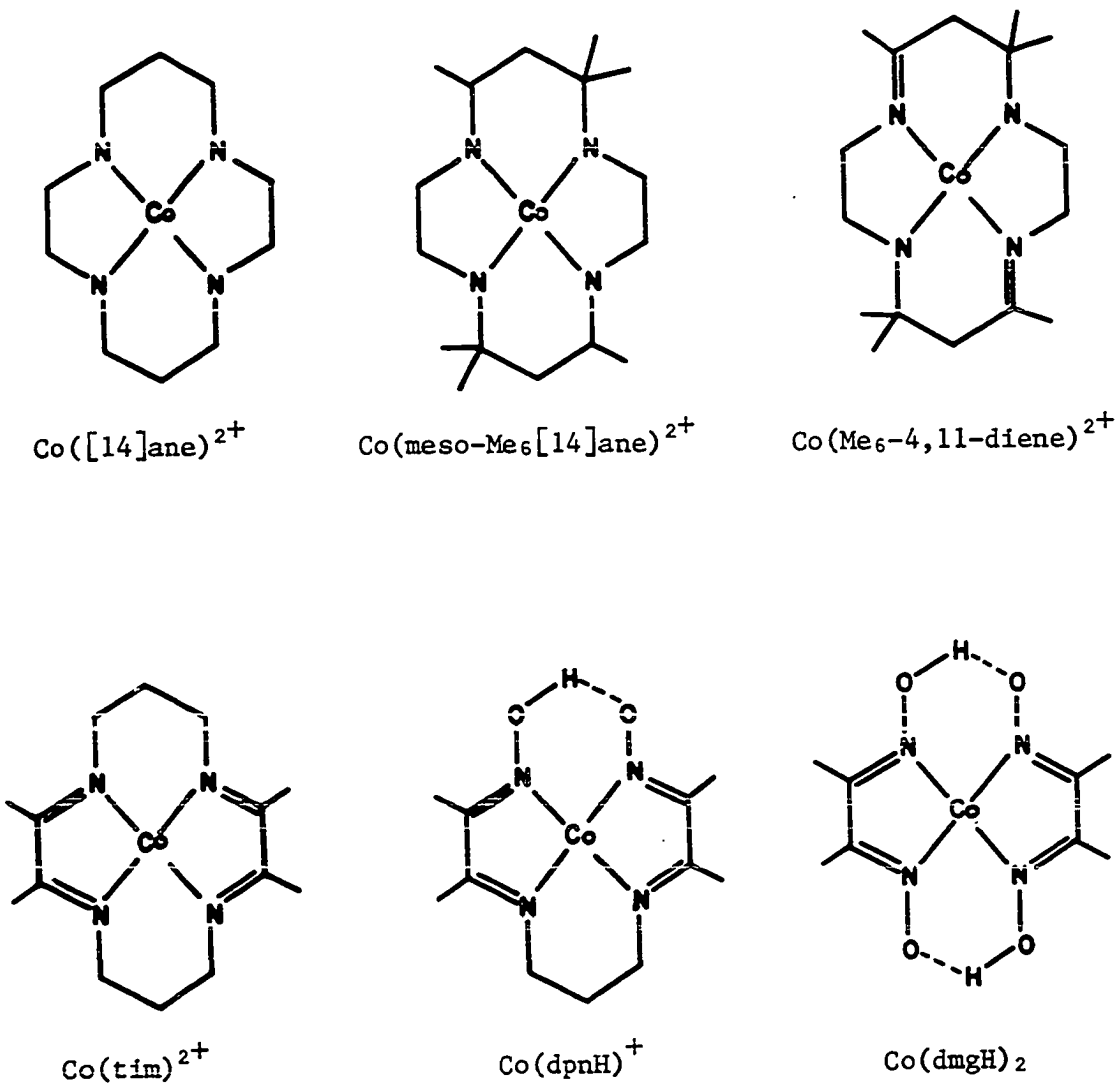

Figure I-2. The structures of the tetraaza macrocycles studied in this work

X-Y the reactions usually follow a two-step mechanism with the formation of radical intermediates as described below.

One of the earliest reactions studied was the ferrous ion catalyzed reaction of H_2O_2 with alcohols (6). The mechanism of reaction was found to involve the initial reaction of Fe^{2+} and H_2O_2 to give Fe^{3+} and $\cdot OH$ (7,8). The hydroxyl radical then was the reactive species toward the alcohol. Carter and Davidson (9) later showed that bromine was reduced by Fe^{2+} in a similar manner; i.e., with the production of bromine atoms as intermediates.

Some interesting reductions by Cr^{2+} that have been studied are those of organic halides. Anet and LeBlanc (10) showed that Cr^{2+} reacted with a benzyl halide to give CrX^{2+} and an organo-chromium product. Kochi and Davis (11) further studied aralkylchromium compounds produced from the reaction of Cr^{2+} with benzyl halides (Equation I-2) or 1,1-dimethyl-2-phenylethylhydroperoxide (Equation I-3). The production of

$$PhCH_2X + 2Cr^{2+} \longrightarrow CrX^{2+} + PhCH_2Cr^{2+} \qquad (I\text{-}2)$$

$$PhCH_2C(CH_3)_2OOH + 2Cr^{2+} + H^+ \longrightarrow PhCH_2Cr^{2+} + Cr^{3+} + (CH_3)_2CO + H_2O \qquad (I\text{-}3)$$

halochromium ion in Equation I-2 and of Cr^{3+} in Equation I-3 demonstrated that each reaction proceeded by inner-sphere atom transfer of halogen or hydroxyl radical and production of a benzyl radical which then reacted with a second chromous ion to give benzylchromium ion.

The mechanism of hydroperoxide reduction by Cr^{2+} was confirmed by the work of Hyde and Espenson (12). They showed that for a variety of hydroperoxides the product of the rate-determining step of the reaction was Cr^{3+} and an alkoxy radical (Equation I-4). The alkoxy radical then

$$ROOH + Cr^{2+} + H^{+} \longrightarrow Cr^{3+} + RO\cdot + H_2O \qquad (I\text{-}4)$$

underwent radical cleavage or hydrogen atom abstraction from the solvent methanol but eventually produced an organochromium species.

The classical study by Taube and Myers (13) of the chromous ion reductions of halogens led in part to the delineation of electron transfer reactions into inner- and outer-sphere mechanisms. The production of halogenated chromium(III) products indicated that the transition state of the reaction had to include the oxidant penetrating the inner coordination sphere of Cr^{2+}. The reaction products were consistent with the production of a halogen atom intermediate.

Recently, Kramer (14) investigated the reactions of Cr^{2+} with a variety of halogen, pseudohalogen, and interhalogen compounds. He demonstrated by product analysis that the reduction of I_2, ClCN, and $S(CN)_2$ proceeded by a mechanism involving inner-sphere atom transfer and the production of a halogen atom or pseudohalogen radical (Equation I-5)

$$Cr^{2+} + X\text{-}Y \longrightarrow CrX^{2+} + Y\cdot \qquad (I\text{-}5)$$

which then combined with another chromous ion to give the final products (Equation I-6). For ICN, BrCN, and $(CN)_2$ the first step was presumed to

$$Cr^{2+} + Y\cdot \longrightarrow CrY^{2+} \qquad \text{(I-6)}$$

involve outer-sphere electron transfer followed by radical ion decomposition and Cr^{2+}—Y recombination (Equations I-7, I-8, and I-6). Product

$$Cr^{2+} + X\text{-}Y \longrightarrow Cr^{3+} + X\text{-}Y^{-} \qquad \text{(I-7)}$$

$$X\text{-}Y^{-} \longrightarrow X^{-} + Y\cdot \qquad \text{(I-8)}$$

analysis and kinetic parameters for the reductions of Cl_2 and Br_2 were best explained by a mechanism wherein the halogen was first hydrolyzed to HOX and then reduced (Equations I-9 to I-12).

$$X_2 + H_2O \rightleftharpoons HOX + X^{-} + H^{+} \qquad \text{(I-9)}$$

$$HOX + Cr^{2+} \longrightarrow CrX^{2+} + \cdot OH \qquad \text{(I-10)}$$

$$\cdot OH + X_2 \longrightarrow HOX + X\cdot \qquad \text{(I-11)}$$

$$Cr^{2+} + X\cdot \longrightarrow CrX^{2+} \qquad \text{(I-12)}$$

Davies, Sutin, and Watkins (15) showed that H_2O_2 oxidized $Cr(CN)_6^{4-}$ by an outer-sphere path but the mechanism proceeded by one-equivalent steps (Equations I-13 and I-14). The hydroxyl radical thus produced

$$Cr(CN)_6^{4-} + H_2O_2 \longrightarrow Cr(CN)_6^{3-} + \cdot OH + OH^{-} \qquad \text{(I-13)}$$

$$Cr(CN)_6^{4-} + \cdot OH \longrightarrow Cr(CN)_6^{3-} + OH^{-} \qquad \text{(I-14)}$$

then oxidized another pentacyanochromate ion. Other authors (16) had earlier stated that the hydrogen peroxide oxidation of Cr^{2+} follows, in part, the same mechanism.

Malin and Swinehart (17) studied the V^{2+} reductions of I_2, I_3^-, and Br_2. They proposed a one-equivalent atom transfer mechanism such as that in Equations I-5 and I-6. For the triiodide reactions I_2^- was produced as an intermediate rather than iodine atoms. Adegite, et al. (18), however, showed that the results of the U^{3+} reductions of I_2, I_3^-, and Br_2 were best interpreted by an outer-sphere mechanism with a halogen radical anion intermediate. The conclusion was based on a free energy correlation with other known outer-sphere oxidants since the substitution lability of uranium(IV) prohibits the identification of any UX^{3+} which would be produced by an inner-sphere mechanism.

Similar reactions have been studied using $Co(CN)_5^{3-}$ as the reducing agent. The substrates Br_2 (19), I_2 (19), H_2O_2 (20,21), NH_2OH (21), ICN (21), and CH_3I and other organic halides (22) have all been shown to undergo reduction by a radical (atom transfer) mechanism (Equations I-15 and I-16). The rate limiting step is represented by Equation I-15 and

$$Co(CN)_5^{3-} + X\text{-}Y \longrightarrow Co(CN)_5X^{3-} + Y\cdot \qquad (I\text{-}15)$$

$$Co(CN)_5^{3-} + Y\cdot \longrightarrow Co(CN)_5Y^{3-} \qquad (I\text{-}16)$$

the rate law is of the form of Equation I-17. Additionally, the order

$$-\frac{d[Co(CN)_5^{3-}]}{dt} = 2k[Co(CN)_5^{3-}][X\text{-}Y] \qquad (I\text{-}17)$$

of reactivity of organic halides with $Co(CN)_5^{3-}$ (22); i.e., $PhCH_2I$ > $PhCH_2Br$ > $PhCH_2Cl$ and $PhCH_2I$ > $(CH_3)_3CI$ > $(CH_3)_2CHI$ > CH_3CH_2I ≃

$CH_3CH_2CH_2I > CH_3I$, is identical to the reactivity order with methyl radical as previously observed (22) and reflects the bond energy of the carbon-halogen bond. In the study of the $Co(CN)_5^{3-}$—H_2O_2 reaction Chock, et al. (21) demonstrated that the hydroxyl radical was indeed a reaction intermediate. When the reaction was done in 0.1 M I^- solution, $ICo(CN)_5^{3-}$ was observed along with $Co(CN)_5OH^{3-}$ as a reaction product as predicted from the known reactivity of hydroxyl radicals (23) (Equations I-18 to I-20).

$$Co(CN)_5^{3-} + H_2O_2 \longrightarrow Co(CN)_5OH^{3-} + \cdot OH \qquad (I\text{-}18)$$

$$\cdot OH + I^- \longrightarrow OH^- + I\cdot \qquad (I\text{-}19)$$

$$Co(CN)_5^{3-} + I\cdot \longrightarrow ICo(CN)_5^{3-} \qquad (I\text{-}20)$$

Woodruff and coworkers (24-26) reported on the Br_2, Br_3^-, I_2, and I_3^- oxidations of Mn(II), Fe(II), and Co(II) complexes of EDTA and CyDTA. A transient halogenated product was observed for the $Co(EDTA)^{2-}$—Br_2 reactions but not for any other reactions since the possible $XM(EDTA)^{2-}$ and $XM(CyDTA)^{2-}$ products are known to undergo rapid elimination of X^- and ring closure. The data were interpreted in terms of inner-sphere coordination of the oxidant (rate limiting in the $Fe(EDTA)^{2-}$ and $Fe(CyDTA)^{2-}$ reductions of Br_2, Br_3^-, and I_2) and subsequent electron transfer (rate limiting in all other cases). The halogen product of the first one-electron reduction was X_2^- which, at least in the Fe(II) reductions, underwent disproportionation to regenerate the halogen (Equation I-21).

$$2X_2^- \longrightarrow X_2 + 2X^- \qquad \text{(I-21)}$$

Reduction reactions by Co(II) complexes of macrocyclic and pseudo-macrocyclic Schiff bases have also been studied although not on the scale of Cr^{2+} and $Co(CN)_5^{3-}$. Researchers have investigated the reactions of $Co(dmgH)_2$ (4,27) and Co(saloph) (28) with benzyl halides and shown them to react analogously to $Co(CN)_5^{3-}$; i.e., forming the Co(III) halide complex and the benzylcobalt species. An anomaly was found in the reaction of Co(salen) with p-nitrobenzyl bromide in CH_2Cl_2 in the presence of excess 1-methylimidazole (29). The reactive form of the complex was Co(salen)(MeIMD)$_2$ which (having both axial coordination sites blocked) reacted with the organic substrate by an outer-sphere electron transfer mechanism in the rate limiting step (Equation I-23).

$$\text{Co(salen)(MeIMD)} + \text{MeIMD} \rightleftharpoons \text{Co(salen)(MeIMD)}_2 \qquad \text{(I-22)}$$

$$\text{Co(salen)(MeIMD)}_2 + \text{RX} \longrightarrow \text{Co(salen)(MeIMD)}_2^+ + \text{RX}^- \qquad \text{(I-23)}$$

The organic radical subsequently produced was then trapped by the Co(II) complex (Equations I-24 and I-25).

$$\text{RX}^- \longrightarrow \text{R}\cdot + \text{X}^- \qquad \text{(I-24)}$$

$$\text{Co(salen)(MeIMD)} + \text{R}\cdot \longrightarrow \text{RCo(salen)(MeIMD)} \qquad \text{(I-25)}$$

Adin and Espenson (30) studied the reactions of $Co(dmgH)_2(H_2O)_2$ with a series of pentaammine complexes of Co(III). The reactions were

found to be inner-sphere (Equation I-26) and exactly analogous to previously studied Cr^{2+} reactions.

$$Co(dmgH)_2(H_2O)_2 + Co(NH_3)_5X^{2+} + 5H^+ \longrightarrow XCo(dmgH)_2(H_2O) + Co^{2+} + 5NH_4^+ + H_2O \qquad (I\text{-}26)$$

Espenson and Martin (31) studied the reactions of a series of macrocyclic tetraammine complexes of Co(II) with several hydroperoxides. Just as was seen for the analogous Cr^{2+} reductions (12), the mechanism involved hydroxyl radical abstraction, alkoxy radical decomposition or reaction with solvent, and alkyl radical—Co(II) recombination to produce an organocobalt species. The effect of the macrocyclic structure was not interpreted.

Roche and Endicott (32) used a radical recombination reaction to prepare some methylcobalt species which were not otherwise obtainable. The two common methods of preparing organocobalt compounds are the S_N2 reactions of Co(I) (33) and the Co(II) radical processes (4,22,27-29). For saturated amine complexes of cobalt, however, the Co(I) state is unattainable and the Co(II) state is generally unreactive towards alkyl halides. Endicott used the photolysis reaction of $Co(NH_3)_5O_2CCH_3^{2+}$ (Equation I-27) as a source of methyl radicals which readily recombined

$$Co(NH_3)_5O_2CCH_3^{2+} + 5H^+ + h\nu \longrightarrow Co^{2+} + 5NH_4^+ + CO_2 + \cdot CH_3 \qquad (I\text{-}27)$$

with the Co(II) complexes to give the organocobalt species in low yield.

The reduction reactions of B_{12r} have been known since shortly after the isolation of crystalline Vitamin B_{12}. Brierly, et al. (34) noted that B_{12r} reacted stoichiometrically with I_2 in an oxidation-reduction process. Since then other workers have studied reactions of B_{12r} with CH_3I (35), and O_2 (36,37). The oxygen reaction is complicated by side products and poorly understood mechanistically.

EXPERIMENTAL

Materials

Cobalt complexes

$Co([14]ane)^{2+}$ Owing to the extreme oxygen sensitivity of (1,4,8,11-tetraazacyclotetradecane)cobalt(II) salts even in the solid state (5) no attempt at isolation was made. Equal volumes of 0.010 M Co^{2+} (as the acetate salt) and 0.010 M [14]ane in neutral aqueous solutions were mixed under a nitrogen atmosphere. Sufficient $HClO_4$ was then added to make the solution 0.10 M in acid.

The solid [14]ane was obtained from Strem Chemical Company.

$[Co([14]ane)(H_2O)_2](ClO_4)_3$ This compound was prepared from the chloro complex by the method of Poon and Tobe (38). A deaerated solution of $CoCl_2 \cdot 6H_2O$ (0.48 g, 2 mmol) in 6 ml methanol was allowed to react with 0.40 g of the ligand (2 mmol) dissolved in 4 ml methanol. Air was bubbled through the solution for one hour and concentrated HCl (0.6 ml, 7.2 mmol) was then added. The color of the solution became dark green. Air was passed through the solution for an additional hour and the solution was filtered to yield green crystals. The filtrate was reduced in volume to obtain additional product (yield - 0.55 g, 75%).

A solution of the dichloro complex (0.55 g, 1.5 mmol) in 25 ml of water was added to a small amount of anion exchange resin (Amberlite IRA400, OH^- form) in a beaker, stirred for 10 minutes, and then passed through an ice-water jacketed column of the same type of resin. The

dark red eluant was concentrated to 1 ml at room temperature. Upon addition of 2 ml 70% $HClO_4$ the solution turned dark green-brown and crystals began to precipitate. The mixture was refrigerated for one hour and the gray-green crystals were filtered, washed with ether, and air-dried (yield - 0.66 g, 74%).

[Co(meso-Me_6[14]ane)]$(ClO_4)_2$ Anhydrous $CoCl_2$ was prepared by stirring $CoCl_2 \cdot 6H_2O$ (1.5 g, 6.3 mmol) in 10 ml 2,2-dimethoxypropane for one hour under a steady flow of dry nitrogen. Following the method of Rillema, et al. (39) Strem Chemical meso-5,7,7,12,14,14-hexamethyl-1,4,8,11-tetraazacyclotetradecane (1.0 g, 3.1 mmol) dissolved in 20 ml DMF was added and the mixture was heated to 70° C for one hour. Cooling yielded blue-green crystals of [Co(meso-Me_6[14]ane)]$(CoCl_4)$ which were filtered, washed with 1:2.5 methanol-ether and with ether, and air-dried (yield - 1.2 g).

The tetrachlorocobaltate salt was then slurried in 30 ml H_2O and NH_4ClO_4 (1.5 g, 13 mmol) was added. The slurry was warmed, with stirring, for five minutes. The slurry was then filtered, washed with 1:5 methanol-ether and ether, and air-dried to yield a pink powder (yield - 1.2 g, 71% of starting ligand).

[Co(Me_6-4,11-diene)]$(ClO_4)_2$ The complex (5,7,7,12,14,14-hexamethyl-1,4,8,11-tetraazacyclotetradeca-4,11-diene)cobalt(II) perchlorate was prepared analogously to the Me_6[14]ane complex using Strem Chemical Me_6-4,11-diene. A yellow product was obtained.

[Co(tim)$(H_2O)_2$]$(ClO_4)_2$ Diaquo(2,3,9,10-tetramethyl-1,4,8,11-tetraazacyclotetradeca-1,3,8,10-tetraene)cobalt(II) perchlorate was

prepared by modification of the procedure of Jackels, et al. (40). Methanol (200 ml) was placed in a 250-ml 3-necked flask. After bubbling with nitrogen for 30 minutes 1,3-diamino-propane (7.5 g, 0.1 mol) was added, followed by dropwise addition of 70% $HClO_4$ (8.5 ml, 0.1 mol) over 20-30 minutes. Biacetyl (8.6 g, 0.1 mol) was then added followed immediately by $Co(C_2H_3O_2)_2 \cdot 4H_2O$ (12.4 g, 0.05 mol). The solution was stirred for four hours under nitrogen at which time 5 ml H_2O and 12.5 ml of 70% $HClO_4$ were added. The methanol was partially removed by vigorously passing nitrogen through the solution for five hours. The reaction mixture was filtered under nitrogen, washed with ether, and vacuum dried (yield - 10 g, 37%).

$\underline{Co(dpnH)^+}$ The divalent compound 3,3'-(trimethylenediimino)bis-(butan-2-oneoximato)cobalt(II) was prepared by the electrolytic reduction of an aqueous solution of $Co(dpnH)(H_2O)_2^{2+}$. Typically, a 1×10^{-3} M solution of $[Co(dpnH)(H_2O)_2](ClO_4)_2$ in 0.10 M $LiClO_4$ was reduced over a mercury pool at a potential of +0.10 V versus sce. About one hour was allowed to ensure complete reduction of 50 ml of such a solution.

In acidic solution $Co(dpnH)^+$ slowly decomposed to uncharacterized products. The rate of this decomposition was sufficiently slow that no interference was seen in the redox reactions studied. At $[H^+] = 0.033$ M and 0.050 M pseudo-first-order rate constants of 3.47×10^{-3} and 6.17×10^{-3} s^{-1} were observed ($\mu = 0.10$ M, ambient temperature).

$\underline{[Co(dpnH)(H_2O)_2](ClO_4)_2}$ The action of $AgClO_4$ (2.5 g, 10.9 mmol) on $Co(dpnH)I_2$ (41) (3.0 g, 5.4 mmol) in 35 ml of water caused the

immediate formation of a brown precipitate. The slurry was stirred for two hours. The precipitate was filtered off and the filtrate was acidified with $HClO_4$ and evaporated to 20 ml. Upon cooling a brown crystalline precipitate was obtained that was filtered, washed with ether, and air-dried. Further evaporation of the filtrate yielded additional product (yield - 2.0 g, 70%).

Co(dmgH)$_2$ Cobaloxime(II) was prepared for use both *in situ* and as a solid. Equal volumes of equimolar solutions of $Co(C_2H_3O_2)_2 \cdot 4H_2O$ and dimethylglyoxime ($dmgH_2$) (obtained from Aldrich Chemical Company), both in 0.1 M aqueous $NaC_2H_3O_2$, were mixed and the product was formed immediately. The solid was prepared by the method of Schrauzer (33). Dimethylglyoxime (11.6 g, 0.1 mol) suspended in 100 ml methanol and $Co(C_2H_3O_2)_2 \cdot 4H_2O$ (12.5 g, 0.05 mol) dissolved in 100 ml methanol were flushed with N_2 for 30 minutes. The Co^{2+} solution was added to the $dmgH_2$ and allowed to react for one-half hour. The suspension was filtered under N_2, washed with deaerated methanol and ether, and vacuum dried (yield - 10 g, 60%).

Of the two methods of preparation, the isolation of solid was the less satisfactory in that the ratio of maximum to minimum absorbances in the visible spectrum (a qualitative indicator of the purity of the Co(II) product) was always less for the redissolved solid compound than for the *in situ* preparation. In general, the complex was used without isolation of the solid.

Adin and Espenson (30) have shown that Co(dmgH)$_2$ is very rapidly decomposed to Co^{2+} and dimethylglyoxime in acidic solution. Their

observation was reproduced here. Therefore, all studies with $Co(dmgH)_2$ were done in 0.10 M NaOAc solution.

$[Co(dmgH)_2(H_2O)_2](ClO_4)$ Diaquocobaloxime(III) perchlorate was prepared by the action of Ag^+ on $H[Co(dmgH)_2Cl_2]$ (42). An aqueous solution of the dichloro complex (3.6 g, 10 mmol) was stirred on a hotplate and $AgClO_4$ (4.1 g, 20 mmol) was added. The solution was heated slightly for several hours to allow for complete aquation of the cobalt complex. The solution was filtered and acidified with $HClO_4$ and the volume was reduced until crystal formation began. The solution was then chilled to produce maximum yield of yellow-brown crystals which were filtered, washed,with ether, and air-dried (yield - 2 g, 45%).

B_{12r} Aquocobalamin, B_{12a}, obtained from Sigma Chemical was reduced under nitrogen by amalgamated zinc in 0.1 M aqueous perchloric acid.

Other reagents Commercial 30% H_2O_2, Br_2, I_2, $HClO_4$, and tert-butanol were used without further purification. Neutralization of a Li_2CO_3 slurry with $HClO_4$, followed by partial evaporation of the solvent and slow cooling yielded crystals of lithium perchlorate. After recrystallization, stock solutions of $LiClO_4$ were standardized by titration of the acid displaced from a cation exchange column by an aliquot of the $LiClO_4$ solution.

Methods

Analyses

Co(II) complexes All of the Co(II) complexes except $Co([14]ane)^{2+}$ have been characterized previously in the literature. The concentrations of solutions of these complexes were most easily determined by the intensity of their absorption spectra (Table I-1 and Figures I-3 to I-9). Vitamin B_{12a} (the chloride salt) was weighed into a small volumetric flask and its concentration was determined from the molecular weight (1382.8 g mol^{-1}) prior to reduction.

An equimolar mixture of Co^{2+} and [14]ane was found not to give a stoichiometric yield of $Co([14]ane)^{2+}$. Rather, the cyclic amine raised the pH of the aqueous solutions sufficiently to cause precipitation of $Co(OH)_2$ which was unreactive toward [14]ane. The slow addition of [14]ane to the Co^{2+} solution gave $Co([14]ane)^{2+}$ as the major cobalt-containing product and addition of $HClO_4$ led to dissolution of the $Co(OH)_2$ and protonation of unreacted [14]ane, but not destruction of the $Co([14]ane)^{2+}$. For purposes of analysis the $Co([14]ane)^{2+}$ was air-oxidized according to Equation I-28 (43) and then separated by cation

$$2Co([14]ane)^{2+} + O_2 \longrightarrow Co([14]ane)\text{-}O_2\text{-}Co([14]ane)^{4+} \qquad \text{(I-28)}$$

exchange chromatography (Sephadex C-25 column) from the uncomplexed Co^{2+}. The concentration of Co^{2+} was determined by complexation with SCN^- in 50% acetone (λ_{max} 623 nm, ε 1842 M^{-1} cm^{-1}) and the concentration of

Table I-1. Electronic spectra of macrocyclic cobalt complexes[a]

mac	Co(II)(mac)	Co(III)(mac)$(H_2O)_2$	BrCo(mac)(H_2O)	ICo(mac)(H_2O)
[14]ane	465 (22)	560 (28) 430 (46)[b]	610 (33)	650 (50) 433 (1400)
meso-Me_6[14]ane	483 (70) 330 (sh)[c]	565 (36) 449 (sh) 257 (4000)[c]	640 (14) 360 (670)	-
Me_6-4,11-diene	446 (130) 335 (2500)[c]	582 (27) 431 (sh)[c]	625 (38) 363 (612)	-
tim	545 (3960) 360 (1005)	575 (sh) 505 (54) 425 (sh)[c]	-	-
dpnH	505 (2050)[d]	-	-	-

[a]Absorption maxima (λ/nm) with molar absorptivity ($\varepsilon/M^{-1}\ cm^{-1}$) in parentheses.

[b]From the aquation of Co(III)(mac)Cl_2.

[c]From Reference 39.

[d]From Reference 31.

Table I-1. (Continued)

mac	Co(II)(mac)	Co(III)(mac)$(H_2O)_2$	BrCo(mac)(H_2O)	ICo(mac)(H_2O)
$(dmgH)_2$	460 (3840)[e]	340 (2000)	-	-
		240 (21000)		
B_{12}	470 (10900)	525 (9950)	354 (20400)[f]	373 (13700)
	410 (6460)	495 (9850)		363 (13700)[f]
	310 (24100)	408 (3150)		
		350 (26200)[f]		

[e]From Reference 30.

[f]From Reference 44.

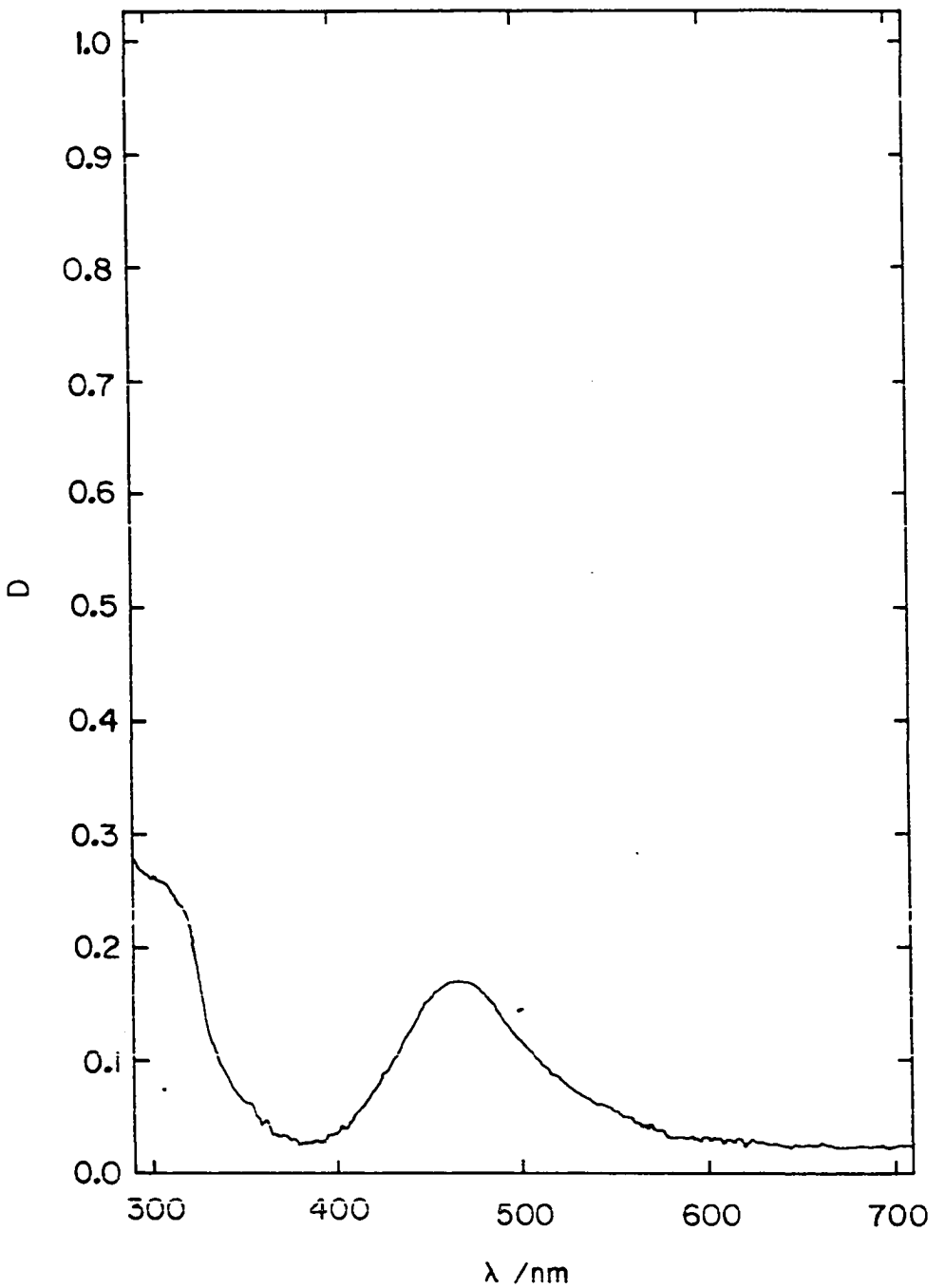

Figure I-3. The electronic spectrum of 1.4×10^{-3} M Co([14]ane)$^{2+}$ (ℓ = 5 cm)

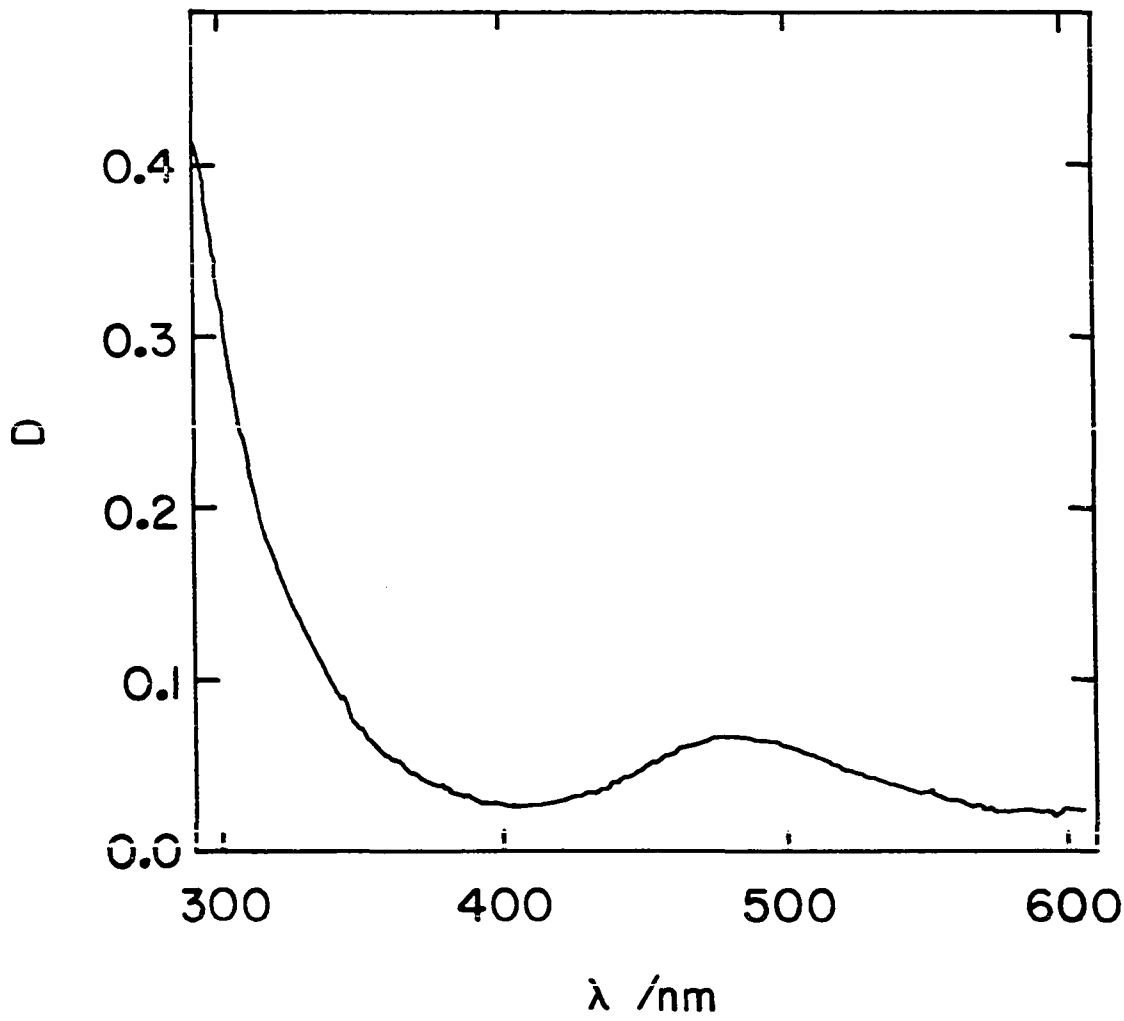

Figure I-4. The electronic spectrum of 2.0×10^{-4} M Co(meso-Me_6[14]ane)$^{2+}$ (ℓ = 5 cm)

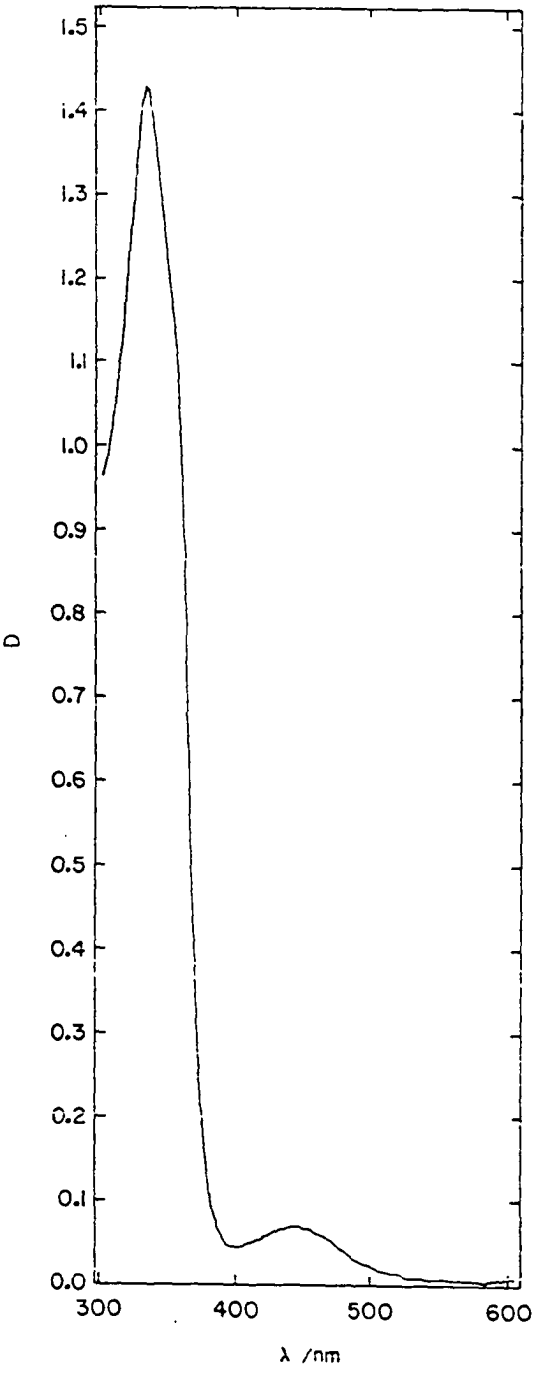

Figure I-5. The electronic spectrum of 1.3×10^{-4} M Co(Me_6-4,11-diene)$^{2+}$ (ℓ = 5 cm)

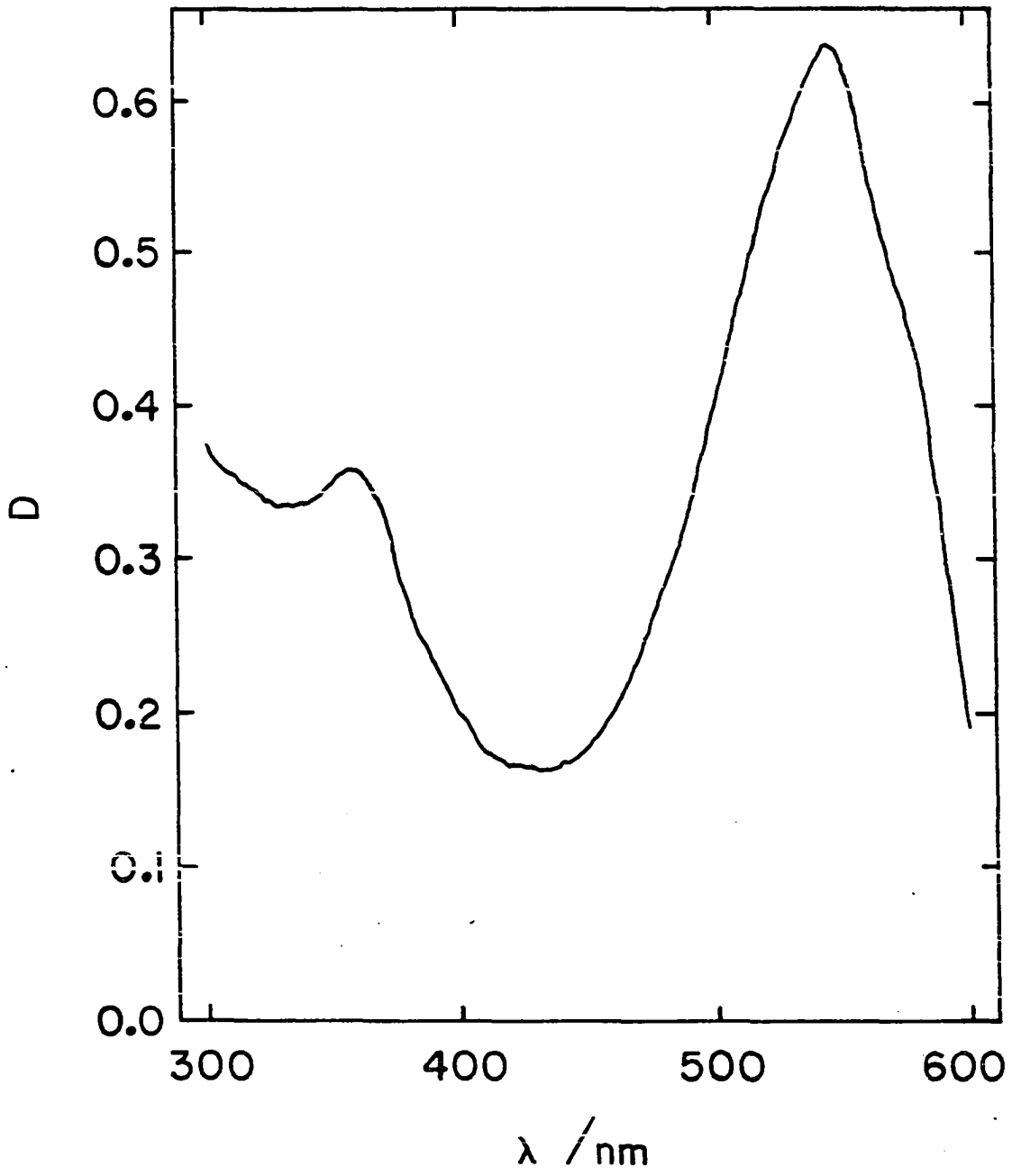

Figure I-6. The electronic spectrum of 1.8×10^{-4} M $Co(tim)^{2+}$ (ℓ = 1 cm)

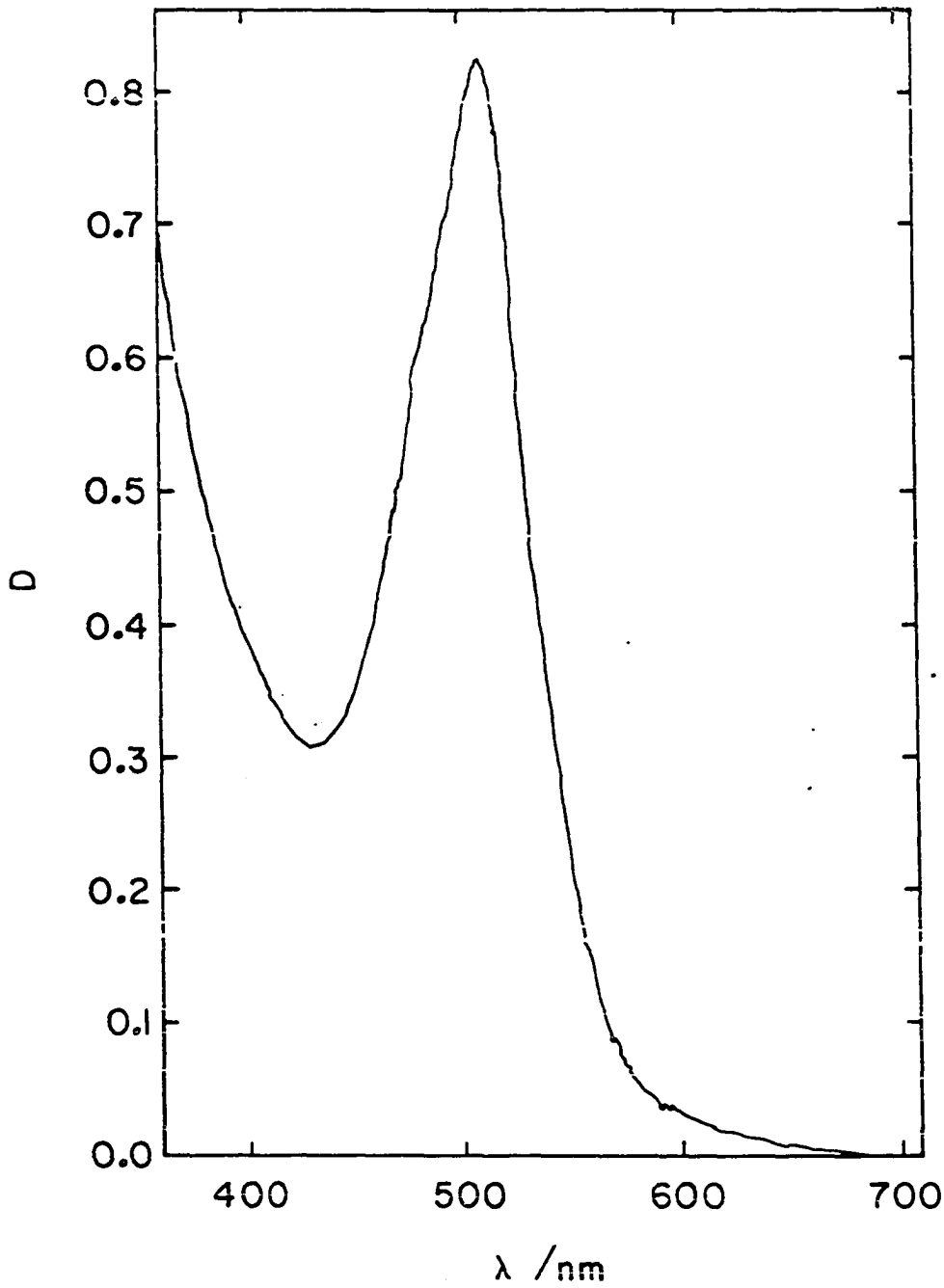

Figure I-7. The electronic spectrum of 4.0×10^{-4} M $Co(dpnH)^{+}$ (ℓ = 1 cm)

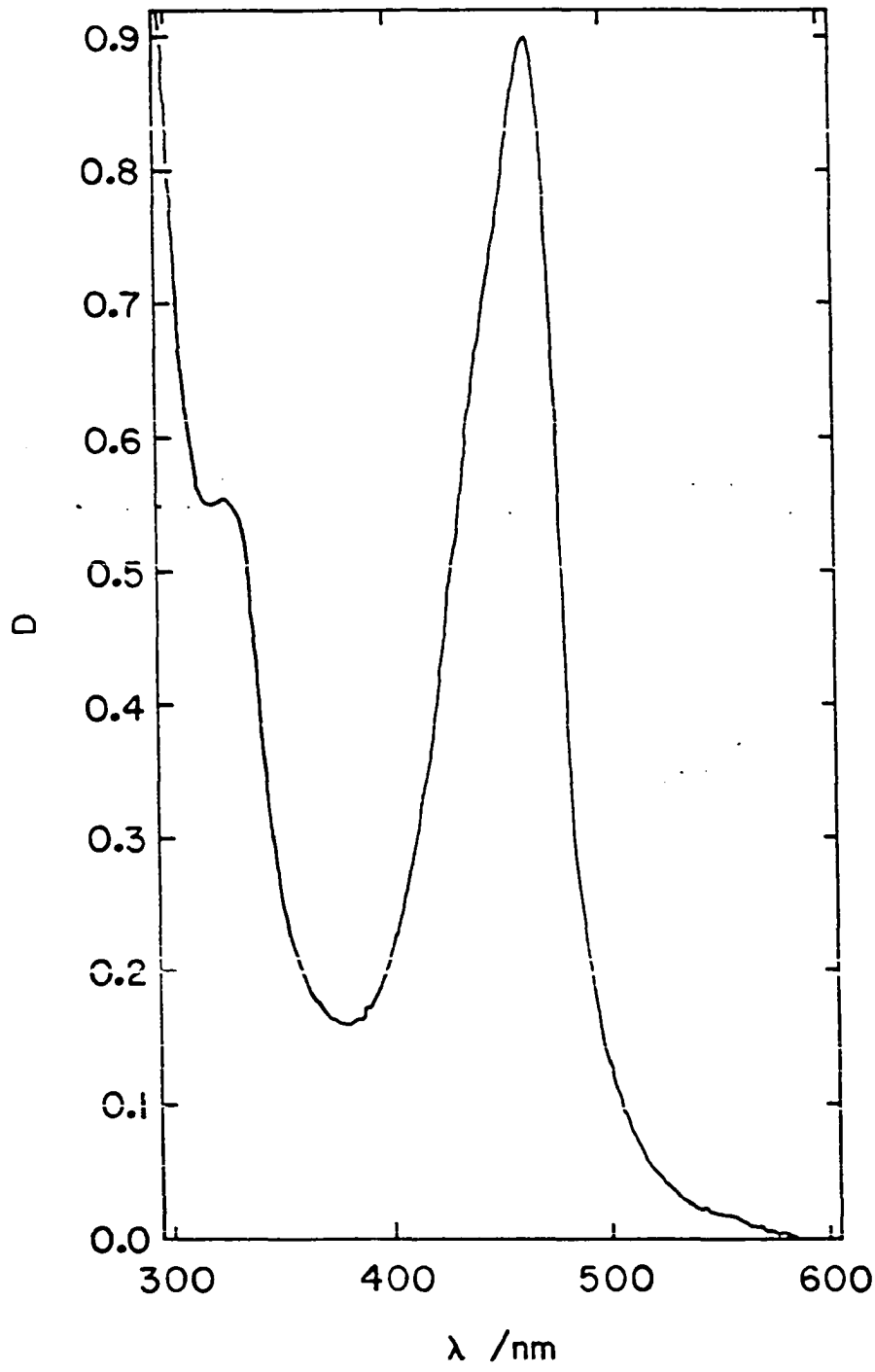

Figure I-8. The electronic spectrum of 1.33×10^{-4} M $Co(dmgH)_2$ (ℓ = 2 cm)

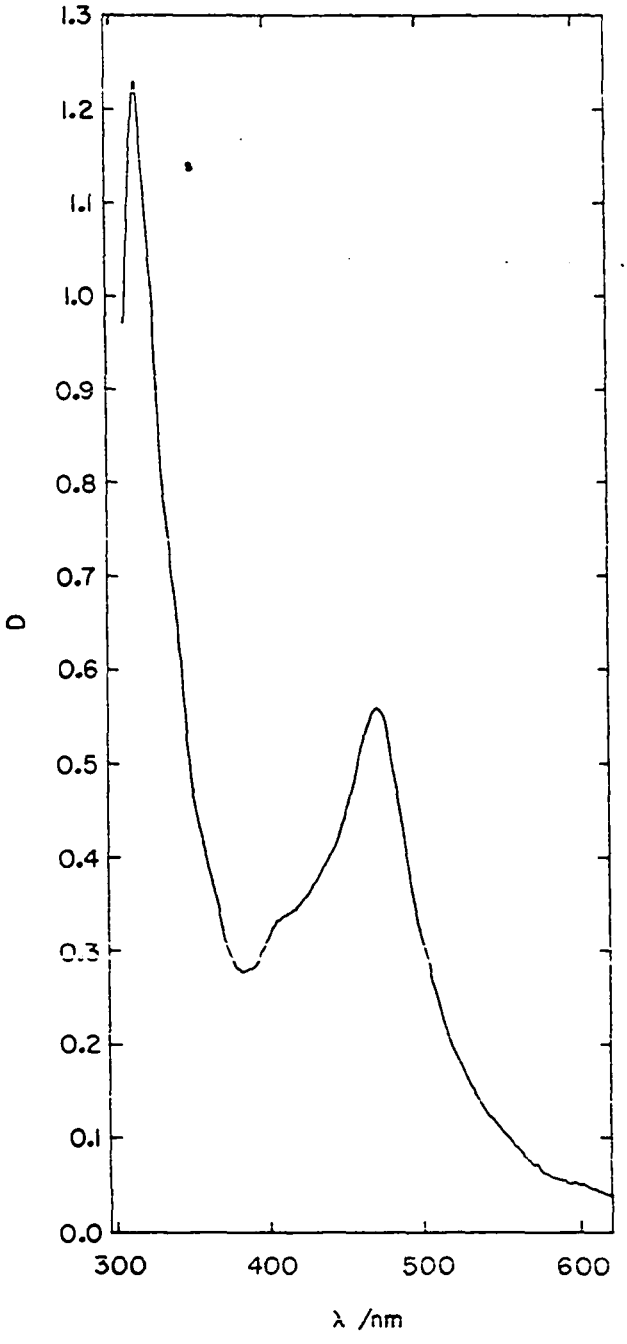

Figure I-9. The electronic spectrum of 5 x 10^{-5} M B_{12r} (ℓ = 1 cm)

$Co([14]ane)^{2+}$ was calculated by difference. Such an analysis was used in all cases where an accurately known concentration of $Co([14]ane)^{2+}$ was required. Otherwise, the concentration was estimated from the quantities of reagents used.

Oxidants Bromine and iodine concentrations were determined by the intensity of their absorptions at 390 (ε 179 M^{-1} cm^{-1}) and 460 nm (ε 787 M^{-1} cm^{-1}), respectively. A concentrated solution of H_2O_2 (30%) was diluted 1:100 and titrated with standardized $S_2O_3^{2-}$ after reaction with excess KI (45).

Reaction products Several of the predicted reaction products have been previously characterized spectrophotometrically in the literature (Table I-1). Where possible these sources were used to identify reaction products.

Endicott's method (46) was used to demonstrate the production of $ICo([14]ane)^{2+}$ in the $Co([14]ane)^{2+}$—I_2 reaction. After cation exchange separation of the yellow band of product from $Co([14]ane)\text{-}O_2\text{-}Co([14]ane)^{4+}$ (produced by air-oxidation of excess $Co([14]ane)^{2+}$), the product solution was photolyzed for several hours under a high-intensity Hg lamp. The iodine produced (Equation I-29) was swept away by a vigorous stream of

$$ICo([14]ane)(H_2O)^{2+} + 2H^+ + h\nu \longrightarrow \tfrac{1}{2}I_2 + Co^{2+} + [14]aneH_2^{2+} + H_2O \qquad (I\text{-}29)$$

N_2 and the remaining Co^{2+} was analyzed as the tetrathiocyanato complex. An identical reaction product solution was reacted with IO_3^- (Equation

I-30) to produce I_2 (47) whose absorbance at 460 nm was used to calculate

$$5ICo([14]ane)(H_2O)^{2+} + IO_3^- + 2H_2O + 6H^+ \longrightarrow 3I_2 + 5Co([14]ane)(H_2O)_2^{3+} \qquad (I\text{-}30)$$

the amount of total iodide in the complex.

Stoichiometry

The stoichiometries of most of the reactions were determined by measuring the fraction of Co(II) complex lost when an aliquot of oxidant was added. Five of the Co(II) complexes studied here were particularly amenable to this method because of strong absorption bands in the visible or near ultraviolet. Alternatively, a plot was made of the observed absorbance (at constant initial concentration of Co(II)) versus the mole ratio of oxidant to Co(II). The break in the curve so obtained indicates the reaction stoichiometry.

Kinetics

Fast kinetic runs were done using a Durrum 110 stopped-flow spectrophotometer. Where reactions were simply single-stage and pseudo-first-order the spectrophotometric data were recorded on a Biomation 802 Transient Recorder and rate constants were calculated using a PDP-15 computer. Slower kinetic runs were done using a Cary 14 spectrophotometer and the data were treated by conventional pseudo-first-order plots of $\log(D - D_\infty)$ versus time.

Some runs were too fast to be studied by pseudo-first-order methods while maintaining reasonable reaction conditions. For several of those

cases second-order conditions were used and rate constants were estimated from the measured half-lives of reaction according to Equation I-31 (48). In Equation I-31 $[A]_o$ and $[B]_o$ correspond to initial reactant

$$k = \frac{a}{t_{\frac{1}{2}}(b[A]_o - a[B]_o)} \ln \frac{a[B]_o}{2a[B]_o - b[A]_o} \qquad \text{(I-31)}$$

concentrations and a and b refer to the stoichiometry of each reagent. An inherent error in the system exists in that because a finite time is required for mixing of reactants, the observed half-life is not necessarily the initial half-life and the calculated rate constant is therefore no better than a lower limit.

Several of the reactions showed biphasic (two-stage) characteristics and the data were treated appropriately (49). For consecutive first-order reactions (Equation I-32) the absorbance at constant wave-

$$A \xrightarrow{k^I} B \xrightarrow{k^{II}} C \qquad \text{(I-32)}$$

length is the sum of the contributions of all three species (Equation I-33). The integrated expressions for each species concentration

$$D = \varepsilon_A \ell[A] + \varepsilon_B \ell[B] + \varepsilon_C \ell[C] \qquad \text{(I-33)}$$

(Equations I-34 to I-36) may be inserted into Equation I-33 and

$$[A] = [A]_o \exp(-k^I t) \qquad \text{(I-34)}$$

$$[B] = [A]_o \left(\frac{k^I}{k^{II} - k^I} \right) [\exp(-k^I t) - \exp(-k^{II} t)] \qquad \text{(I-35)}$$

$$[C] = [A]_o - [A]_o \left(\frac{1}{k^{II} - k^I} \right) [k^{II} \exp(-k^I t) - k^I \exp(-k^{II} t)] \qquad \text{(I-36)}$$

rearranged to give the absorbance as a sum of two terms exponential in time (Equation I-37). The term $\varepsilon_C \ell [A]_o$ is equivalent to the absorbance

$$D = \alpha \exp(-k^I t) - \beta \exp(-k^{II} t) + \varepsilon_C \ell [A]_o \qquad \text{(I-37)}$$

$$\alpha = \left(\varepsilon_A + \varepsilon_B \frac{k^I}{k^{II} - k^I} - \varepsilon_C \frac{k^{II}}{k^{II} - k^I} \right) \ell [A]_o \qquad \text{(I-38)}$$

$$\beta = (\varepsilon_B - \varepsilon_C) \left(\frac{k^I}{k^{II} - k^I} \right) \ell [A]_o \qquad \text{(I-39)}$$

at infinite time. A plot of $\ln(D - D_\infty)$ versus time gives a straight

$$D - D_\infty = \alpha \exp(-k^I t) - \beta \exp(-k^{II} t) \qquad \text{(I-40)}$$

line at long times whose slope and (extrapolated) intercept are equal to $-k^{II}$ and $-\beta$, respectively, provided that $k^I > k^{II}$. A plot of $\ln[\beta \exp(-k^{II} t) - (D - D_\infty)]$ versus time at short times gives a straight line of slope equal to $-k^I$.

The iodide anation of $Co([14]ane)^{3+}$ and the aquation of $ICo([14]-ane)^{2+}$ were quite slow reactions. Therefore, their reaction rates were determined by initial rate studies. For the anation reaction Equation I-41 applied, where the differential was determined from observed

$$k_{an} = \frac{d[ICo([14]ane)(H_2O)^{2+}]/dt}{[Co([14]ane)(H_2O)_2{}^{3+}][I^-]} \qquad (I-41)$$

absorbance changes (< 10% of the total reaction) and known molar absorptivities. Equation I-42 applied to the aquation reaction.

$$k_{aq} = \frac{-d[ICo([14]ane)(H_2O)^{2+}]/dt}{[ICo([14]ane)(H_2O)^{2+}]} \qquad (I-42)$$

Reduction potentials

Reduction potentials for all the complexes studied except B_{12r} were determined by cyclic voltametry using a PAR Model 173 Potentiostat/Galvanostat and Model 175 Universal Programmer. A platinum disc electrode was used for the $Co(tim)^{2+}$ determination and a hanging mercury drop was used for the others, with a saturated calomel reference in all cases. For the [14]ane, dpnH, and dimethylglyoxime complexes the Co(III) complex was used, while the Co(II) complex was used for the tim, meso-Me_6[14]ane, and Me_6-4,11-diene complexes. All studies except that of $Co(dmgH)_2(H_2O)_2^+$ were done in 0.10 M $HClO_4$ while the cobaloxime was done in 0.10 M $NaClO_4$. Due to limited solubility, the meso-Me_6[14]ane and Me_6-4,11-diene complexes were studied at 1×10^{-4} M concentrations and all others were at 1×10^{-3} M.

A standard reduction potential, E°, was determined for the Co([14]ane)$(H_2O)_2^{3+}$/Co([14]ane)$^{2+}$ couple by a method similar to that of Liteplo and Endicott (50). A 9.57 x 10^{-4} M solution of Co([14]ane)-$(H_2O)_2^{3+}$ in 0.10 M $HClO_4$ was titrated with 0.10 ml aliquots of 9.8 x 10^{-2} M Cr^{2+}. After each addition of chromous the potential of the solution was measured. The resulting potentials were corrected for junction potentials and cell characteristics by calibration with a similar potentiometric titration of a 2.21 x 10^{-3} M Fe^{3+} solution. The standard reduction potential is the observed potential at equal concentrations of oxidized and reduced species.

The half-wave potentials were calculated as the average of the potentials of the anodic and cathodic waves (Figure I-10) and were reproducible to ± 0.01 V. The theoretical separation between waves is 0.059 volts for a completely reversible reaction and is independent of the scan rate used. No attempt was made to determine whether the systems under study were completely reversible, although at the scan rates used (1-5 V s^{-1}) all complexes except Co([14]ane)$^{3+/2+}$ showed peak separations of 60-90 mV.

Electrochemical studies were done with the assistance of Mr. Garry Kirker.

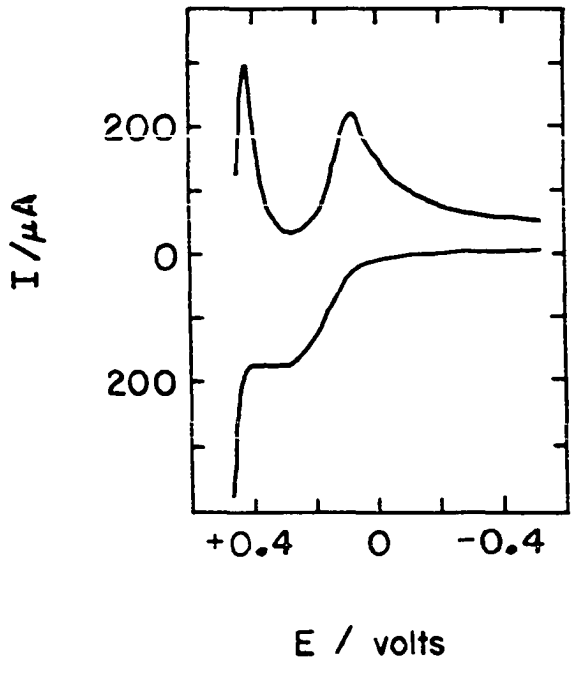

(a)

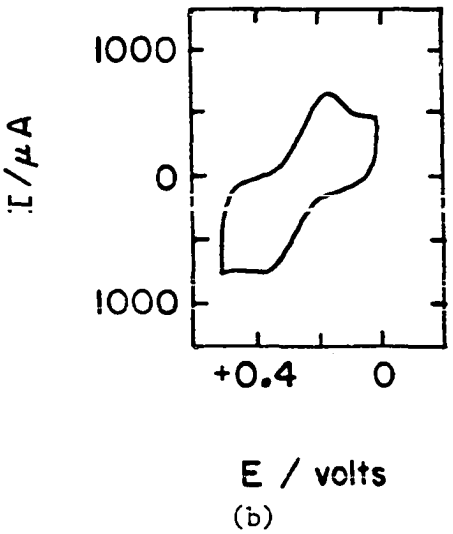

(b)

Figure I-10. Cyclic voltammograms for (a) 1.0×10^{-3} M Co([14]ane)$^{3+}$ using a hanging mercury drop electrode and (b) 1.0×10^{-3} M Co(tim)$^{2+}$ at a platinum disc electrode

RESULTS

Reactions of H_2O_2

Stoichiometry

The stoichiometries for the reduction of H_2O_2 by the seven cobalt(II) complexes studied here have not been reported previously. The stoichiometries in most cases were determined by measuring the loss of intensity of a prominent peak in the electronic spectrum of the Co(II) reagent.

A spectrophotometric titration of 3.17×10^{-3} M $Co([14]ane)^{2+}$ with H_2O_2 was followed at 400 nm (essentially, a shoulder of $Co([14]ane)(H_2O)_2^{3+}$). A plot of $D\ell^{-1}[Co([14]ane)^{2+}]^{-1}$ versus the mole ratio of H_2O_2 to $Co([14]ane)^{2+}$ (Figure I-11) showed a break at 0.53, implying a stoichiometry of 2:1 $Co([14]ane)^{2+}$:H_2O_2.

All of the other Co(II)—H_2O_2 reaction stoichiometries (except that for $Co(dpnH)^+$) were determined, and Table I-2 shows that all stoichiometries were 1:1. Additionally, the stoichiometry for the $Co(tim)^{2+}$ reaction was confirmed by spectrophotometric titration of $Co(tim)^{2+}$ with H_2O_2. A plot of $D\ell^{-1}[Co(tim)^{2+}]^{-1}$ versus mole ratio of H_2O_2 to $Co(tim)^{2+}$ (Figure I-12) showed a break at 1.08. Table I-2 shows that the addition of tert-butanol had no effect on the stoichiometry of the $Co(tim)^{2+}$—H_2O_2 reaction.

The reaction stoichiometry of $Co(dpnH)^+$ with H_2O_2 was not determined. However, by analogy with $Co(tim)^{2+}$ and $Co(dmgH)_2$ the stoichiometry was presumed to be 1:1.

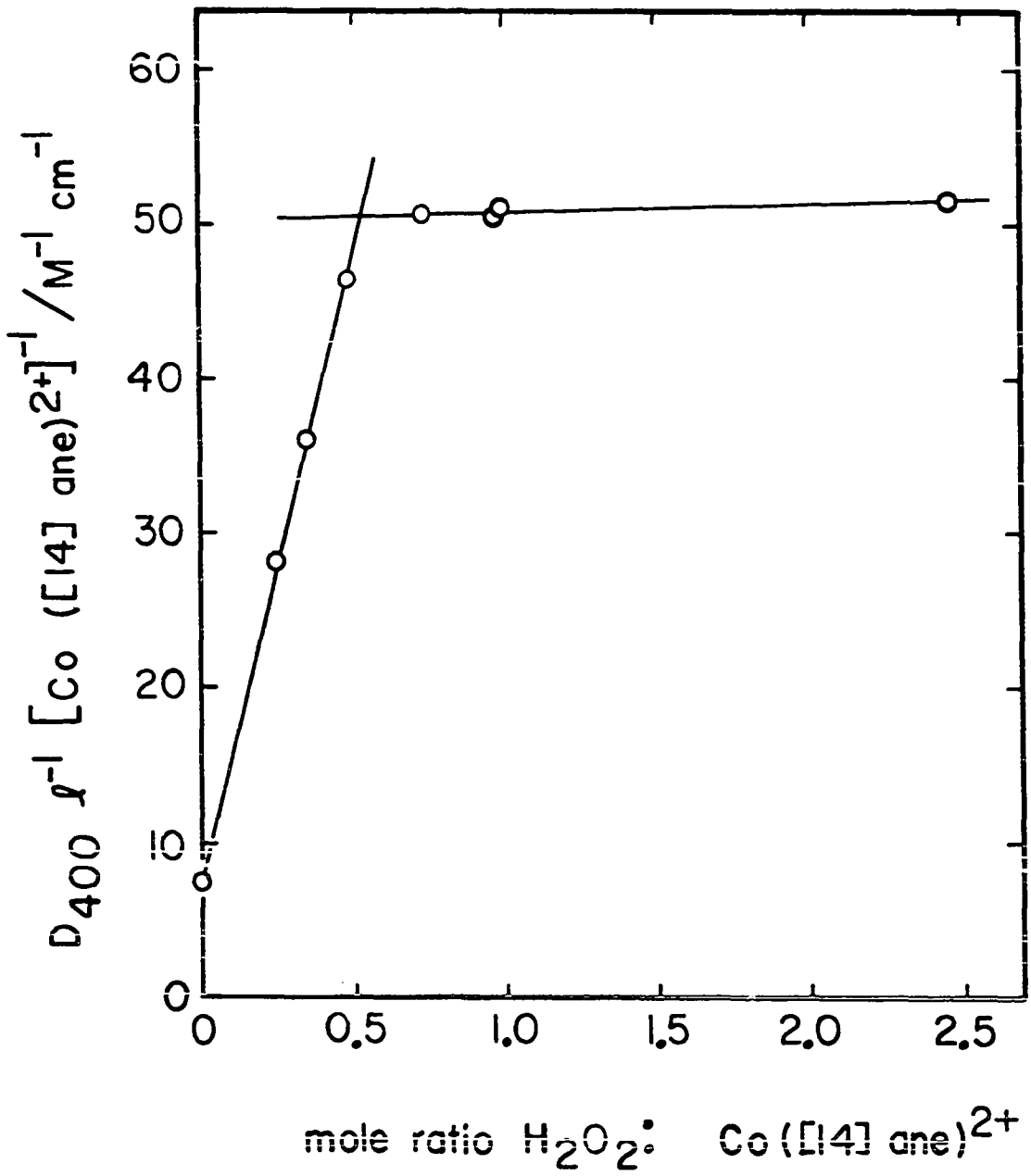

Figure I-11. Spectrophotometric titration of $Co([14]ane)^{2+}$ with H_2O_2

Table I-2. Determination of reaction stoichiometries for the reactions of Co(II)(mac) with H_2O_2

mac	Conditions	10^4[Co(II)]/M	10^4[H_2O_2]/M	Δ[Co(II)]/[H_2O_2]
meso-Me_6[14]ane	μ = [H^+] = 0.05 M	1.87	0.33	1.63
		1.87	0.49	0.73
		1.87	0.65	0.60
		1.87	1.63	0.85
Me_6-4,11-diene	μ = [H^+] = 0.1 M	3.03	0.33	1.19
		3.03	1.63	1.00
		3.03	2.29	1.00
tim	μ = [H^+] = 0.1 M	3.21	0.98	0.97
		3.21	1.63	1.02
		3.21	2.28	0.95
tim	μ = [H^+] = 0.1 M	3.21	0.65	1.07
	1 M t-BuOH	3.21	0.98	0.98
		3.21	1.63	1.08
		3.21	2.28	1.13
tim	μ = [H^+] = 0.1 M	3.21	0.98	1.07
	50% t-BuOH-H_2O	3.21	1.63	0.88
		3.21	2.28	1.06

Table I-2. (Continued)

mac	Conditions	$10^4[Co(II)]/M$	$10^4[H_2O_2]/M$	$\Delta[Co(II)]/[H_2O_2]$
$(dmgH)_2$	μ = 0.1 M NaOAc	1.33	0.33	0.91
		1.33	0.65	1.05
		1.33	0.98	1.02
B_{12r}	$\mu = [H^+] = 0.1$ M	0.67	0.33	1.19
		1.00	0.33	1.21

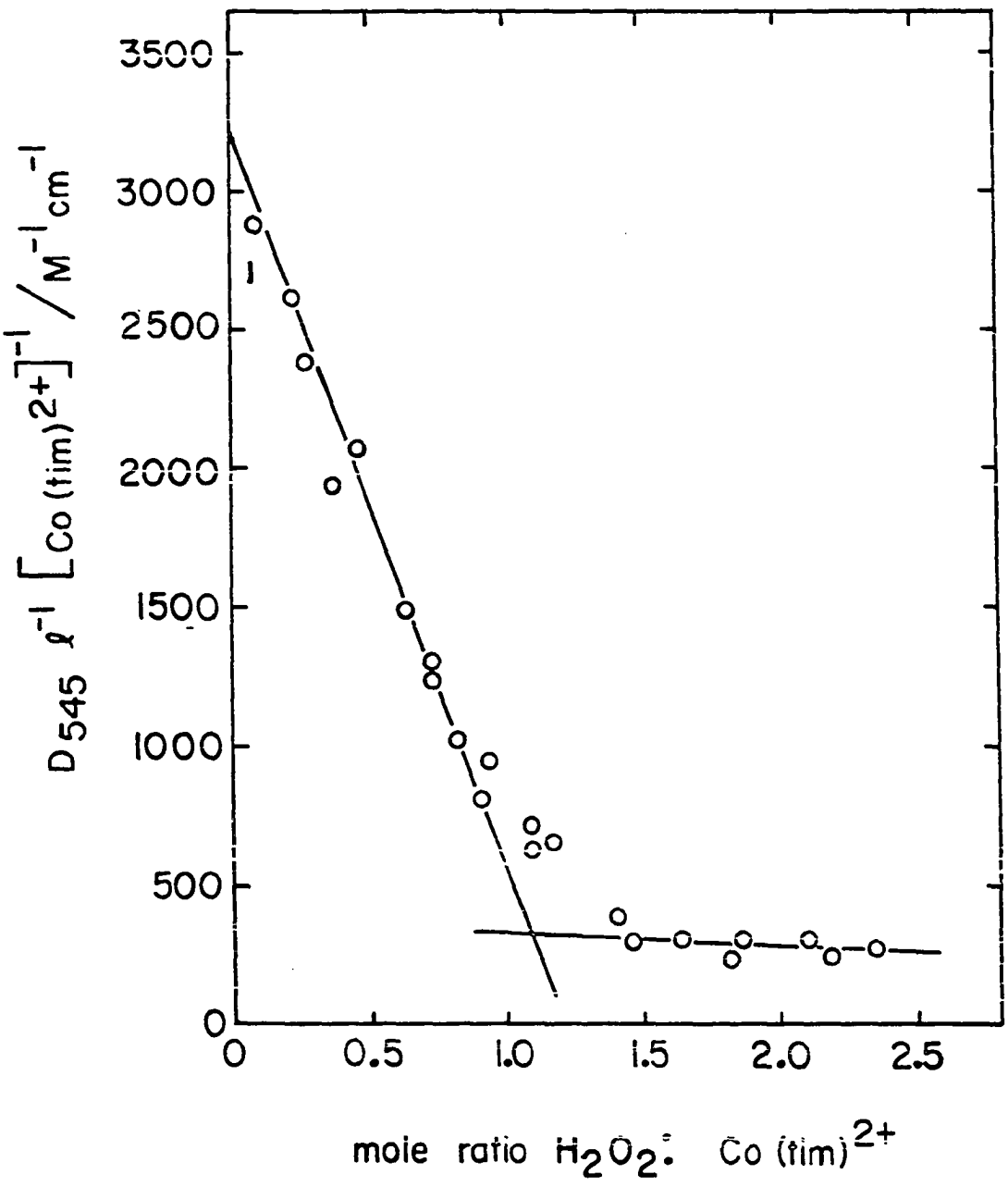

Figure I-12. Spectrophotometric titration of $Co(tim)^{2+}$ with H_2O_2

Products of reaction

By analogy with the previously reported reductions of H_2O_2 with Cr^{2+} (16), Fe^{2+} (7,8), and $Co(CN)_5^{3-}$ (21) the expected products of reaction in this study were of the type $Co(III)(macrocycle)(H_2O)_2^{n+}$. Electronic spectra of the diaquo cobalt(III) complexes of several of the macrocycles have been reported in the literature and those data are shown in Table I-1.

The most thoroughly studied complexes were $Co(dmgH)_2$ and B_{12r}. The product spectrum of $B_{12r} + H_2O_2$ (Figure I-13) clearly shows the principal features of aquocobalamin B_{12a} (λ_{max} at 525, 495, 408, and 350 nm) although an uncharacteristic shoulder is also apparent at 460 nm. A mixture of 3.0×10^{-4} M B_{12r} and 2.9×10^{-4} M H_2O_2 in 0.1 M $HClO_4$ was allowed to react for 10 minutes and then loaded onto a column of Sephadex cation exchange resin. Elution with 0.10 M $HClO_4$ resolved the product into two well-separated bands of red followed by yellow. The spectrum of the red product compared very well to that of authentic B_{12a} while the yellow product had absorption bands at 480 (sh), 450, 430 (sh), 345, and 300 nm (Figure I-14). The yield of B_{12a} was 51%. Reaction with a large excess of H_2O_2 showed production of larger quantities of the yellow product.

The electronic spectrum of $Co(dmgH)_2(H_2O)_2^+$ is featureless in the visible although the uv shows a shoulder at 340 nm with an intense maximum at 240 nm (Figure I-15). Reaction of 1.0×10^{-3} M $Co(dmgH)_2$ with 1.0×10^{-3} M H_2O_2 in 0.10 M $NaC_2H_3O_2$ gave a yellow product solution

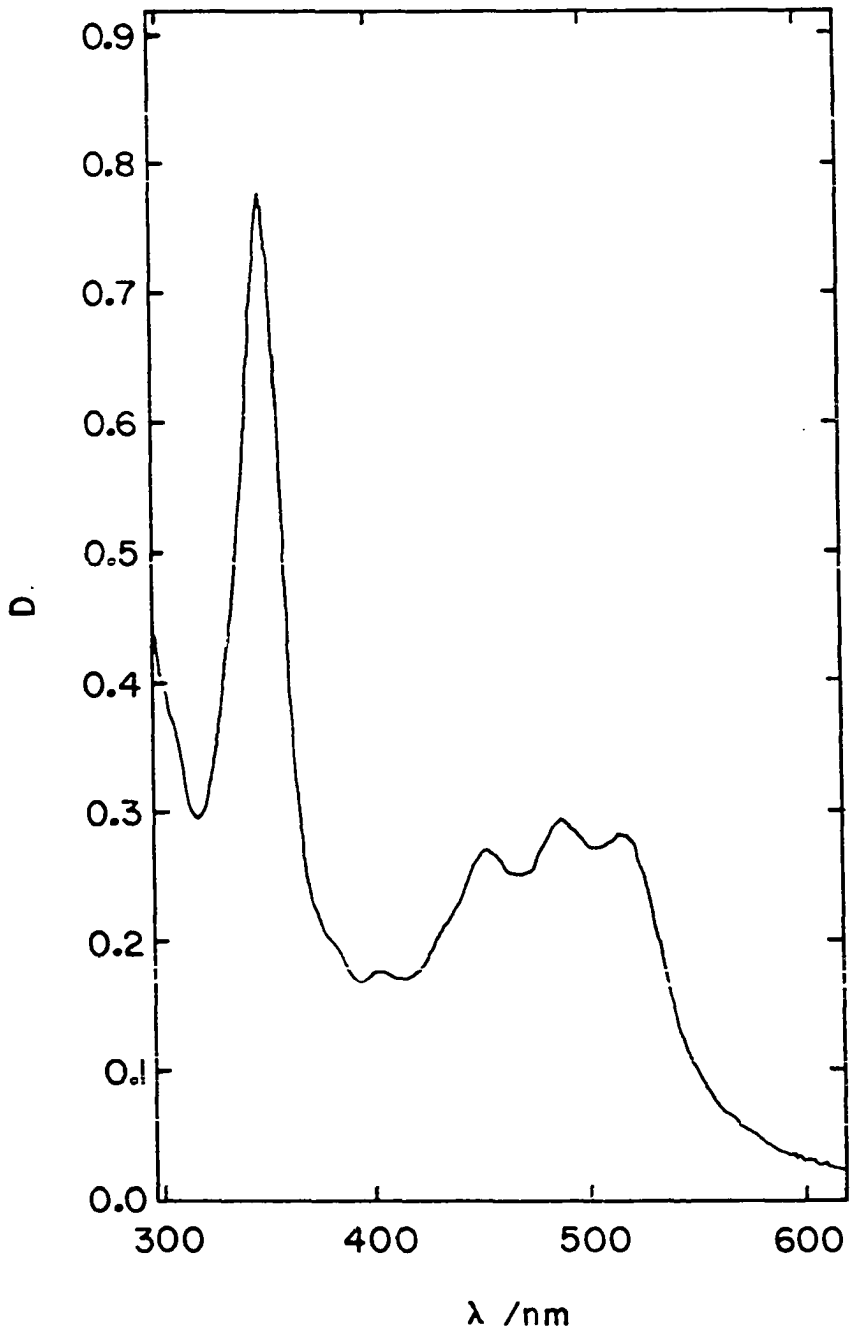

Figure I-13. The spectrum of the product mixture from the reaction of 5.0×10^{-5} M B_{12r} with 4.9×10^{-3} M H_2O_2

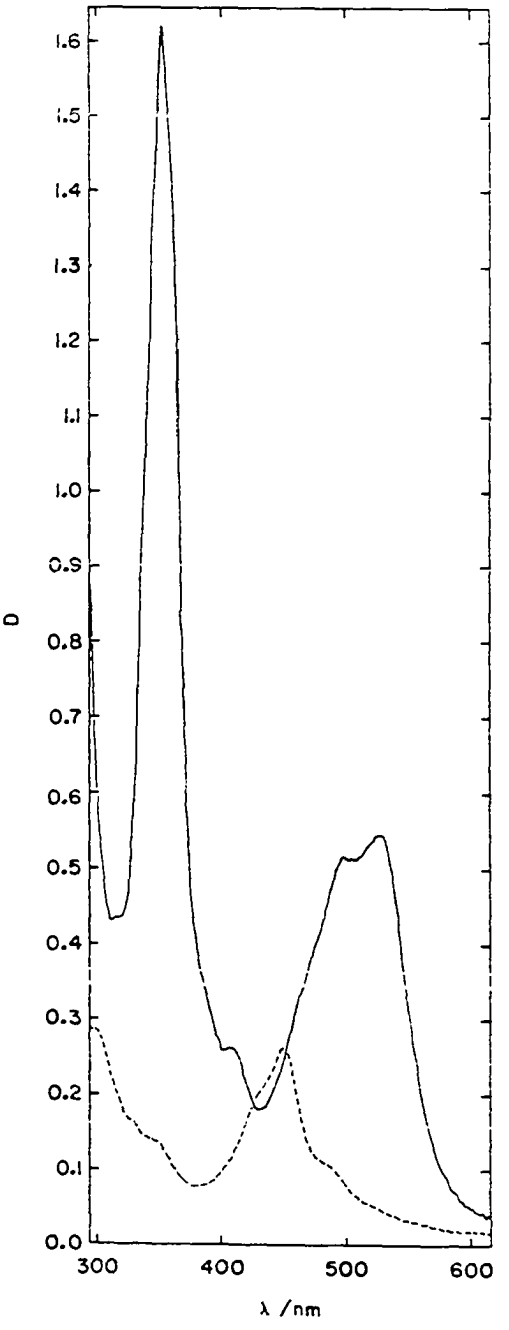

Figure I-14. The spectra of the two products from the reaction of B_{12r} with H_2O_2

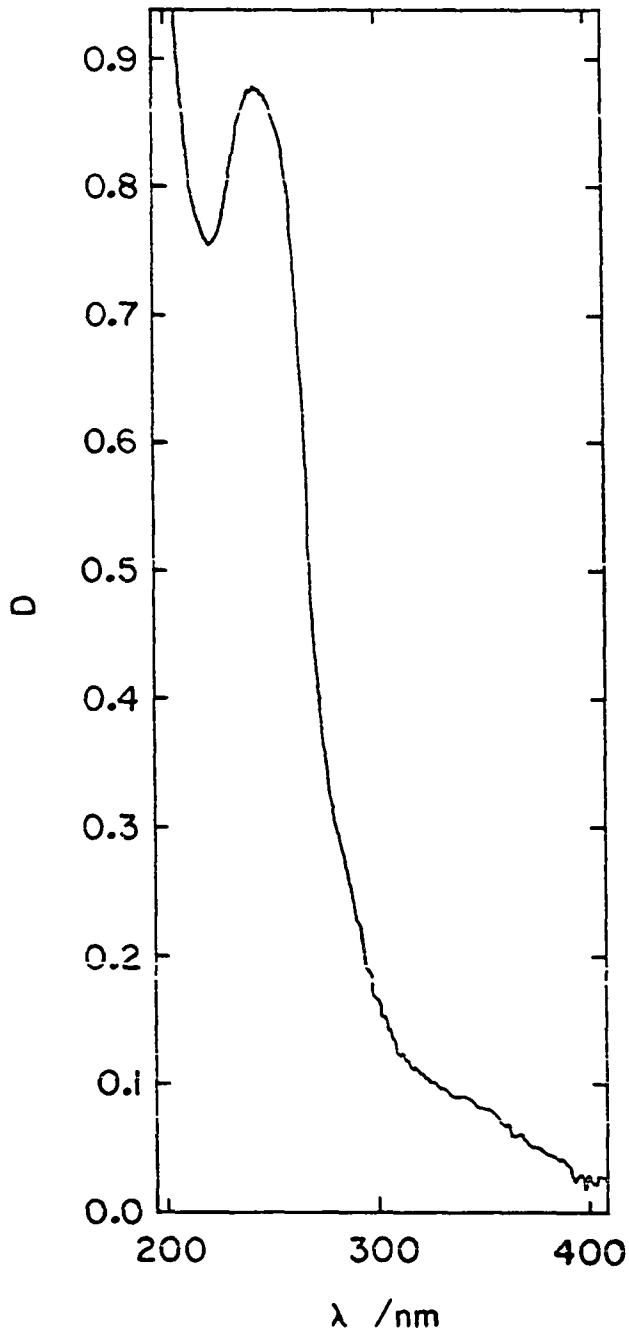

Figure I-15. The electronic spectrum of 2.0×10^{-5} M $Co(dmgH)_2(H_2O)_2^+$ (ℓ = 2 cm)

which was loaded onto a Sephadex column and eluted with 0.10 M $HClO_4$. Two well-resolved yellow bands were collected and their spectra showed maxima at 230 nm (first band) and 235 nm (second band) (Figure I-16). Assuming that the second band was $Co(dmgH)_2(H_2O)_2^+$, the yield of diaquo product was 40%.

The reaction of $Co([14]ane)^{2+}$ with H_2O_2 yielded a product whose spectrum was very much like that of $Co([14]ane)(H_2O)_2^{3+}$ (Figure I-17). This result along with the results of stoichiometry studies led to the conclusion that $Co([14]ane)(H_2O)_2^{3+}$ was the sole product of reaction.

The reaction of 7.00×10^{-4} M $Co(meso\text{-}Me_6[14]ane)^{2+}$ with excess H_2O_2 yielded a product whose spectrum had maxima at 550, 430 (sh), and $\simeq$ 245 nm. Because of the similarity of this spectrum to that of $Co([14]ane)(H_2O)_2^{3+}$ the product was assumed to be the analogous $Co(meso\text{-}Me_6[14]ane)(H_2O)_2^{3+}$ although modification of peripheral substituents of the ligand may not be apparent spectrophotometrically.

The visible spectra of the products of reaction of $Co(tim)^{2+}$ and $Co(dpnH)^+$ with H_2O_2 had no prominent features on which to base any identification. The product of the $Co(Me_6\text{-}4,11\text{-diene})^{2+}$—$H_2O_2$ reaction was not studied in detail. However, when the reaction was done in 2 M CH_3OH (hydroxyl radical scavenger), no $HOCH_2Co(Me_6\text{-}4,11\text{-diene})^{2+}$ was detected (51).

Two additional experiments were done using halide ions as hydroxyl radical scavengers. The reaction of 3.6×10^{-3} M $Co([14]ane)^{2+}$ containing 0.01 M Br^- with excess H_2O_2 gave a product whose spectrum was

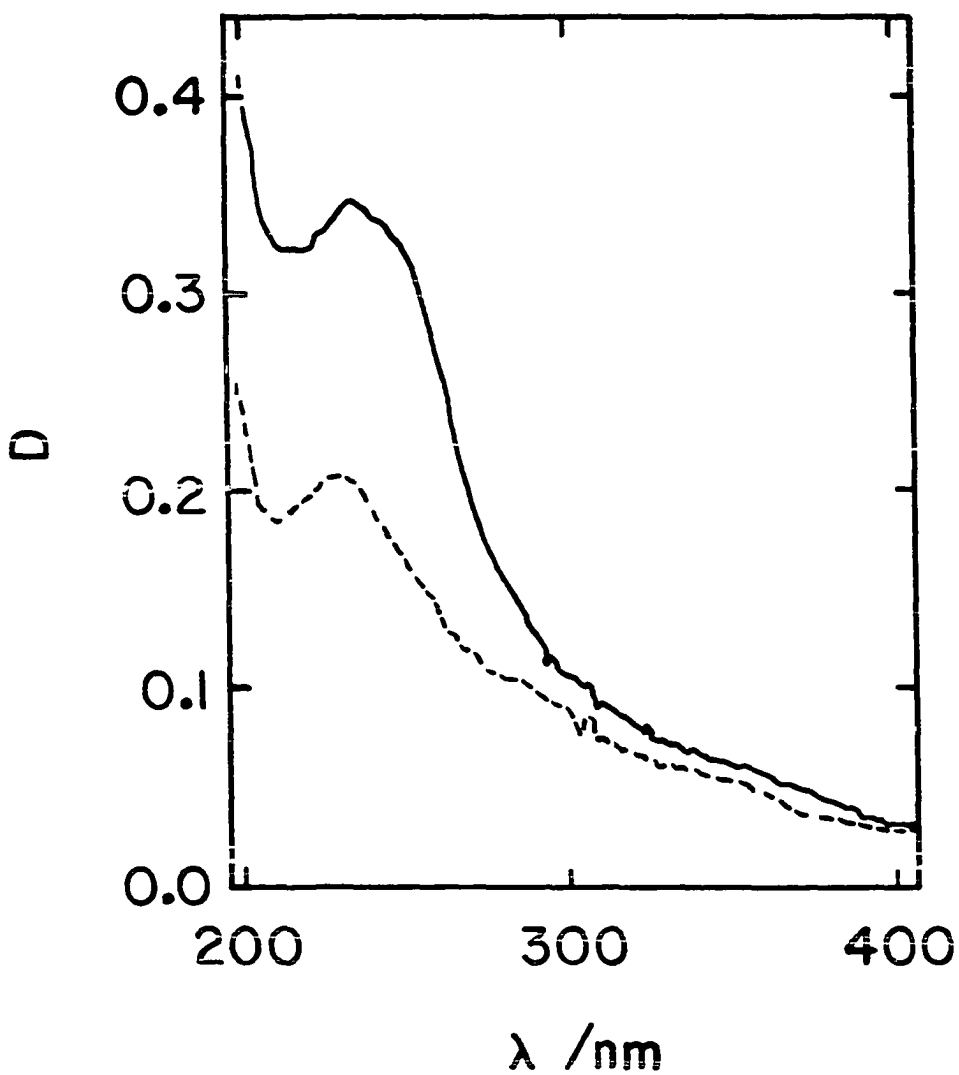

Figure I-16. The spectra of the two products from the reaction of $Co(dmgH)_2$ with H_2O_2

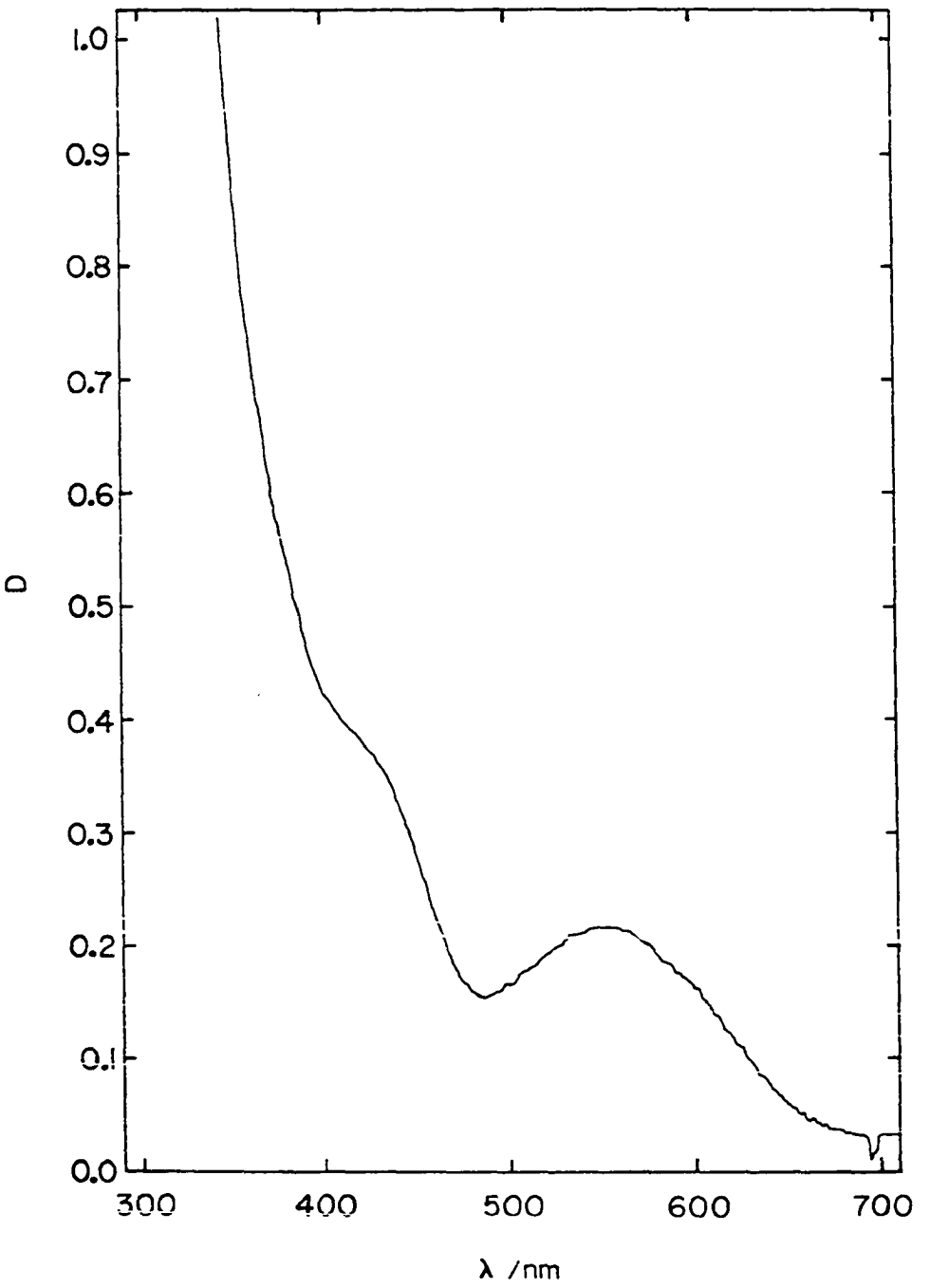

Figure I-17. The electronic spectrum of the product of the reaction of 1.4×10^{-3} M Co([14]ane)$^{2+}$ with 1.4×10^{-3} M H_2O_2

similar to, but not identical to, the calculated spectrum of a mixture of 1.8×10^{-3} M Co([14]ane)$(H_2O)_2^{3+}$ and 1.8×10^{-3} M BrCo([14]ane)-$(H_2O)^{2+}$. With 0.1 M Br^- the discrepancy between calculated and observed spectra was worse, possibly owing to the formation of $Br_2Co([14]ane)^+$. The latter species could have arisen either from rapid anation of BrCo-([14]ane)$(H_2O)^{2+}$ or from the bromine atom oxidation of BrCo([14]ane)$^+$. Rapid anation of the monobromo product is unlikely because of the known slow anation of the analogous chloro complex (52).

A solution of 3.72×10^{-3} M Co([14]ane)$^{2+}$ with $[I^-] = 0.01$ M and $[H^+] = 0.10$ M was allowed to react with a slight excess of H_2O_2. A portion of the reaction mixture was loaded onto a cation exchange column and eluted with 0.3 M $HClO_4$. Two cationic bands which had the electronic spectra of ICo([14]ane)$(H_2O)^{2+}$ and Co([14]ane)$(H_2O)_2^{3+}$ were collected in 40% and 60% yields, respectively.

Kinetics

All reactions of H_2O_2 with the Co(II) complexes were studied kinetically under pseudo-first-order conditions with H_2O_2 in excess. All reaction traces so obtained gave good plots of $\log(D - D_\infty)$ versus time on those occasions when plots were made to confirm computer-generated results. Tables I-3 to I-9 give the pseudo-first-order rate constants, k_{obs}, and second-order rate constants, k, obtained. Plots of k_{obs} versus $[H_2O_2]$, Figures I-18 to I-24, were also linear in all cases, with intercepts at the origin, showing the first-order dependence of the reaction on H_2O_2 concentration. The rate law for this set of reactions

Table I-3. Kinetic data for the reaction of $Co([14]ane)^{2+}$ with H_2O_2. Conditions: $[Co([14]ane)^{2+}] = 2.5 \times 10^{-4}$ M, $\mu = [H^+] = 0.10$ M, T = 25° C, λ = 300 nm

$10^3[H_2O_2]/M$	k_{obs}/s^{-1}	$10^{-3}k/M^{-1}\ s^{-1}$ [a,b]
0.92	7.69	4.19
1.42	15.4	5.43
1.97	15.8	4.02
3.75	24.6	3.28
5.64	39.7	3.52
9.39	63.3	3.37

[a] $k = \frac{1}{2}k_{obs}[H_2O_2]^{-1}$.

[b] Average value is (3.97 ± 0.80) x $10^3\ M^{-1}\ s^{-1}$.

Table I-4. Kinetic data for the reaction of $Co(meso\text{-}Me_6[14]ane)^{2+}$ with H_2O_2. Conditions: $[Co(meso\text{-}Me_6[14]ane)^{2+}] = 7 \times 10^{-5}$ M, $\mu = [H^+] = 0.10$ M, $T = 25^\circ$ C, $\lambda = 300$ nm

$10^2[H_2O_2]/M$	k_{obs}/s^{-1}	$10^{-2}k/M^{-1}\ s^{-1}$ [a,b]
0.21	0.538	2.56
0.45	1.19	2.64
0.92	2.43	2.66
2.46	6.63	2.70
2.57	6.85	2.66
2.80	7.44	2.66

[a] $k = k_{obs}[H_2O_2]^{-1}$.

[b] Average value is $(2.65 \pm 0.05) \times 10^2\ M^{-1}\ s^{-1}$.

Table I-5. Kinetic data for the reaction of $Co(Me_6\text{-}4,11\text{-diene})^{2+}$ with H_2O_2. Conditions: $[Co(Me_6\text{-}4,11\text{-diene})^{2+}] = 9.5 \times 10^{-5}$ M, $\mu = [H^+] = 0.10$ M, T = 25° C, λ = 335 nm

$10[H_2O_2]/M$	k_{obs}/s^{-1}	$k/M^{-1}\ s^{-1}$ [a,b]
0.17	1.57	92[c,d]
0.17	1.39	82[d]
0.19	1.55	81.6
0.48	2.97	61.8
0.95	7.05	74.2
1.53	12.2	79.8
1.91	15.1	79.0
2.67	23.1	86.4
4.76	36.2	76.0

[a] $k = k_{obs}[H_2O_2]^{-1}$.

[b] Average value is (77.0 ± 7.8) $M^{-1}\ s^{-1}$.

[c] Contained 0.13 M NaBr.

[d] Run not included in average or least squares fit.

Table I-6. Kinetic data for the reaction of $Co(tim)^{2+}$ with H_2O_2. Conditions: $[Co(tim)^{2+}] = 5.8 \times 10^{-5}$ M, $\mu = [H^+] = 0.10$ M, T = 25° C, λ = 545 nm

$10^2[H_2O_2]$/M	$[Br^-]$/M	k_{obs}/s^{-1}	$10^{-2}k/M^{-1}\ s^{-1}$ [a,b]
0.373	0.0	0.507	1.36
0.746	0.0	1.18	1.58
2.24	0.0	2.98	1.33
3.73	0.0	5.16	1.39
5.97	0.0	8.39	1.40
7.46	0.0	9.76	1.30
11.2	0.0	16.3	1.46
18.7	0.0	28.3	1.52
4.4	0.0	6.22	1.41
4.4	0.2	7.41	1.83[c]
4.4	0.3	11.1	2.75[c]
4.4	0.4	13.7	3.11[c]
4.4	0.5	37.2	8.45[c]

[a] $k = k_{obs}[H_2O_2]^{-1}$.

[b] Average value is $(1.42 \pm 0.10) \times 10^2\ M^{-1}\ s^{-1}$.

[c] Not used in computing average or least squares fit.

Table I-7. Kinetic data for the reaction of $Co(dpnH)^{+}$ with H_2O_2. Conditions: $[Co(dpnH)^{+}] = 1.0 \times 10^{-4}$ M, $[H^{+}] = 0.05$ M, $\mu = 0.10$ M, T = 25° C, $\lambda = 505$ nm

$10^2[H_2O_2]$	k_{obs}/s^{-1}	$10^{-2}k/M^{-1}\ s^{-1}$ [a,b]
0.24	1.18	4.92
0.34	1.49	4.42
0.48	2.32	4.79
0.97	4.36	4.48
1.47	6.76	4.61
1.96	8.83	4.52
2.45	11.3	4.62

[a] $k = k_{obs}[H_2O_2]^{-1}$.

[b] Average value is $(4.62 \pm 0.18) \times 10^2\ M^{-1}\ s^{-1}$.

Table I-8. Kinetic data for the reaction of $Co(dmgH)_2$ with H_2O_2. Conditions: $[Co(dmgH)_2] = 6.0 \times 10^{-5}$ M, $\mu = 0.10$ M $NaC_2H_3O_2$, T = 25° C, λ = 460 nm

$10^3[H_2O_2]/M$	k_{obs}/s^{-1}	$10^{-3}k/M^{-1}\ s^{-1}$ [a,b]
0.46	1.01	2.20
0.46	1.04	2.26
1.20	2.46	2.05
1.20	2.39	1.99[c]
2.42	4.43	1.83
2.42	4.14	1.71[d]
2.42	4.39	1.81[e]
3.64	6.47	1.78
4.38	7.67	1.75
4.86	8.59	1.77

[a] $k = k_{obs}[H_2O_2]^{-1}$.

[b] Average value is $(1.92 \pm 0.20) \times 10^3\ M^{-1}\ s^{-1}$.

[c] Run contained 10% t-butanol.

[d] Run contained 8×10^{-5} M $dmgH_2$.

[e] Run contained 4×10^{-5} M Co^{2+}.

Table I-9. Kinetic data for the reaction of B_{12r} with H_2O_2. Conditions: $[B_{12r}] = 5.0 \times 10^{-5}$ M, $\mu = [H^+] = 0.10$ M, $T = 25°$ C, $\lambda = 468$ nm

$10^2[H_2O_2]/M$	k_{obs}/s^{-1}	$10^{-2}k/M^{-1}\ s^{-1}$ [a,b]
0.49	0.62	1.27
0.98	1.47	1.50
2.94	3.80	1.29
4.89	6.33	1.29
6.85	8.98	1.31
7.83	9.96	1.27
9.79	13.2	1.34

[a] $k = k_{obs}[H_2O_2]^{-1}$.

[b] Average value is $(1.32 \pm 0.08) \times 10^2\ M^{-1}\ s^{-1}$.

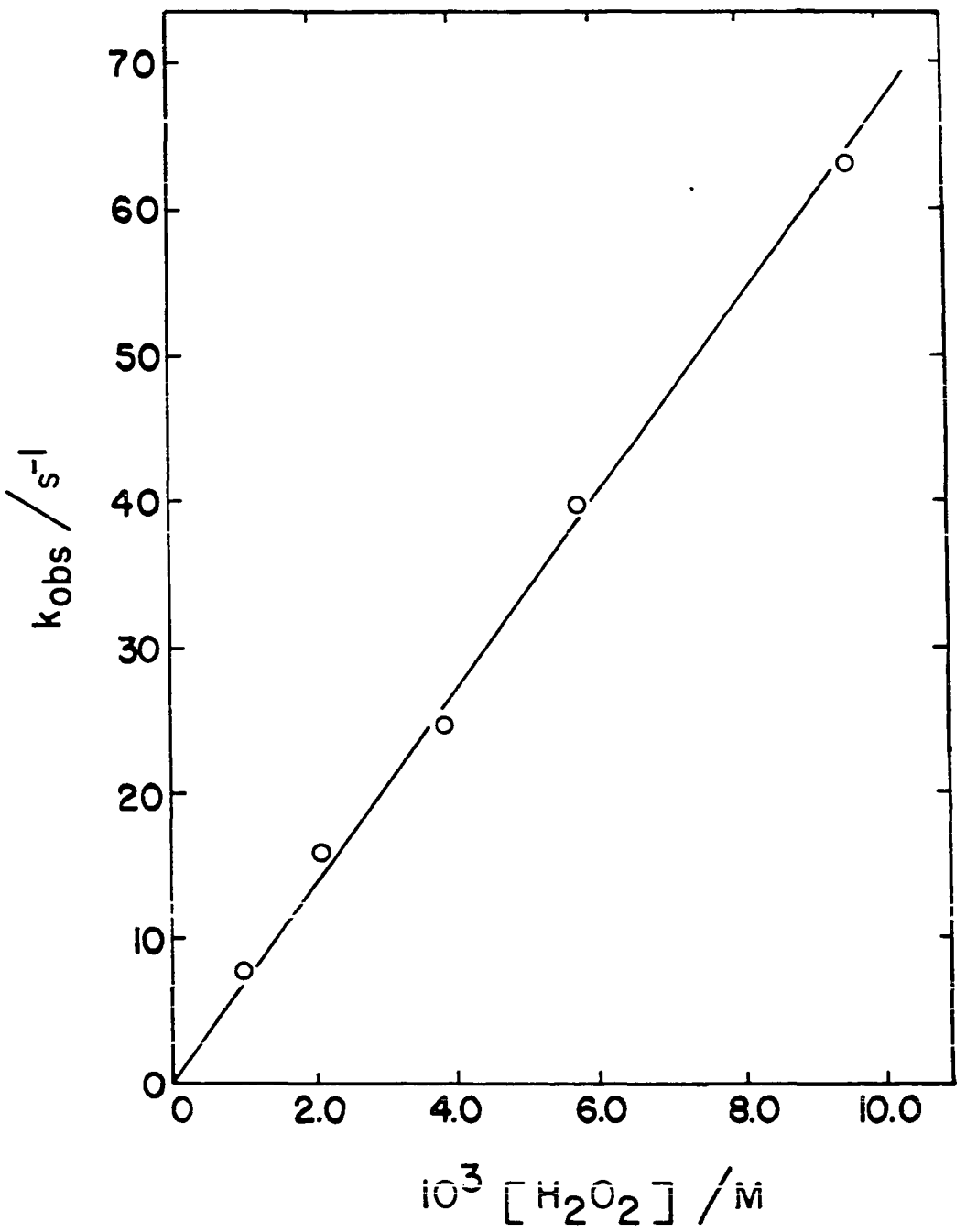

Figure I-18. The dependence of k_{obs} on $[H_2O_2]$ for the reaction of $Co([14]ane)^{2+}$ with H_2O_2

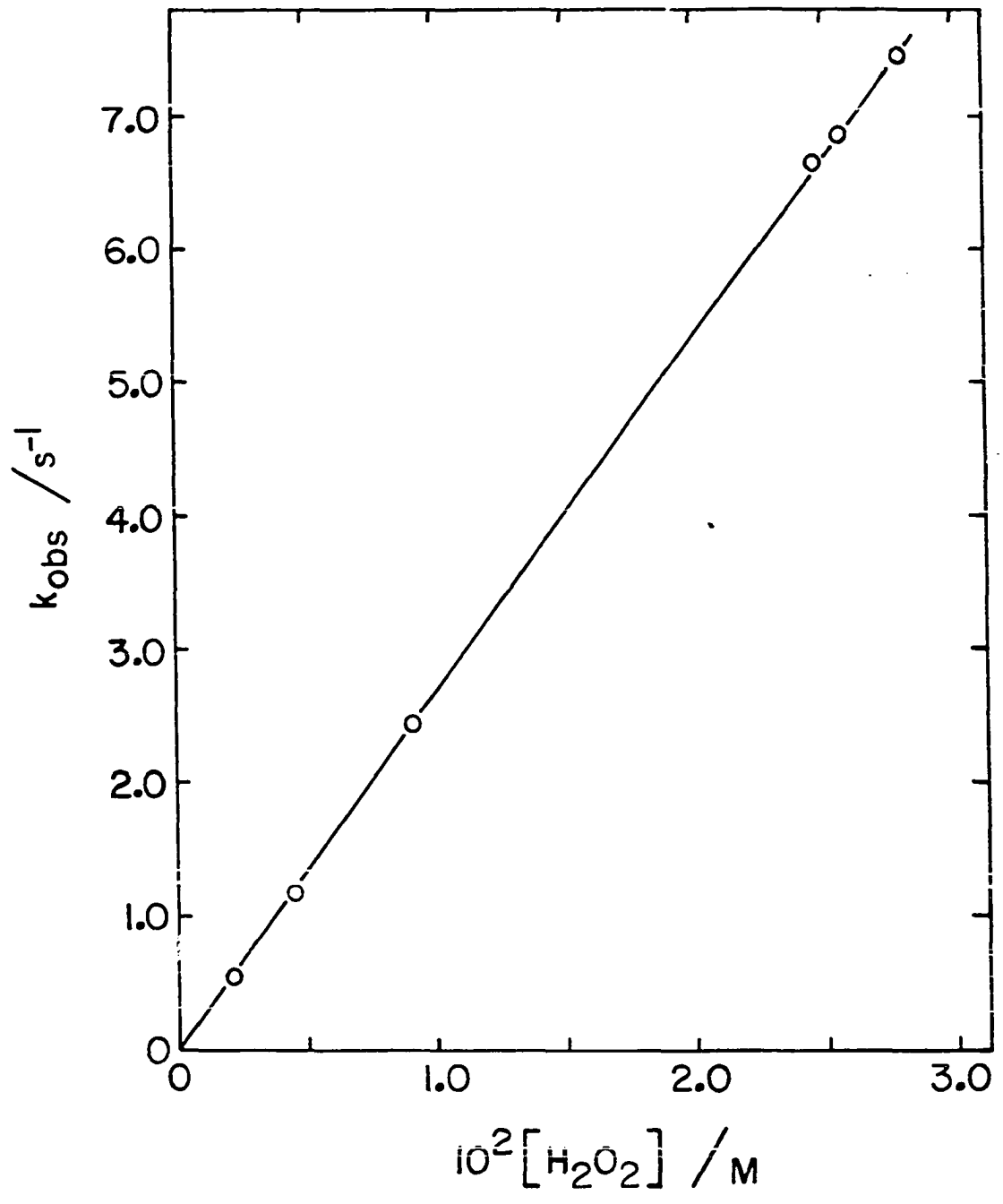

Figure I-19. The dependence of k_{obs} on $[H_2O_2]$ for the reaction of Co(meso-Me_6[14]ane)$^{2+}$ with H_2O_2

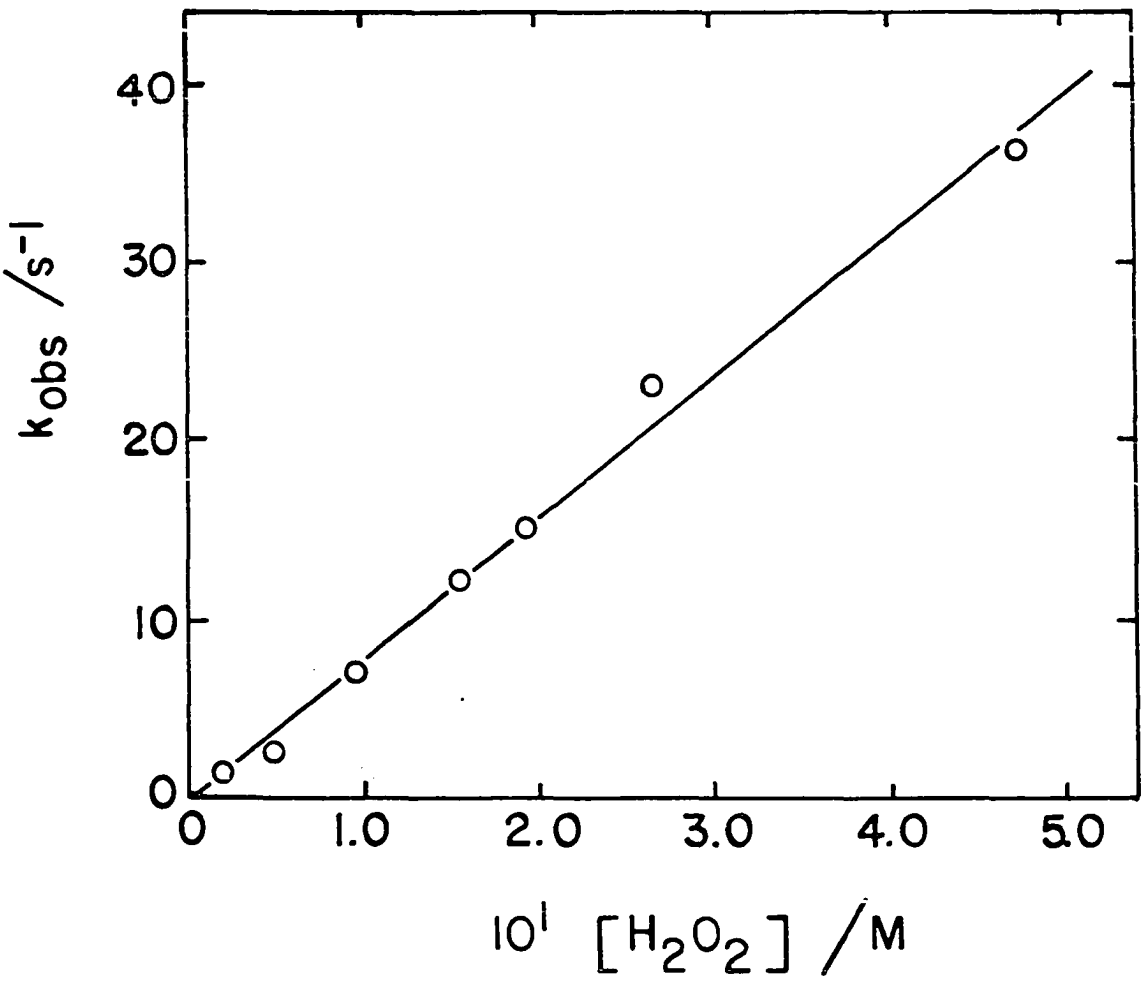

Figure I-20. The dependence of k_{obs} on $[H_2O_2]$ for the reaction of $Co(Me_6\text{-}4,11\text{-diene})^{2+}$ with H_2O_2

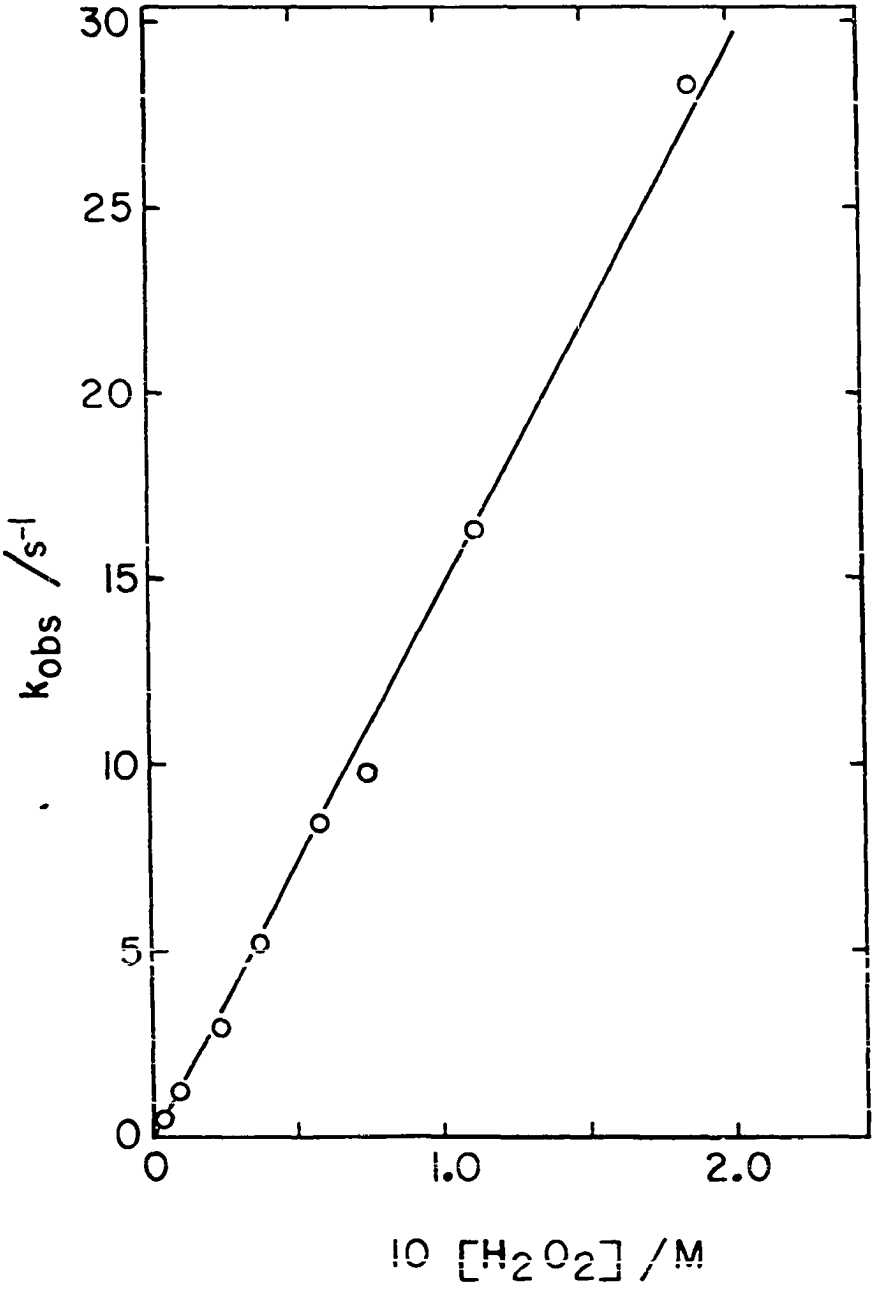

Figure I-21. The dependence of k_{obs} on $[H_2O_2]$ for the reaction of $Co(tim)^{2+}$ with H_2O_2

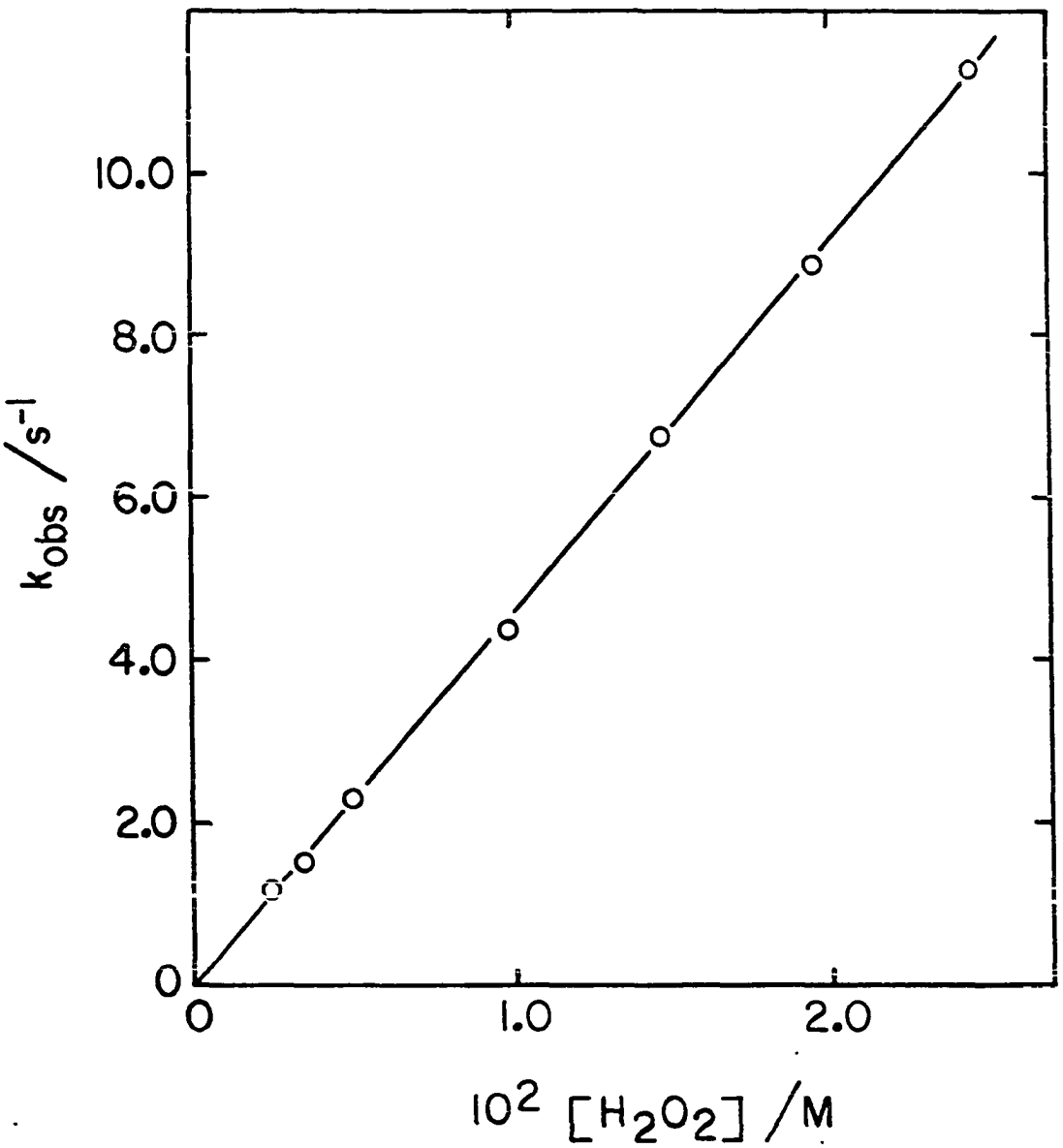

Figure I-22. The dependence of k_{obs} on $[H_2O_2]$ for the reaction of $Co(dpnH)^+$ with H_2O_2

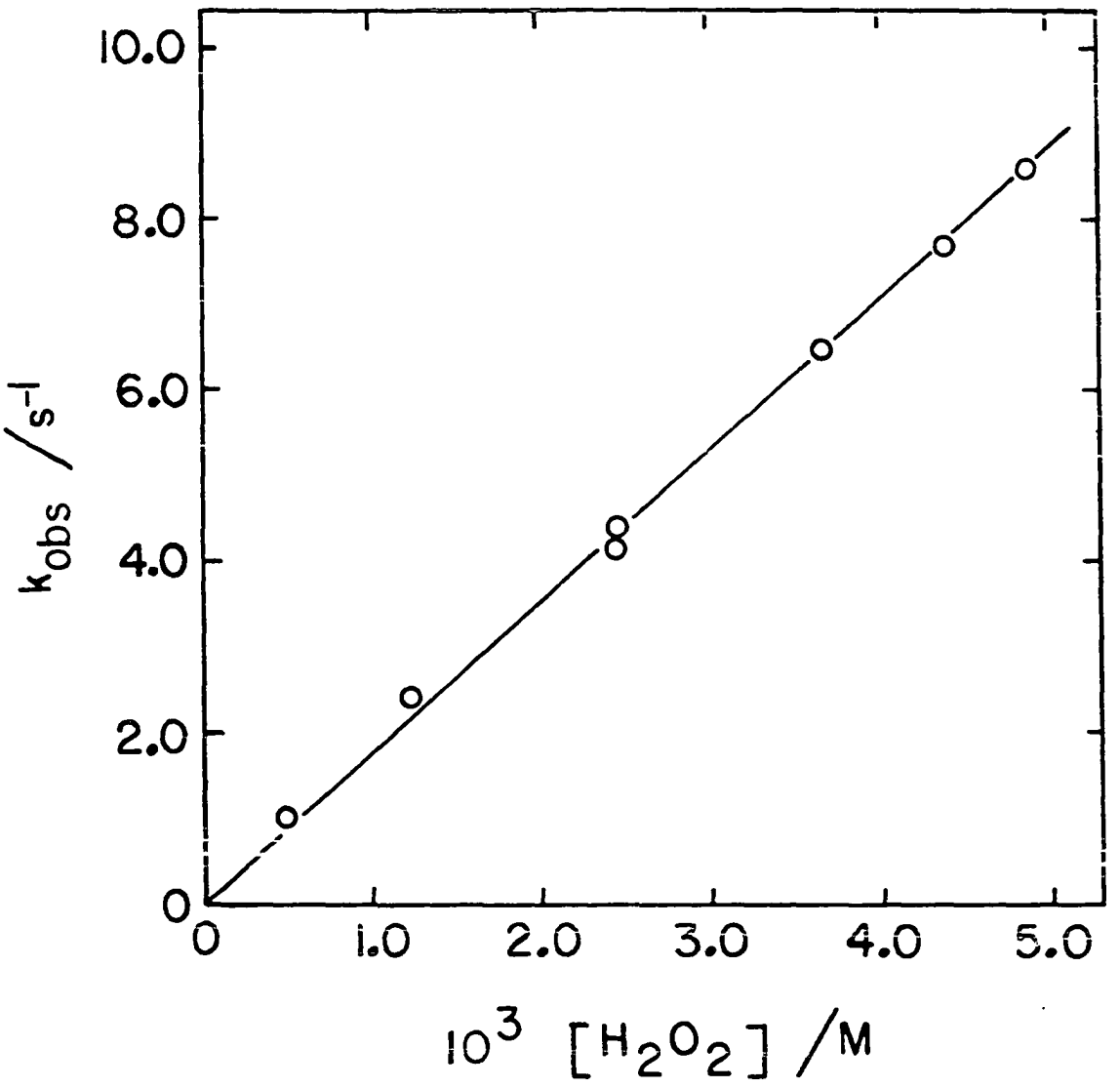

Figure I-23. The dependence of k_{obs} on $[H_2O_2]$ for the reaction of $Co(dmgH)_2$ with H_2O_2

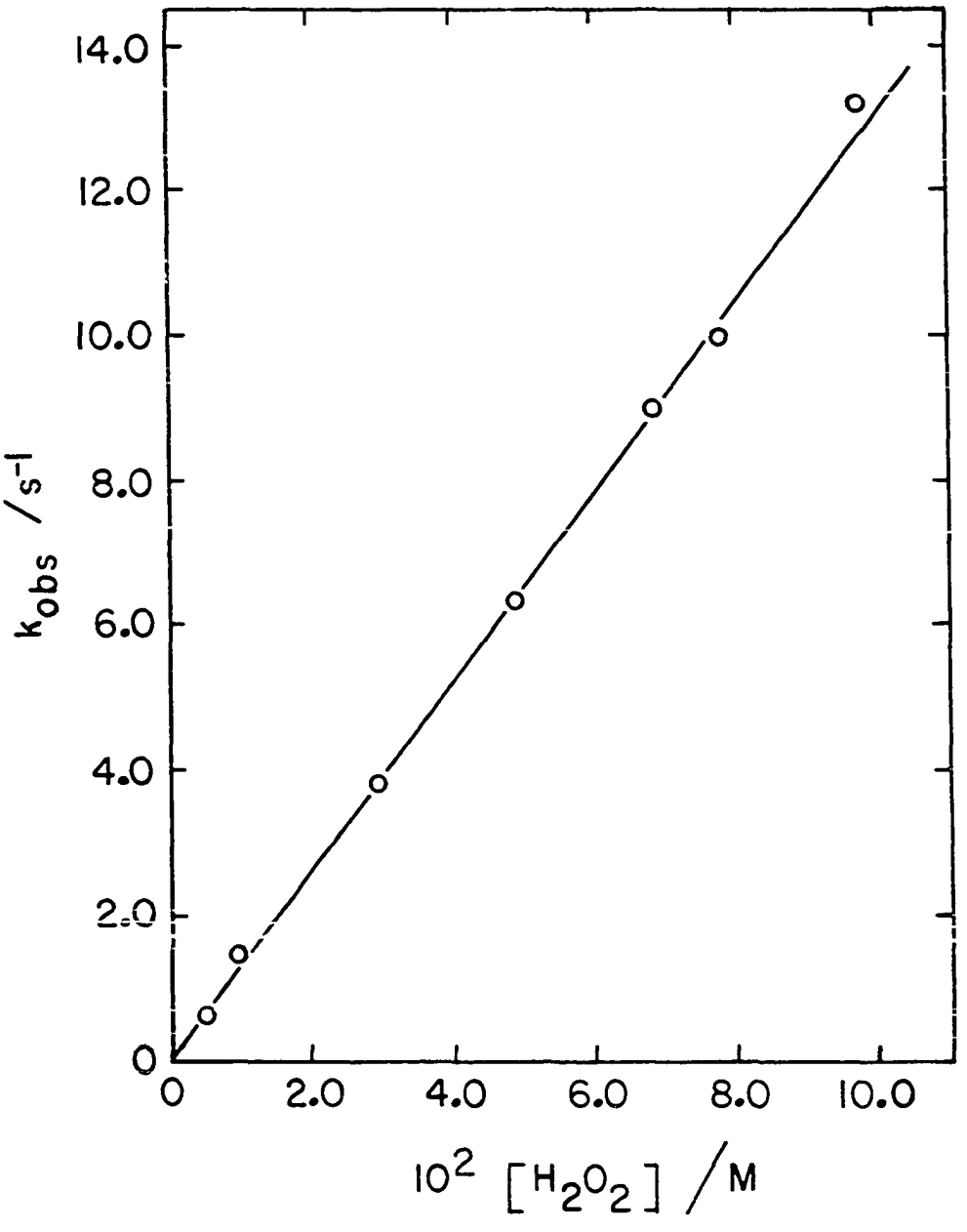

Figure I-24. The dependence of k_{obs} on $[H_2O_2]$ for the reaction of B_{12r} with H_2O_2

can therefore be written as in Equation I-43. The factor of n in the

$$-\frac{d[Co(II)]}{dt} = nk[Co(II)][H_2O_2] \qquad (I-43)$$

rate law is the stoichiometric correction. Since the stoichiometry of the $Co([14]ane)^{2+}$ reaction with H_2O_2 is 2:1, n must equal 2. Therefore, the plot of k_{obs} versus $[H_2O_2]$ gives slope = 2k or k = ½(slope) = (3.75 ± 0.53) x 10^3 M^{-1} s^{-1}. For all other complexes, where n = 1, rate constants of 267 ± 1 ($Co(meso\text{-}Me_6[14]ane)^{2+}$), 75.4 ± 3.2 ($Co(Me_6\text{-}4,11\text{-}diene)^{2+}$), 141 ± 3 ($Co(tim)^{2+}$), 461 ± 7 ($Co(dpnH)^{+}$), (1.78 ± 0.06) x 10^3 ($Co(dmgH)_2$), and 131 ± 1 M^{-1} s^{-1} (B_{12r}) were obtained.

The effect of added Br^-, which should act as a hydroxyl radical scavenger, is also noted in Tables I-5 and I-6 for the hydrogen peroxide reactions with $Co(Me_6\text{-}4,11\text{-}diene)^{2+}$ and $Co(tim)^{2+}$. The increase in the pseudo-first-order rate constant is most likely due to a Br^- catalyzed reaction path.

Reactions of Br_2

Stoichiometry

Reaction stoichiometries were found to be 2:1 Co(II):Br_2 for the bromine reactions with $Co([14]ane)^{2+}$ (Figure I-25), $Co(Me_6\text{-}4,11\text{-}diene)^{2+}$ (Figure I-26), and $Co(tim)^{2+}$ (Figure I-27). The complexes $Co(meso\text{-}Me_6[14]ane)^{2+}$ and $Co(dpnH)^{+}$ were presumed to react similarly. The stoichiometry of the B_{12r}—Br_2 reaction was unclear since rapid subsequent reactions occurred (see below).

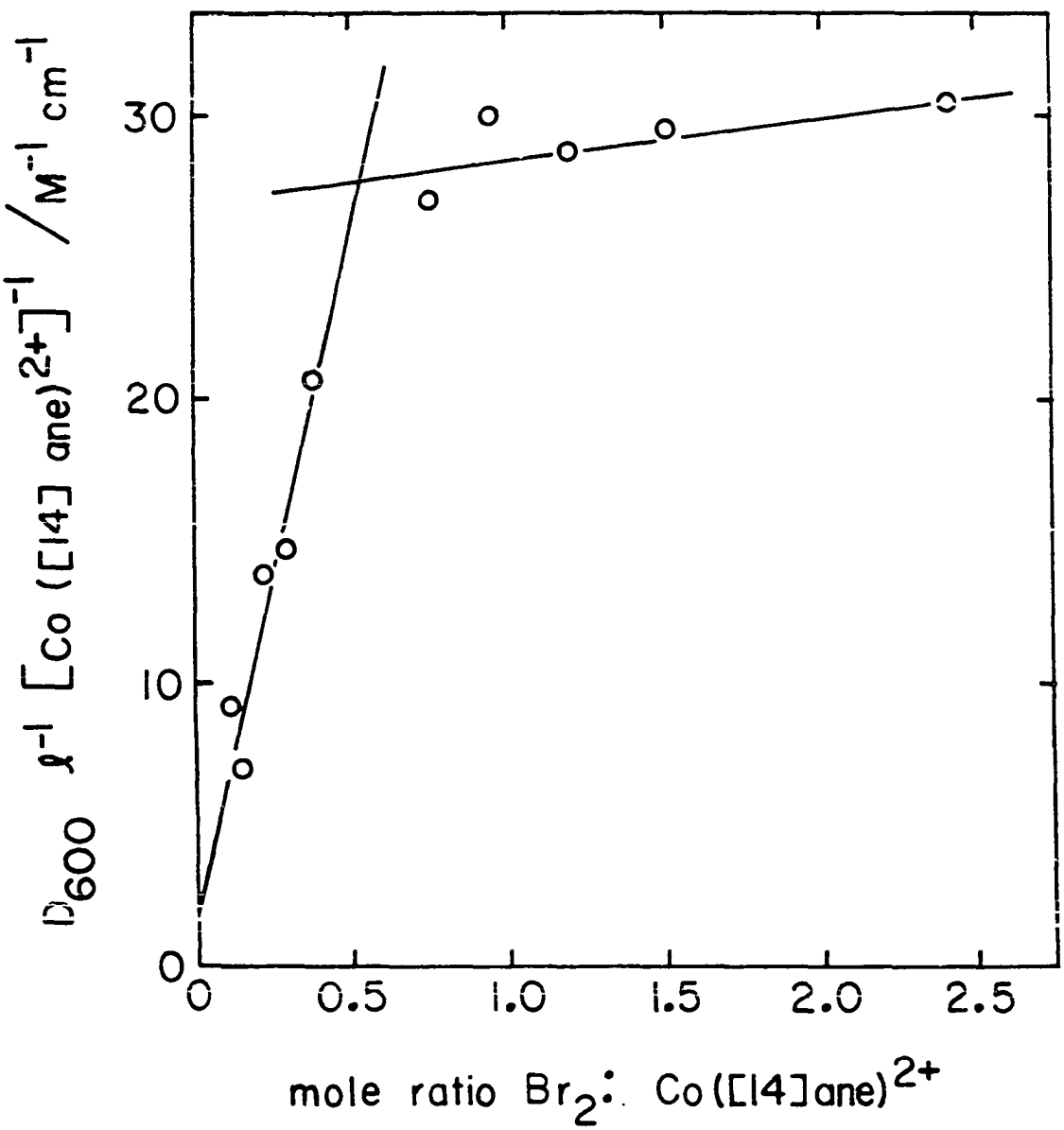

Figure I-25. Spectrophotometric titration of Co([14]ane)$^{2+}$ with Br_2

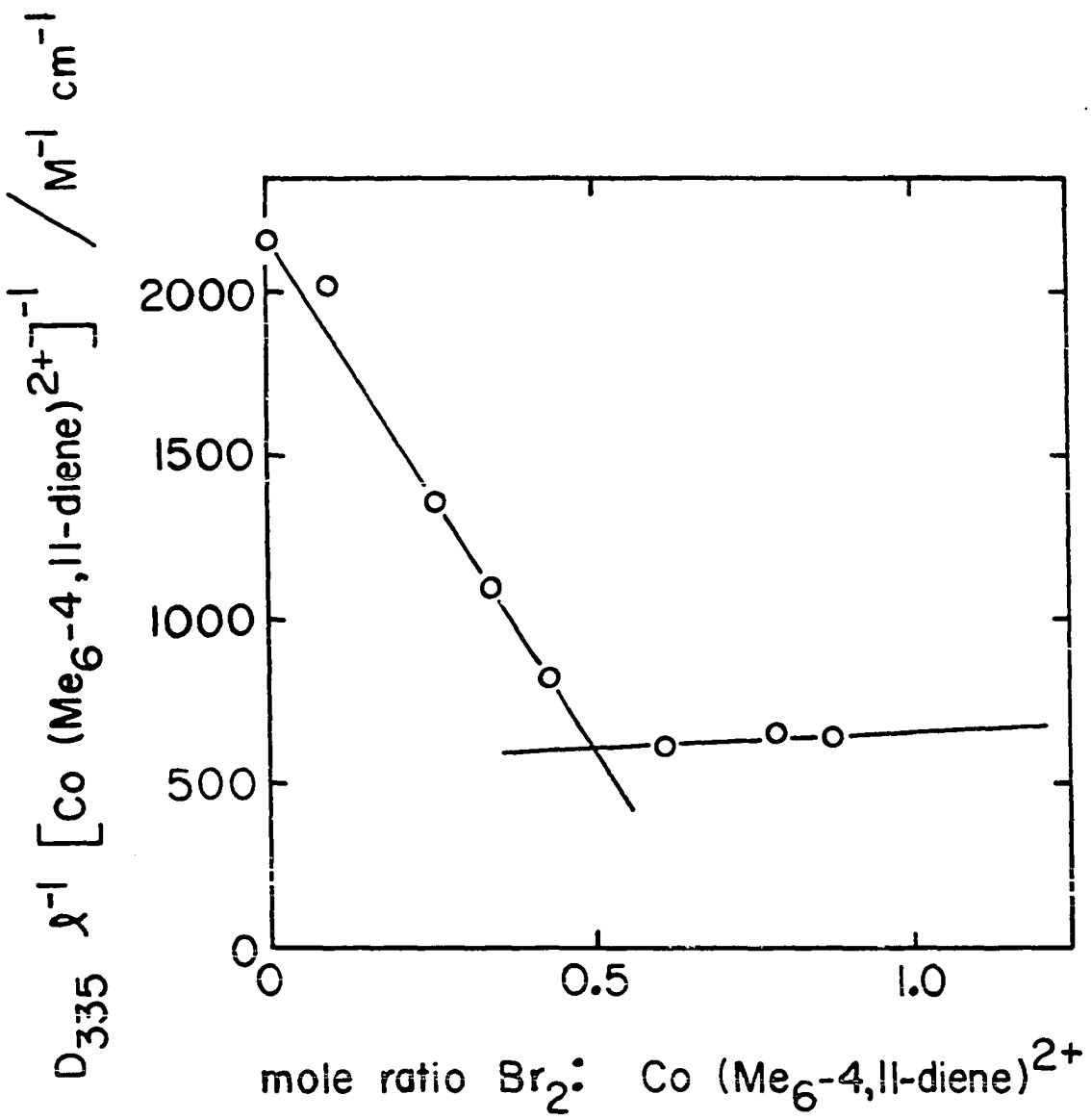

Figure I-26. Spectrophotometric titration of Co(Me_6-4,11-diene)$^{2+}$ with Br_2

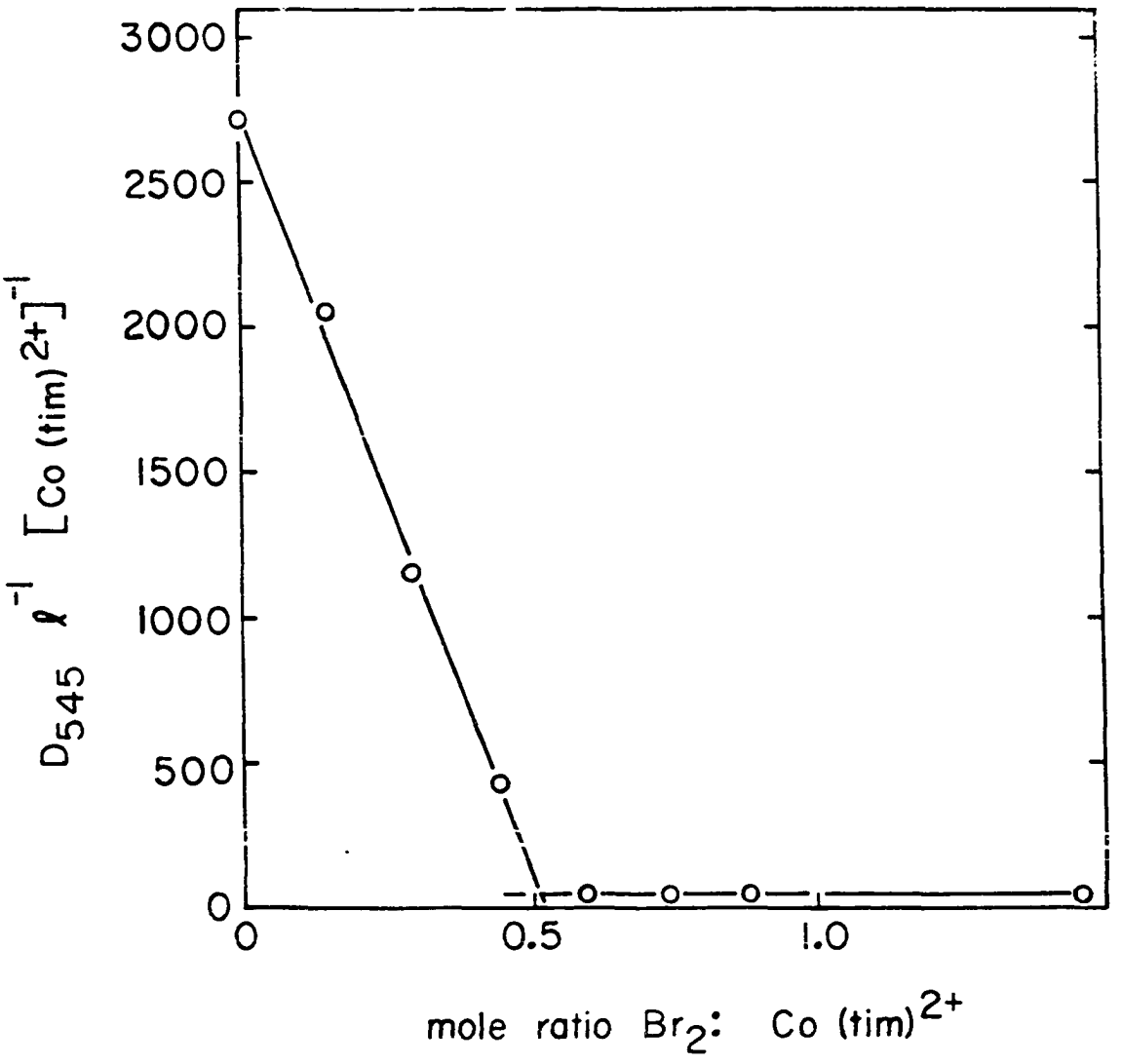

Figure I-27. Spectrophotometric titration of $Co(tim)^{2+}$ with Br_2

Products of reaction

Little information is available in the literature on the electronic spectra of aquobromo Co(III) complexes. Therefore, conclusions as to the identity of reaction products were based largely on differences between observed product spectra and spectra of other known compounds which could be possible products (e.g., the diaquo derivatives), and on subsequent reactions which could be attributed to aquation of a monobromo species. Table I-1 shows the principal spectral features of the initial bromination products. Due to the extreme acid lability of $Co(dmgH)_2$ and the necessity of keeping the Br_2 in acidic media, the $Co(dmgH)_2$—Br_2 reaction was not studied.

Bromine was reduced by $Co([14]ane)^{2+}$ to give a product with absorption bands at 610 and 450 (sh) nm. The difference between this spectrum and that of $Co([14]ane)(H_2O)_2^{3+}$ suggested that a brominated product was indeed formed, which was tentatively formulated as $BrCo([14]ane)(H_2O)^{2+}$.

The reaction of $Co(meso\text{-}Me_6[14]ane)^{2+}$ with Br_2 produced an initial product spectrum with maxima at 640 and 360 (sh) nm. The initial product then slowly decayed to a final stable product. Spectral scans during the second-stage reaction showed isosbestics at 610 and 500 nm, and the final spectrum had a maximum at 555 nm ($\varepsilon \simeq 47\ M^{-1}\ cm^{-1}$). Because of the similarity to the spectrum of $Co([14]ane)(H_2O)_2^{3+}$ the final product was formulated as $Co(meso\text{-}Me_6[14]ane)(H_2O)_2^{3+}$ and the product of the first-stage reaction as $BrCo(meso\text{-}Me_6[14]ane)(H_2O)^{2+}$.

The reaction of $Co(Me_6\text{-}4,11\text{-}diene)^{2+}$ with Br_2 was very similar to that of $Co(meso\text{-}Me_6[14]ane)^{2+}$. A two-stage reaction was observed with

the initial product spectrum showing maxima at 625 and 363 nm and the final product spectrum showing maxima at 570 and 400 (sh) nm. Even though no literature spectra are available for $BrCo(Me_6\text{-}4,11\text{-diene})(H_2O)^{2+}$, a sequence of reactions such as that described for Co(meso-Me_6[14]ane)$^{2+}$ seems very likely.

The products of reaction of $Co(tim)^{2+}$ and $Co(dpnH)^{+}$ with Br_2 were characterized only to the extent that featureless visible spectra were obtained upon reaction. The monobrominated compounds $BrCo(tim)(H_2O)^{2+}$ and $BrCo(dpnH)(H_2O)^{+}$ were the presumed products.

The oxidation of B_{12r} by Br_2 was the least well-behaved of all reactions studied. Addition of less than twice equimolar amounts of Br_2 to a 6.65×10^{-5} M solution of B_{12r} gave product spectra similar to the spectrum of B_{12a} (λ at 535, 515, 410, and 350 nm) (Figure I-28). However, upon addition of further excess of Br_2 very rapid decay of the B_{12a} spectral features was observed. At $[B_{12r}] = 6.65 \times 10^{-5}$ M and $[Br_2] = 5.67 \times 10^{-4}$ M maxima were seen at 530 (sh), 475, 450 (sh), 390 (sh), and 350 nm with apparent ε values of 1080, 2510, 2030, 2750, and 3700, respectively. Similarly, reaction of 6.65×10^{-5} M B_{12a} with 5.67×10^{-4} M Br_2 gave slow ($\simeq$ two hours) decay to a spectrum with maxima at 550, 470, 380 (sh), and 350 nm (Figure I-29), with apparent molar absorptivities of 950, 1470, 2350, and 3260 M^{-1} cm^{-1}, respectively. The most plausible explanation of these observations is that B_{12r} reacts with Br_2 to give initially bromocobalamin which rapidly aquates to B_{12a}. The bromocobalamin which might be expected to have been produced initially would not have been seen due to its known rapid aquation to B_{12a}

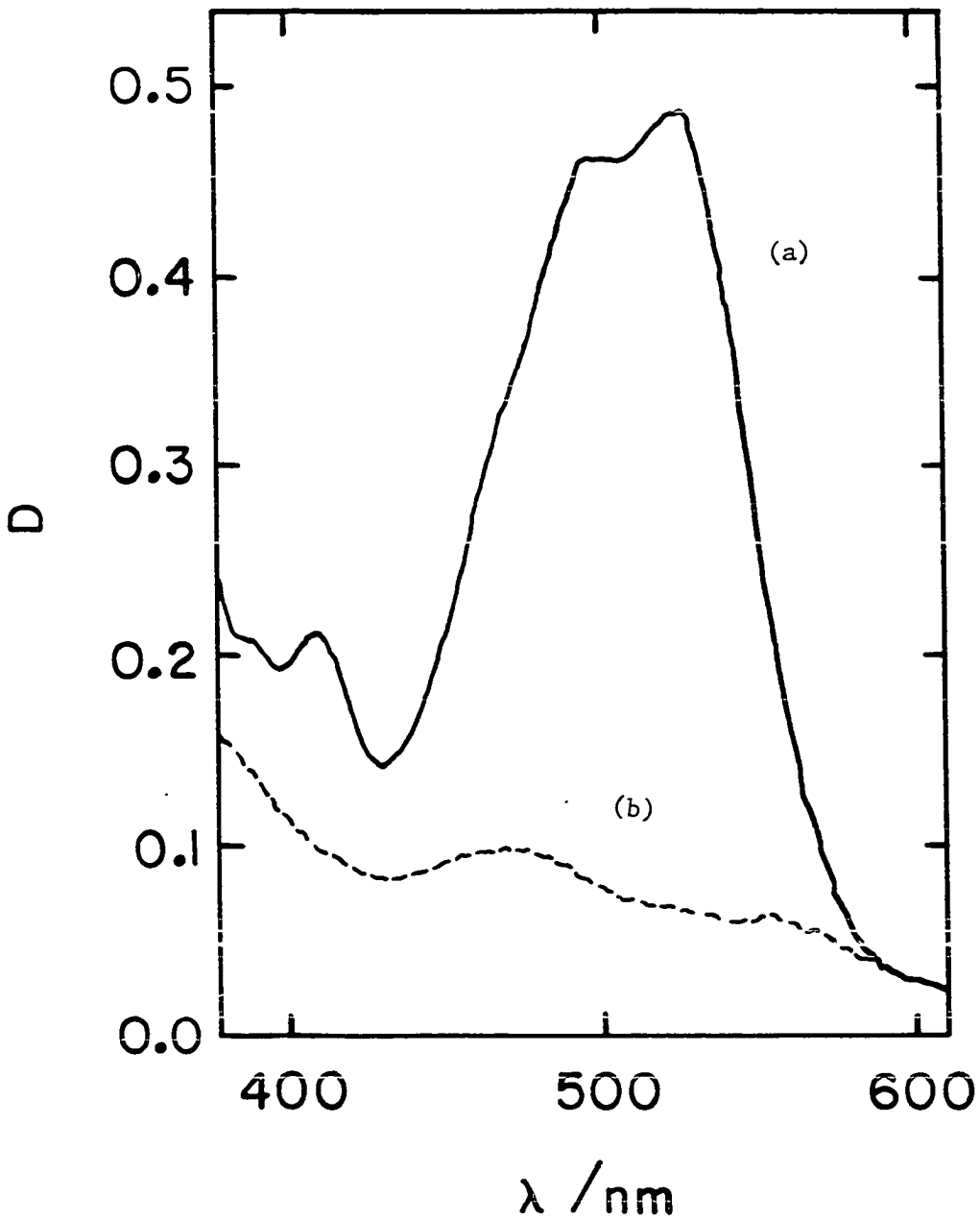

Figure I-28. The electronic spectrum of the products of the reaction of 6.7×10^{-5} M B_{12r} with (a) 1.1×10^{-4} M Br_2 and (b) 5.7×10^{-4} M Br_2

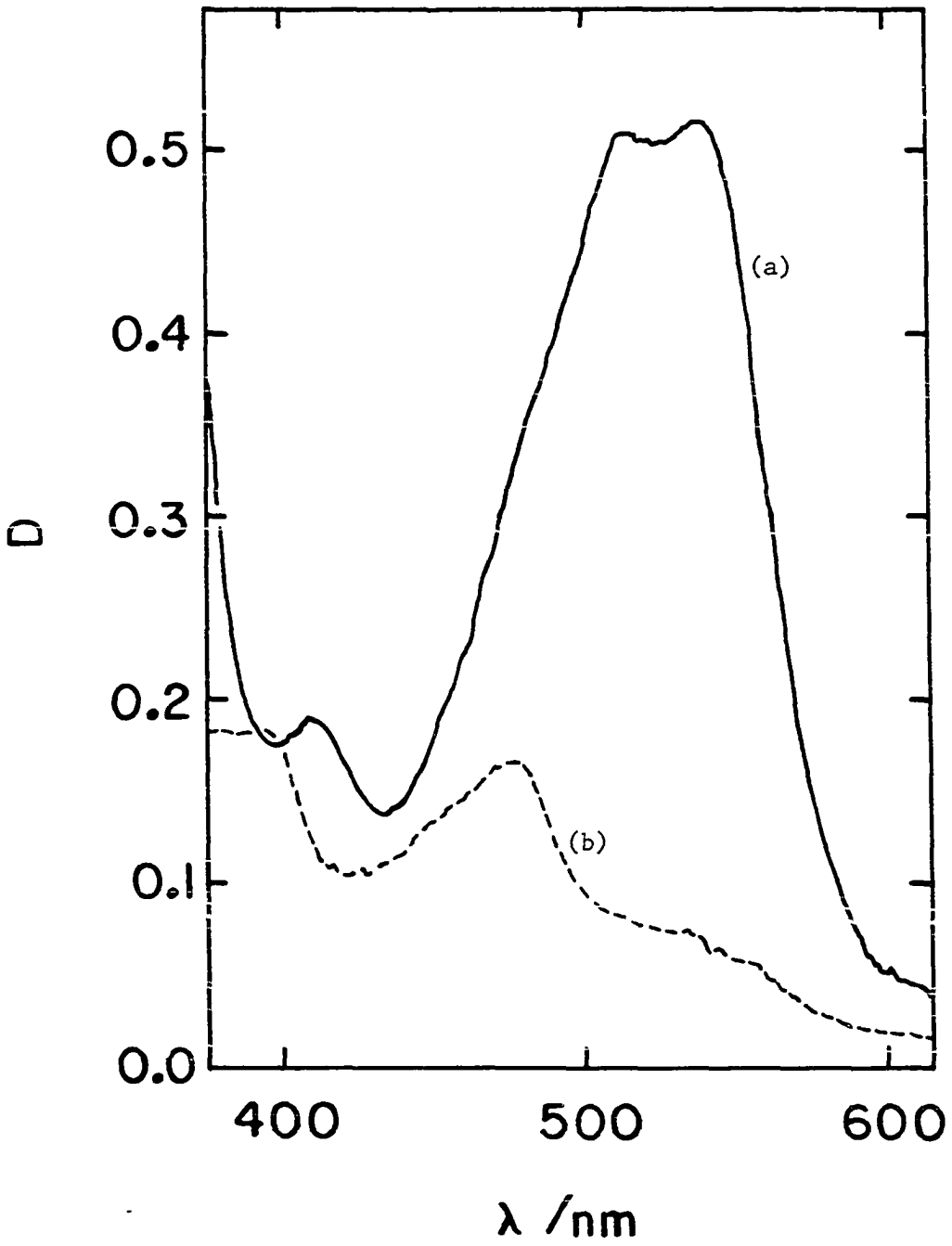

Figure I-29. The electronic spectrum of the products of the reaction of 6.7×10^{-5} M B_{12a} with 5.7×10^{-4} M Br_2 at (a) mixing and (b) two hours

($k = 590\ s^{-1}$) (53). The B_{12a} then reacts with Br_2 in a Br^- or $Br\cdot$ catalyzed reaction to yield a modified chromophore.

Kinetics

The bromination of $Co([14]ane)^{2+}$ was found to be extremely fast. No exponential traces were seen on the stopped-flow spectrophotometer when equal volumes of 1.00×10^{-4} M $Co([14]ane)^{2+}$ and 6.54×10^{-5} M Br_2 were mixed ($\mu = [H^+] = 0.10$ M). Since the mixing time of the instrument was 3-5 ms the half-life for reaction must have been less than 3 ms. A lower limit for the second-order rate constant was then estimated from Equation I-31 to be $k > 1 \times 10^7\ M^{-1}\ s^{-1}$, where a = 2, b = 1 for $A_o = [Co([14]ane)^{2+}]$, $B_o = [Br_2]$.

The reaction of $Co(meso\text{-}Me_6[14]ane)^{2+}$ with Br_2 was found to give good first-order kinetic traces when studied with a pseudo-first-order excess of Br_2. Rate constants are given in Table I-10. A plot of k_{obs} versus Br_2 (Figure I-30) was linear with a zero intercept and $k = \frac{1}{2}(\text{slope}) = (4.93 \pm 0.24) \times 10^4\ M^{-1}\ s^{-1}$. The rate law consistent with these results is given in Equation I-44. Two runs at $\mu = [H^+] = 0.05$ M

$$-\frac{d[Co(II)]}{dt} = 2k[Co(II)][Br_2] \qquad (I\text{-}44)$$

showed the lack of effect of variations in acidity and ionic strength on the first-stage rate constant. As noted above a slow second-stage reaction, identified as an aquation reaction, was also observed. One preliminary kinetic run at $[BrCo(meso\text{-}Me_6[14]ane)(H_2O)^{2+}] = 2.3 \times 10^{-4}$ M, $[H^+] = 0.007$ M, T = 25° C, $\lambda = 360$ nm gave $k_{obs} = 1.4 \times 10^{-3}\ s^{-1}$.

Table I-10. Kinetic data for the reaction of $Co(meso\text{-}Me_6[14]ane)^{2+}$ with Br_2. Conditions: $[Co(meso\text{-}Me_6[14]ane)^{2+}] = (0.7 - 1.2) \times 10^{-4}$ M, $[H^+] = 0.10$ M, $\mu = 1.0$ M, T = 25° C, $\lambda = 300$ nm

$10^3[Br_2]/M$	k_{obs}/s^{-1}	$10^{-4}k/M^{-1}\ s^{-1}$ [a,b]
0.17	21.9	6.44
0.28	30.3	5.41
0.29	30.3	5.22
0.51	52.6	5.15
0.71	71.0	5.00[c]
0.95	100	5.26
1.33	128	4.81
1.45	134	4.68[c]

[a] $k = \frac{1}{2}k_{obs}[Br_2]^{-1}$.

[b] Average value is $(5.25 \pm 0.54) \times 10^4\ M^{-1}\ s^{-1}$.

[c] Runs done at $\mu = [H^+] = 0.05$ M, $\lambda = 360$ nm.

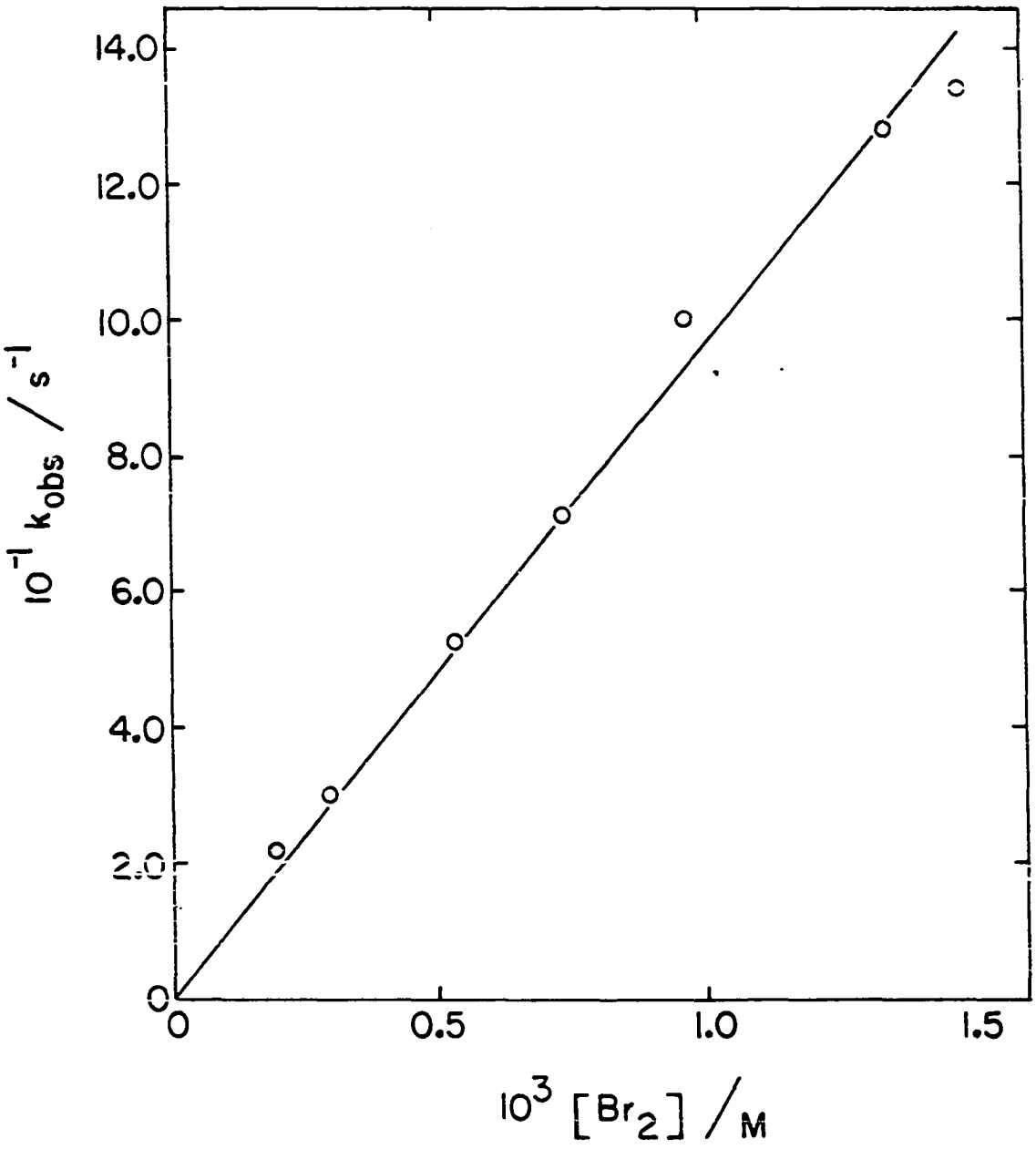

Figure I-30. The dependence of k_{obs} on $[Br_2]$ for the reaction of $Co(meso\text{-}Me_6[14]ane)^{2+}$ with Br_2

The complex $Co(Me_6\text{-}4,11\text{-diene})^{2+}$ reacted very similarly with Br_2. The fast first-stage reaction was found to follow Equation I-44. Pseudo-first-order rate constants and the conditions of the study are given in Table I-11. The second-order rate constant obtained from a plot of k_{obs} versus $[Br_2]$ (Figure I-31) was $(1.70 \pm 0.21) \times 10^4\ M^{-1}\ s^{-1}$. Again, no influence of acidity or ionic strength was seen. Three runs were done to gain information on the second-stage reaction. A run at $[BrCo(Me_6\text{-}4,11\text{-diene})(H_2O)^{2+}] = 0.69 \times 10^{-4}$ M, $[H^+] = 0.10$ M (formed by reaction of 1.54×10^{-3} M Br_2 with 0.69×10^{-4} M $Co(Me_6\text{-}4,11\text{-diene})^{2+}$) gave a rate constant of $6.81 \times 10^{-4}\ s^{-1}$. A solution of $BrCo(Me_6\text{-}4,11\text{-diene})(H_2O)^{2+}$ prepared from reaction of 9.87×10^{-4} M Br_2 and 7.62×10^{-4} M $Co(Me_6\text{-}4,11\text{-diene})^{2+}$ in 0.10 M $HClO_4$ gave an aquation rate constant of $6.25 \times 10^{-4}\ s^{-1}$ after the excess Br_2 had been flushed out of the reaction cell by a vigorous stream of N_2. Thus, the independence of the rate constant with respect to the presence of excess halogen was demonstrated. One run at $[BrCo(Me_6\text{-}4,11\text{-diene})(H_2O)^{2+}] = 2.8 \times 10^{-4}$ M, $[H^+] = 0.014$ M gave $k_{obs} = 1.1 \times 10^{-3}\ s^{-1}$ which showed that the second-stage reaction rate was inversely dependent on acid concentration. Such inverse acid concentration dependence is very characteristic of aquation reactions of metal complexes.

Table I-12 gives results of kinetic studies for the reaction of $Co(tim)^{2+}$ with Br_2 and Figure I-32 shows a plot of k_{obs} versus $[Br_2]$. The value of k from the plot is $(1.03 \pm 0.21) \times 10^6\ M^{-1}\ s^{-1}$.

The reaction of $Co(dpnH)^+$ with Br_2 was too fast to be studied either under pseudo-first-order or a range of second-order conditions.

Table I-11. Kinetic data for the reaction of $Co(Me_6\text{-}4,11\text{-diene})^{2+}$ with Br_2. Conditions: $[Co(Me_6\text{-}4,11\text{-diene})^{2+}] = (0.7 - 1.7) \times 10^{-4}$ M, $[H^+] = 0.10$ M, $\mu = 1.0$ M, T = 25° C, $\lambda = 350$ nm

$10^3[Br_2]/M$	k_{obs}/s^{-1}	$10^{-4}k/M^{-1}\ s^{-1}$ [a,b]
0.31	9.24	1.49
0.49	12.8	1.31
0.65	23.9	1.85
0.68	21.5	1.58[c]
1.36	56.4	2.07[c]
1.89	70.0	1.85
2.43	102	2.10
2.93	135	2.30
3.15	108	1.70

[a] $k = \frac{1}{2}k_{obs}[Br_2]^{-1}$.

[b] Average value is $(1.81 \pm 0.32) \times 10^4\ M^{-1}\ s^{-1}$.

[c] Runs done at $\mu = [H^+] = 0.05$ M, $\lambda = 360$ nm.

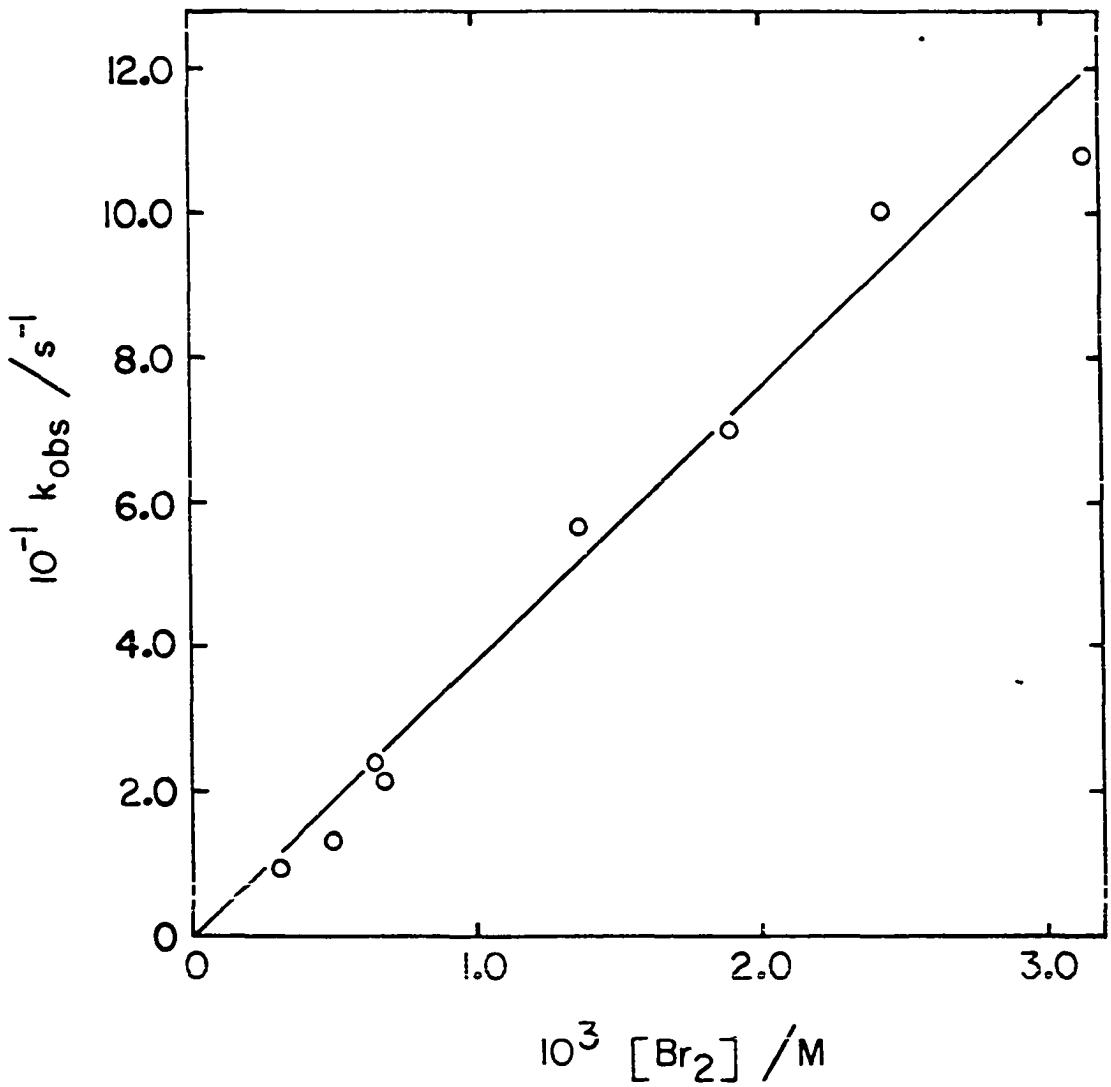

Figure I-31. The dependence of k_{obs} on [Br_2] for the reaction of Co(Me_6-4,11-diene)$^{2+}$ with Br_2

Table I-12. Kinetic data for the reaction of $Co(tim)^{2+}$ with Br_2. Conditions: $[Co(tim)^{2+}] = (0.6 - 1.7) \times 10^{-5}$ M, $\mu = [H^+] = 0.10$ M, T = 25° C, λ = 545 nm

$10^4[Br_2]/M$	k_{obs}/s^{-1}	$10^{-6}k/M^{-1}\ s^{-1}$ [a,b]
0.19	60.7	1.60[c]
0.24	33.5	0.70
0.42	104	1.24
0.50	119	1.19
0.50	171	1.71
1.30	254	0.98
1.33	166	0.62[c]
1.53	309	1.01
2.23	470	1.05
3.42	526	0.77[c]

[a] $k = \frac{1}{2}k_{obs}[Br_2]^{-1}$.

[b] Average value is $(1.13 \pm 0.31) \times 10^6\ M^{-1}\ s^{-1}$.

[c] Run not included in computation of average or least squares fit.

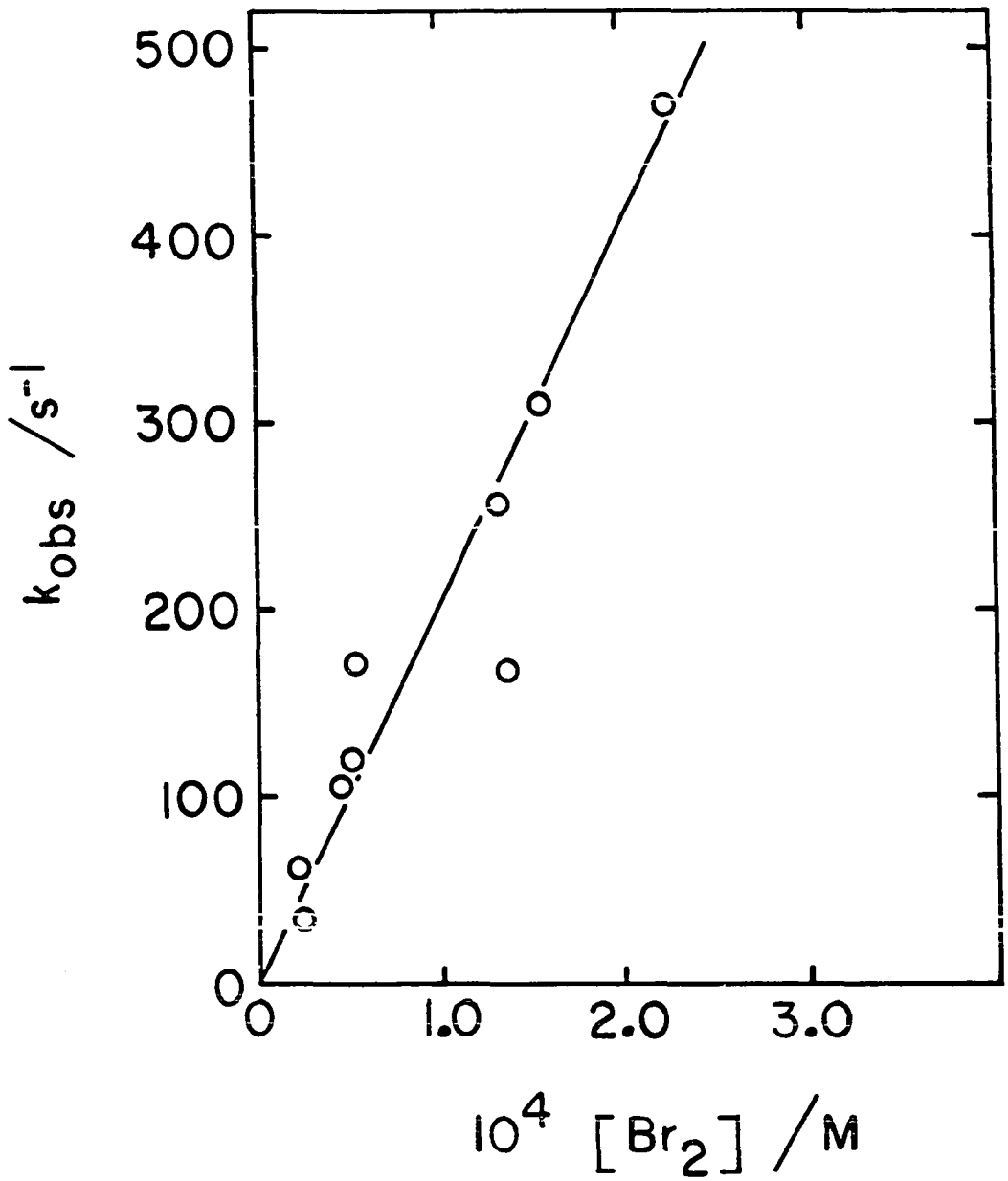

Figure I-32. The dependence of k_{obs} on [Br_2] for the reaction of $Co(tim)^{2+}$ with Br_2

Two identical runs at $[Co(dpnH)^{+}]$ = 1.03 x 10^{-5} M, $[Br_2]$ = 0.76 x 10^{-5} M, $[H^{+}]$ = 0.05 M, μ = 0.10 M, followed at 505 nm gave half-lives of 2.8 and 4 ms, which corresponded to second-order rate constants of 3.8 x 10^{7} and 2.9 x 10^{7} M^{-1} s^{-1} (using Equation I-31, a = 2, b = 1). Considering the noise in the traces and the inherent error in measuring second-order rates on a stopped-flow system, the above values can only be considered to be an approximation and/or a lower limit of the true value of k.

Similarly, the rate of the B_{12r}—Br_2 reaction could only be approximated. When followed at 350 nm, reaction conditions of $[B_{12r}]$ = 1.43 x 10^{-5} M, $[Br_2]$ = 0.38 x 10^{-5} M, and $[B_{12r}]$ = 2.85 x 10^{-5} M, $[Br_2]$ = 0.76 x 10^{-5} M, in 0.10 M $HClO_4$ gave half-lives of 7 and 5 ms and second-order rate constants of 7.5 x 10^{6} and 5.3 x 10^{6} M^{-1} s^{-1}, respectively (using Equation I-31, a = 2, b = 1).

Reactions of I_2

Stoichiometry

Table I-13 shows the yield of $ICo([14]ane)(H_2O)^{2+}$ from the reaction of $Co([14]ane)^{2+}$ and I_2. In the runs shown, I_2 was essentially quantitatively converted to $ICo([14]ane)(H_2O)^{2+}$ indicating a stoichiometry of 2:1 $Co([14]ane)^{2+}$:I_2.

The reduction of one mole of I_2 was assumed to require two moles of $Co(meso\text{-}Me_6[14]ane)^{2+}$ or $Co(Me_6\text{-}4,11\text{-}diene)^{2+}$. Unfortunately, because of the slowness of the two reactions and the subsequent aquation reactions, the assumption could not be confirmed.

Table I-13. Stoichiometry for the reaction of $Co([14]ane)^{2+}$ with I_2. Conditions: $\mu = [H^+] = 0.45$ M, $\lambda = 433$ nm

$10^4[Co(II)]/M$	$10^4[I_2]/M$	$10^4[ICo(III)]/M$	$\Delta[ICo(III)]/[I_2]$
6.67	2.29	4.53	1.98
8.33	2.84	5.57	1.96
8.33	2.20	4.16	1.89
13.3	2.29	4.21	1.84
16.7	2.84	5.07	1.79
16.7	2.20	4.10	1.86
16.7	2.29	4.67	2.04

The reaction of $Co(tim)^{2+}$ with I_2 was clearly shown to be 2:1 $Co(tim)^{2+}:I_2$ (Table I-14). The complex $Co(dpnH)^{+}$ was presumed to behave similarly.

Previous workers (34) have demonstrated a 2:1 stoichiometry for the B_{12r}—I_2 reaction. Their results were confirmed here (Table I-14).

Products of reaction

As with the Br_2 reactions, the reduction of I_2 by Co(II) complexes was expected to produce the aquoiodo derivative of Co(III). Also, as in the case of Br_2 little data has been published on the electronic spectra and properties of these compounds. Therefore, the identity of reaction products was convincingly demonstrated in the reaction of two of the complexes, strongly implied in two more, and presumed in the last two. Again, the $Co(dmgH)_2$—I_2 reaction was not studied due to the incompatibility of acidic and non-acidic media required for I_2 and $Co(dmgH)_2$, respectively.

The reduction of I_2 by $Co([14]ane)^{2+}$ gave a yellow product whose electronic spectrum showed a maximum at 433 nm (ε 1400 M^{-1} cm^{-1}). The product was isolable from excess of either starting material or uncomplexed Co^{2+} by ion exchange with 0.3 M $HClO_4$ on a Sephadex column. The product was shown to be different than $Co([14]ane)(H_2O)_2^{3+}$ by the distinct elution patterns of the two species, the diaquo complex eluting more slowly with 0.3 M $HClO_4$. A sample of the product in 0.3 M $HClO_4$ was photolyzed for 1½ hours with a high-intensity Hg lamp (Equation I-29). The I_2 produced (46) was swept out by a vigorous stream of N_2

Table I-14. Stoichiometry for the reactions of $Co(tim)^{2+}$ and B_{12r} with I_2.

mac	Conditions	$10^4[Co(II)]/M$	$10^4[I_2]/M$	$\Delta[Co(II)]/[I_2]$
tim	$\mu = [H^+] = 0.1$ M	3.08	0.51	1.47
		3.08	0.85	1.87
		3.08	1.19	1.97
B_{12r}	$\mu = [H^+] = 0.1$ M	1.00	0.20	2.08
		1.00	0.39	2.25

and the $[Co^{2+}]$ was found to be 2.76×10^{-4} M. Another portion of the same product solution was analyzed for I^- content by reaction with IO_3^- (Equation I-30) and was found to have $[I^-]$ (complexed or free) equal to 2.82×10^{-4} M. This experiment conclusively demonstrated that the product contained one mole of iodide per mole of cobalt and the product was therefore formulated as $ICo([14]ane)(H_2O)^{2+}$.

Additional confirmation of the formulation was obtained by aquation and anation reaction studies. A mixture of 5.0×10^{-4} M $Co([14]ane)(H_2O)_2^{3+}$ and 4.0×10^{-4} M I^- was found to react slowly to form a product with an absorption maximum at 433 nm. Similarly, a solution of $ICo([14]ane)(H_2O)^{2+}$ prepared from the reaction of 5.0×10^{-4} M $Co([14]ane)^{2+}$ and 2.0×10^{-4} M I_2 slowly decomposed (aquated) until a small residual absorbance at 433 nm remained. One solution with $[ICo([14]ane)(H_2O)^{2+}] = 2.36 \times 10^{-4}$ M initially and $[H^+] = 0.6$ M was allowed to stand at room temperature for 60 hours. At that time the residual concentration of $ICo([14]ane)(H_2O)^{2+}$ (as determined from D_{433}) was 2.23×10^{-5} M. A formation constant of 490 M^{-1} was calculated in accord with Equations I-45 and I-46.

$$Co([14]ane)(H_2O)_2^{3+} + I^- \underset{k_{aq}}{\overset{k_{an}}{\rightleftharpoons}} ICo([14]ane)(H_2O)^{2+} + H_2O \qquad \text{(I-45)}$$

$$K = \frac{[ICo([14]ane)(H_2O)^{2+}]}{[Co([14]ane)(H_2O)_2^{3+}][I^-]} \qquad \text{(I-46)}$$

The reactions of Co(meso-Me_6[14]ane)$^{2+}$ and Co(Me_6-4,11-diene)$^{2+}$ with I_2 were both biphasic with the two stages of reaction being of similar magnitude so that isolation of the presumed iodo complexes was precluded. Spectral characterization of the iodo complexes was also impossible. Kinetic behavior (as discussed below) was consistent with the assignment first-stage redox reaction and second-stage aquation.

The Co(tim)$^{2+}$ and Co(dpnH)$^{+}$ reductions of I_2 were also presumed to produce the iodo-cobalt complexes although spectral features in the visible were too weak to allow a determination. The Co(tim)$^{2+}$ reaction also produced a precipitate at too high reaction concentrations, such as [Co(tim)$^{2+}$] = 3.6 x 10^{-5} M, [I_2] = 7.33 x 10^{-4} M in 0.10 M $HClO_4$.

The reaction of $B_{12}r$ with I_2 gave a red product whose spectrum was identical to that of $B_{12}a$. Kinetic studies at an absorption maximum for iodocobalamin, however, showed a two-stage reaction as expected for formation of iodocobalamin and rapid aquation (see below).

Kinetics

The reduction of I_2 by Co([14]ane)$^{2+}$ was studied kinetically by monitoring the formation of ICo([14]ane)(H_2O)$^{2+}$ at 433 nm with [H^+] = 0.1 M, μ = 1.0 M. Pseudo-first-order conditions with excess Co([14]ane)$^{2+}$ were used and the rate constants so obtained are shown in Table I-15. A plot of k_{obs} versus Co([14]ane)$^{2+}$ was linear (Figure I-33) with slope = k = (2.83 ± 0.08) x 10^3 M^{-1} s^{-1}. The rate law was therefore written as Equation I-47. One run at significantly greater acidity (0.842 M) gave

$$-\frac{d[Co(II)]}{dt} = 2k[Co(II)][I_2] \qquad (I-47)$$

Table I-15. Kinetic data for the reaction of $Co([14]ane)^{2+}$ with I_2. Conditions: $[I_2] = (2.8 - 4.6) \times 10^{-5}$ M, $[H^+] =$ 0.13 M, $\mu = 1.00$ M, T = 25° C, $\lambda = 430$ nm

$10^3[Co([14]ane)^{2+}]/M$	k_{obs}/s^{-1}	$10^{-3}k/M^{-1}\ s^{-1}$ [a,b]
0.23	0.68	2.93
0.28	0.92	3.33
0.41	1.18	2.85
0.74	1.94	2.64
0.82	2.97	3.61[c]
0.96	2.75	2.88
1.16	3.28	2.82
1.42	4.07	2.87
1.77	4.32	2.44
1.79	5.46	3.04

[a] $k = k_{obs}[Co([14]ane)^{2+}]^{-1}$.

[b] Average value is $(2.87 \pm 0.25) \times 10^3\ M^{-1}\ s^{-1}$.

[c] Run done at $[H^+] = 0.84$ M, $\mu = 1.02$ M, and not included in average or least squares fit.

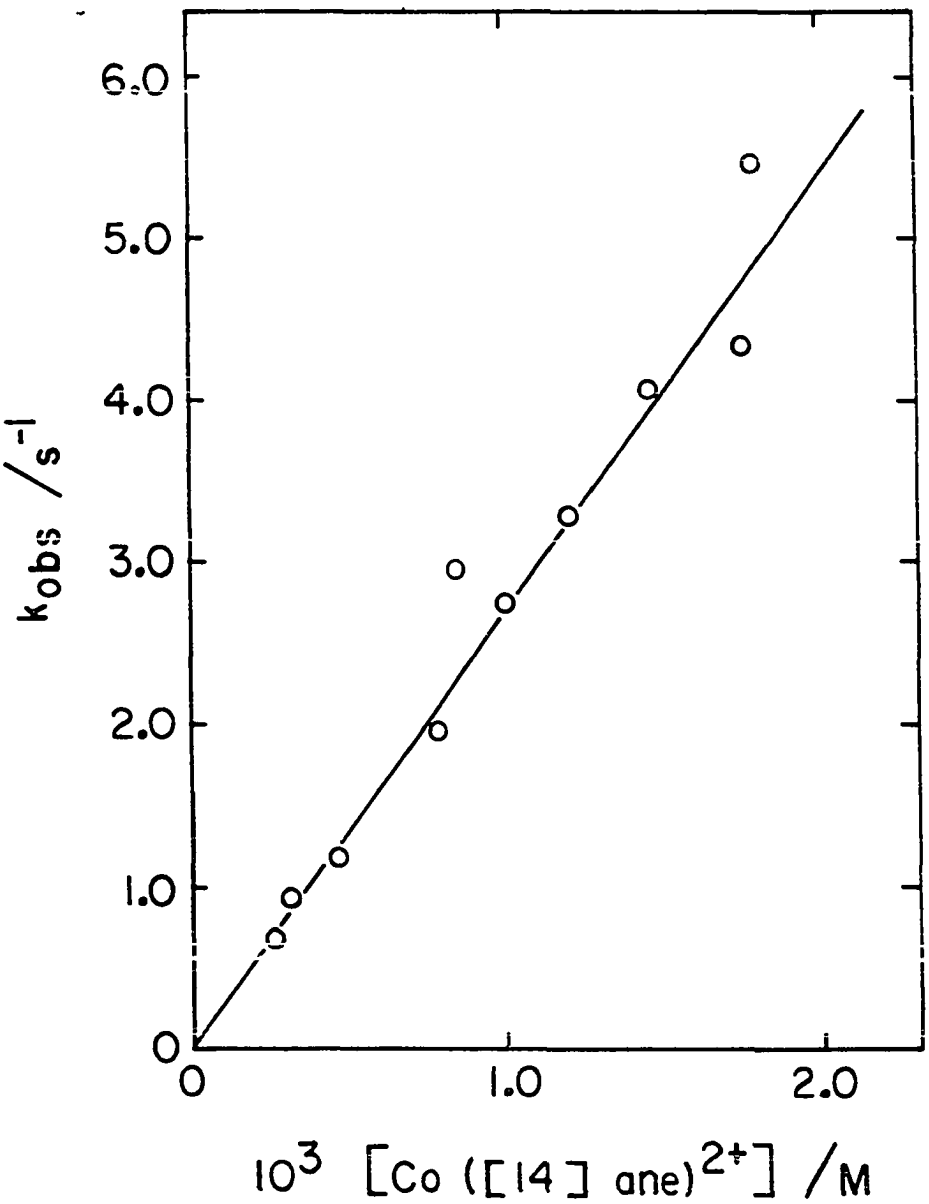

Figure I-33. The dependence of k_{obs} on [Co([14]ane)$^{2+}$] for the reaction of Co([14]ane)$^{2+}$ with I_2

a somewhat higher value of k_{obs}, but the magnitude of the difference was not such as to warrant further investigation.

The aquation of $ICo([14]ane)(H_2O)^{2+}$ was sufficiently slow so as not to interfere with the redox reaction. Table I-16 shows the results for preliminary studies of the aquation reaction and Table I-17 shows preliminary results for the anation of $Co([14]ane)(H_2O)_2^{3+}$ by I^-. Rate constants for the reactions were determined from the initial rates of the reaction (Equations I-41 and I-42).

For an equilibrium reaction the equilibrium constant is equal to the ratio of the forward to the reverse rate constants (Equation I-48)

$$K = k_{an}/k_{aq} \qquad \text{(I-48)}$$

and the value so obtained may be compared to the thermodynamically obtained value. From Tables I-16 and I-17 an estimate of the equilibrium constant is available. Using rate constants for the aquation reaction at $[ICo([14]ane)(H_2O)^{2+}] = 8.56 \times 10^{-4}$ M, $[H^+] = 0.45$ M ($k_{obs} = 9.4 \times 10^{-6}$ s^{-1}) and the anation reaction at $[Co([14]ane)(H_2O)_2^{3+}] = 6.27 \times 10^{-3}$ M, $[I^-] = 8.5 \times 10^{-3}$ M, $[H^+] = 0.492$ M ($k_{obs} = 2.85 \times 10^{-3}$ M^{-1} s^{-1}) gave $k = 300$ M^{-1}, a value in reasonable agreement with the thermodynamic value when differences in acidity and ionic strength and the crudeness of the measurements are taken into account.

The two predominant features of the data in Tables I-16 and I-17 are the effect of acidity and $[Co([14]ane)^{2+}]$. Both the aquation and anation rate constants show an inverse dependence on $[H^+]$ and a direct

Table I-16. Kinetic data for the aquation of $ICo([14]ane)(H_2O)^{2+}$ as determined by initial rates. Conditions: $\mu = [H^+]$, T = 25° C, λ = 433 nm

$10^4[ICo([14]ane)(H_2O)^{2+}]/M$	$10^4[Co([14]ane)^{2+}]/M$ [a]	$[H^+]/M$	$10^4 k/s^{-1}$
4.23	0.00	0.045	0.985[b]
3.75	2.92	0.045	1.67[b]
4.11	5.89	0.045	2.13[b]
4.94	11.7	0.045	2.28[b]
4.38	20.6	0.045	5.71[b]
4.94	11.7	0.027	5.06[c]
3.43	13.2	0.125	5.47[c]
4.19	12.5	0.273	4.77[c]
2.99	13.7	0.372	5.85[c]
4.51	12.1	0.519	3.60[c]
8.56	0.00	0.45	0.094[b]

[a] Calculated from added amounts of Co^{2+} and [14]ane; therefore, the concentration is only an estimate.

[b] $\mu = [H^+]$.

[c] μ = 0.52 M.

Table I-17. Kinetic data for the I^- anation of $Co([14]ane)(H_2O)_2^{3+}$ as determined by initial rates. Conditions: $[Co([14]ane)(H_2O)_2^{3+}] = 6.27 \times 10^{-3}$ M, $[I^-] = 8.5 \times 10^{-3}$ M, μ = 0.49 M, T = 25° C, λ = 433 nm

$10^4[Co([14]ane)^{2+}]/M$[a]	$[H^+]/M$	$10^2k/M^{-1}\ s^{-1}$
0.00	0.049	0.778
0.00	0.098	0.674
0.00	0.295	0.354
0.00	0.492	0.285
1.67	0.492	1.62
4.17	0.492	2.87
8.33	0.049	4.42
8.33	0.295	4.11
8.33	0.492	3.66
16.7	0.49	4.84

[a]Calculated from added amounts of Co^{2+} and [14]ane; therefore, the concentration is only an estimate.

dependence on $[Co([14]ane)^{2+}]$. Such catalytic dependencies are particularly characteristic of transition metal aquation reactions.

Both $Co(meso\text{-}Me_6[14]ane)^{2+}$ and $Co(Me_6\text{-}4,11\text{-}diene)^{2+}$ as well as I_2 have limited solubility in aqueous $HClO_4$. Therefore, the range of concentrations studied for the redox reactions was rather small. Further, the second-stage of the reactions of the two complexes with I_2 was sufficiently rapid to interfere with the treatment of first-stage data, but too slow to be followed conveniently. The reactions were therefore studied at 0.010 M $HClO_4$ (μ = 0.010 M) which allowed greater solubility of the Co(II) complexes and a shorter half-life for the second-stage reactions. Iodine was used as the limiting reagent because of the greater solubility of the complexes in 0.010 M $HClO_4$ and the lack of intense absorption maxima in the visible spectrum for the Co(II) species.

Table I-18 gives rate constants obtained for the reaction of $Co(meso\text{-}Me_6[14]ane)^{2+}$ with I_2. The average of k^I was 5.0 ± 1.0 M^{-1} s^{-1}. The large standard deviation is primarily a function of the poor resolution of rate constants of similar magnitude by a biphasic treatment of data. The second-stage rate constants varied somewhat with the change in concentration of excess reagent. This implied a $Co(meso\text{-}Me_6[14]ane)^{2+}$ catalysis of the aquation such as that seen for $Co([14]ane)^{2+}$.

Only two runs were done for the reaction of $Co(Me_6\text{-}4,11\text{-}diene)^{2+}$ and I_2 as shown in Table I-19. The average value of k^I was 4.0 M^{-1} s^{-1}. The second-stage rate constant again showed a strong dependence on the concentration of the Co(II) complex.

Table I-18. Kinetic data for the reaction of Co(meso-Me_6[14]ane)$^{2+}$ with I_2. Conditions: $\mu = [H^+] = 0.010$ M, T = 25° C, λ = 460 nm

10^4[Co(meso-Me_6[14]ane)$^{2+}$]/M	$10^4[I_2]$/M	$10^3 k^I_{obs}/s^{-1}$	$k^I/M^{-1}\ s^{-1}$ [a,b]	$10^3 k^{II}_{obs}/s^{-1}$
3.81	0.27	1.5	4.3	0.66
4.78	0.66	2.3	5.6	0.65
5.65	0.51	2.0	4.0	0.72
10.5	1.02	5.7	6.0	1.7

[a] $k^I = k^I_{obs}$[Co(meso-Me_6[14]ane)$^{2+}$]$^{-1}$.

[b] Average value of k^I is 5.0 ± 1.0 $M^{-1}\ s^{-1}$.

Table I-19. Kinetic data for the reaction of Co(Me_6-4,11-diene)$^{2+}$ with I_2. Conditions: $\mu = [H^+] = 0.010$ M, T = 25° C, λ = 460 nm

10^4[Co(Me_6-4,11-diene)$^{2+}$]/M	$10^4[I_2]$/M	$10^3 k^I_{obs}/s^{-1}$	$k^I/M^{-1}\ s^{-1}$ [a,b]	$10^3 k^{II}_{obs}/s^{-1}$
3.82	0.51	1.4	4.2	0.73
7.64	1.0	2.6	3.8	1.7

[a] $k^I = k^I_{obs}$[Co(Me_6-4,11-diene)$^{2+}$]$^{-1}$.

[b] Average value of k^I is 4.0 ± 0.2 $M^{-1}\ s^{-1}$.

The range of concentrations studied for the $Co(tim)^{2+}$—I_2 reaction was limited by the precipitation of the reaction product. At the range of concentrations given in Table I-20 the precipitation did not interfere. A plot of k_{obs} versus $[I_2]$ (Figure I-34) was very scattered, the slope giving a rate constant of $k = (6.1 \pm 1.3) \times 10^4\ M^{-1}\ s^{-1}$.

Iodine was reduced by $Co(dpnH)^+$ at a slightly greater rate as shown by the data in Table I-21. Figure I-35 shows k_{obs} versus $[I_2]$ with $k = (8.7 \pm 1.4) \times 10^4\ M^{-1}\ s^{-1}$.

The B_{12r}—I_2 reaction was followed at three wavelengths as shown in Table I-22. The loss of B_{12r} was followed at 310 nm; 555 nm showed the two stages of formation and aquation of iodocobalamin (Figures I-36 and I-37) while 535 nm was an isosbestic for the B_{12a}—iodocobalamin equilibrium (Figures I-36 and I-38). Table I-22 shows that the first-stage reaction rate constant was independent of wavelength with $k^I = (5.85 \pm 0.60) \times 10^4\ M^{-1}\ s^{-1}$ (from Figure I-39). The two values determined for the second-stage (aquation) rate constant gave an average of $37\ s^{-1}$, in good agreement with the value of $35\ s^{-1}$ determined by Thusius (53).

Reduction Potentials

The determination of the standard reduction potential of $Fe^{3+/2+}$ done here gave $E^\circ = +0.479$ V versus the saturated calomel electrode. The value of E° cited by Liteplo and Endicott (50) under the same conditions of acidity and ionic strength ($[H^+] = 0.6$ M, $\mu = 1.0$ M) was +0.499 V, a difference of 0.020 V which was used as a correction for

Table I-20. Kinetic data for the reaction of $Co(tim)^{2+}$ with I_2. Conditions: $[Co(tim)^{2+}] = 1.8 \times 10^{-5}$ M, μ = $[H^+] = 0.10$ M, T = 25° C, λ = 545 nm

$10^4[I_2]/M$	k_{obs}/s^{-1}	$10^{-3}k/M^{-1}\ s^{-1}$ [a,b]
0.81	1.07	6.69
1.13	1.02	4.55
1.89	2.19	5.82
2.36	4.22	8.98
2.83	4.77	8.46
3.63	4.93	6.81

[a] $k = \frac{1}{2}k_{obs}[I_2]^{-1}$, using average $[I_2]$ in each run.

[b] Average value is $(6.89 \pm 1.64) \times 10^3\ M^{-1}\ s^{-1}$.

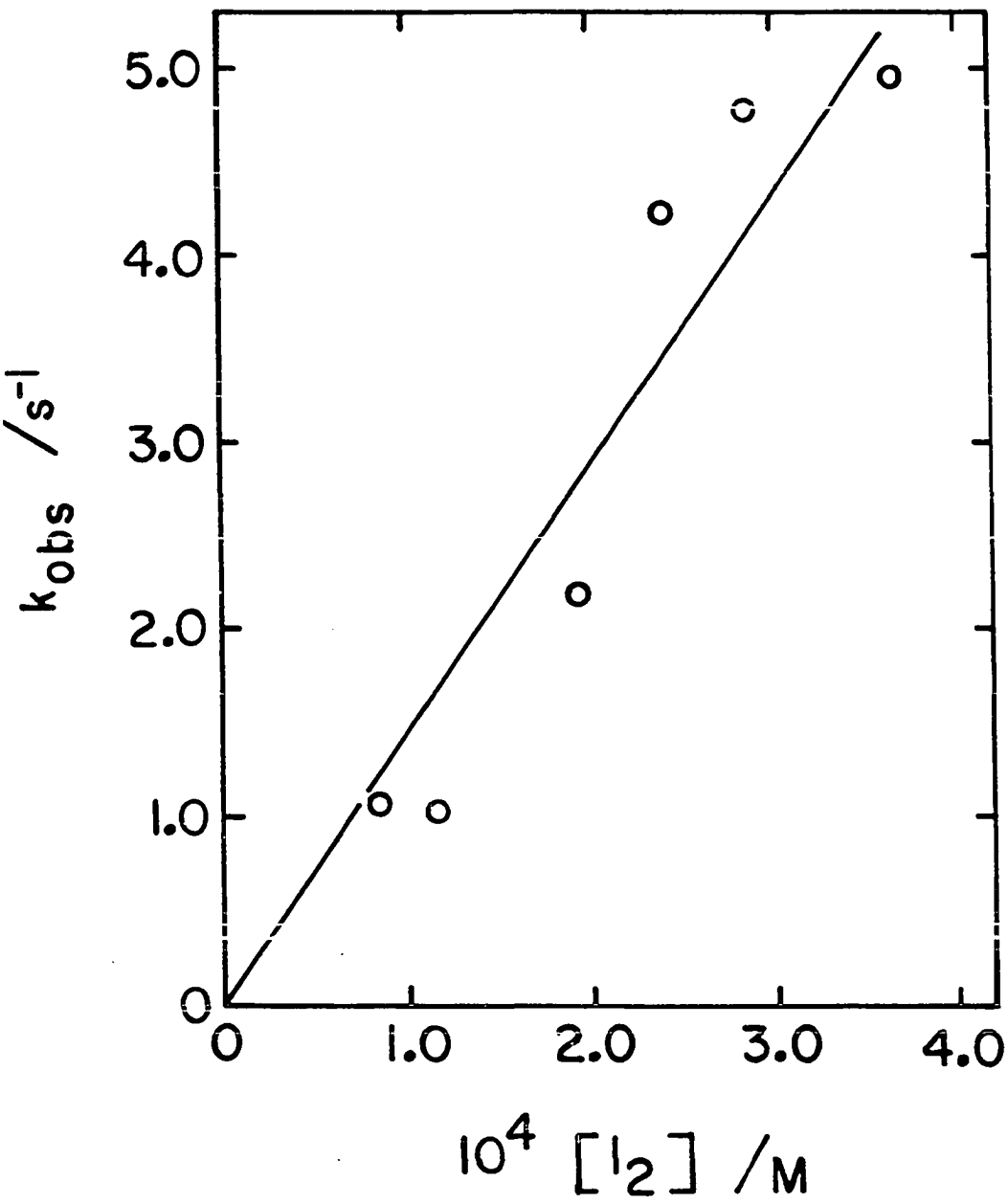

Figure I-34. The dependence of k_{obs} on $[I_2]$ for the reaction of $Co(tim)^{2+}$ with I_2

Table I-21. Kinetic data for the reaction of $Co(dpnH)^{+}$ with I_2. Conditions: $[Co(dpnH)^{+}] = (0.8 - 2.5) \times 10^{-5}$ M, $[H^{+}] = 0.05$ M, $\mu = 0.10$ M, T = 25° C, $\lambda = 505$ nm

$10^4[I_2]/M$	k_{obs}/s^{-1}	$10^{-4}k/M^{-1}\ s^{-1}$ [a,b]
0.35	9.03	12.9
1.54	27.4	8.90
2.24	35.1	7.83
3.05	53.7	8.80
3.86	59.6	7.72

[a] $k = \frac{1}{2}k_{obs}[I_2]^{-1}$, using average $[I_2]$ in each run.

[b] Average value is $(9.23 \pm 2.17) \times 10^4\ M^{-1}\ s^{-1}$.

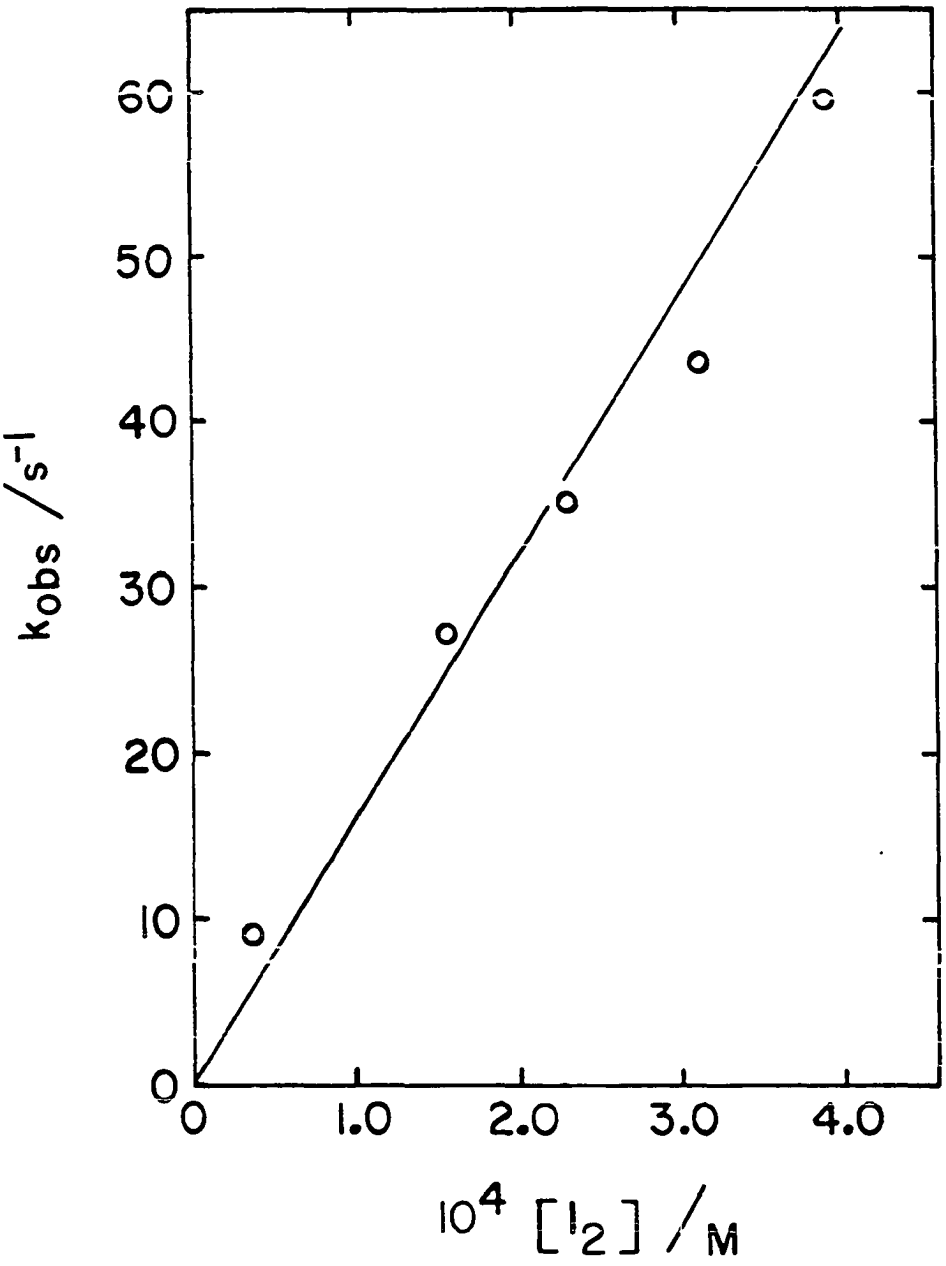

Figure I-35. The dependence of k_{obs} on $[I_2]$ for the reaction of $Co(dpnH)^+$ with I_2

Table I-22. Kinetic data for the reaction of B_{12r} with I_2. Conditions: $[B_{12r}] = (1.0 - 2.0) \times 10^{-5}$ M, $\mu = [H^+] = 0.10$ M, T = 25° C

$10^5[B_{12r}]/M$	$10^4[I_2]/M$	λ/nm	k^I_{obs}/s^{-1}	$10^{-4}k^I/M^{-1}\ s^{-1}$ [a,b]	k^{II}_{obs}
1.0	0.70	310	8.55	6.11	-
1.14	0.93	535	15.7	8.44	-
1.14	1.89	535	23.4	6.19	-
2.0	2.13	310	25.3	5.94	-
1.14	2.85	535, 555	33.3	5.84	31.5
2.0	3.58	310	39.1	5.46	-
1.14	3.81	535, 555	44.9	5.89	42.1
2.0	5.03	310	48.9	4.86	-

[a] $k^I = \frac{1}{2}k^I_{obs}[I_2]^{-1}$, using average $[I_2]$ in each run.

[b] Average value is $(6.09 \pm 1.04) \times 10^4\ M^{-1}\ s^{-1}$.

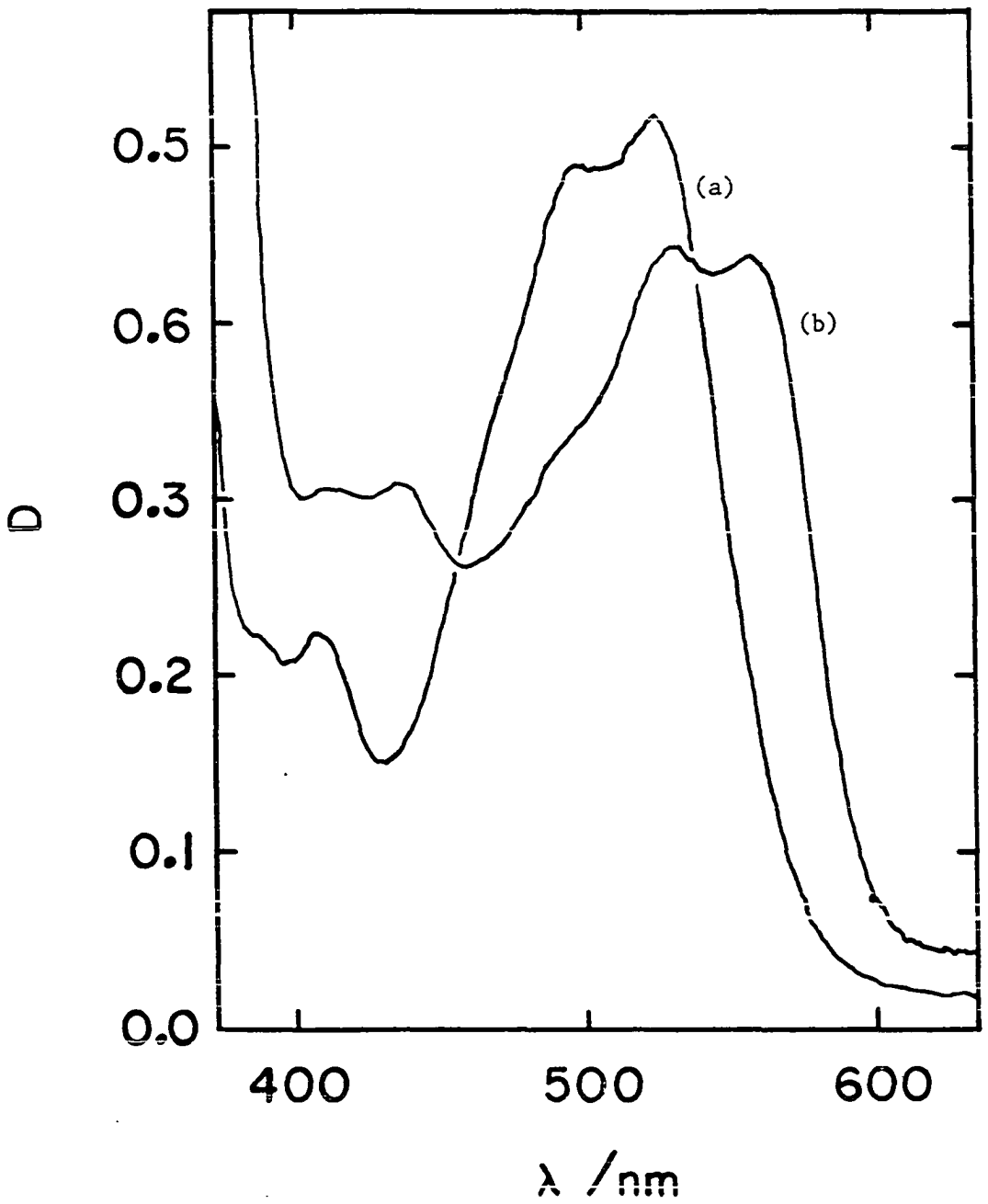

Figure I-36. The electronic spectrum of (a) 6.0×10^{-5} M B_{12a} and (b) iodocobalamin

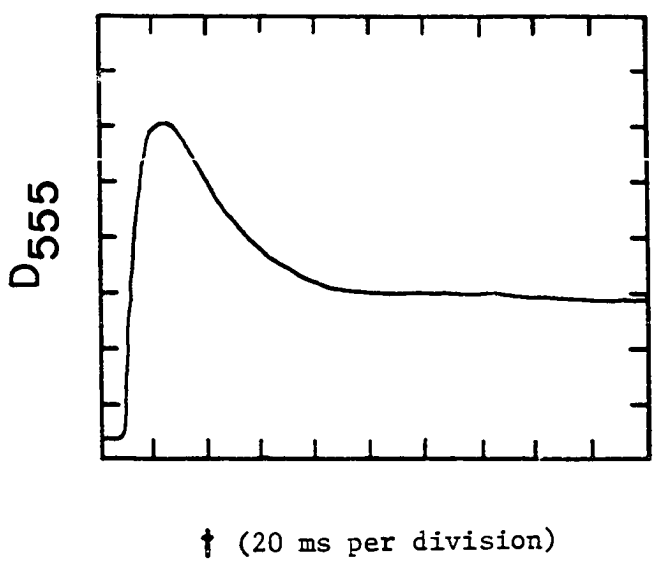

Figure I-37. The time dependence of the absorbance at 555 nm for the reaction of 1.14×10^{-5} M B_{12r} with 3.84×10^{-4} M I_2

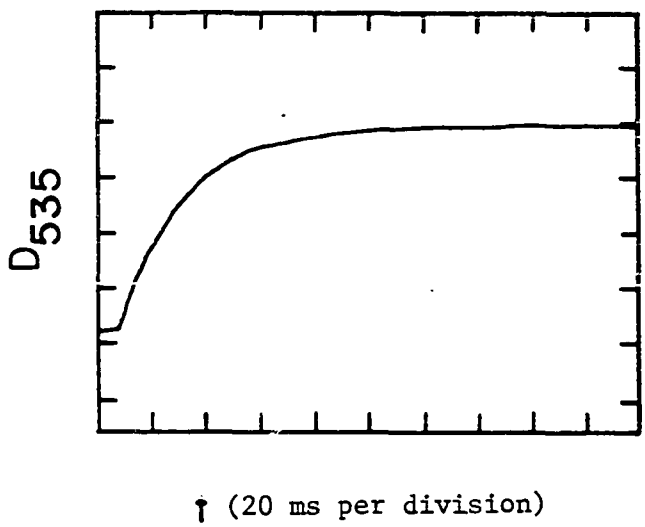

Figure I-38. The time dependence of the absorbance at 535 nm for the reaction of 1.14×10^{-5} M B_{12r} with 3.84×10^{-4} M I_2

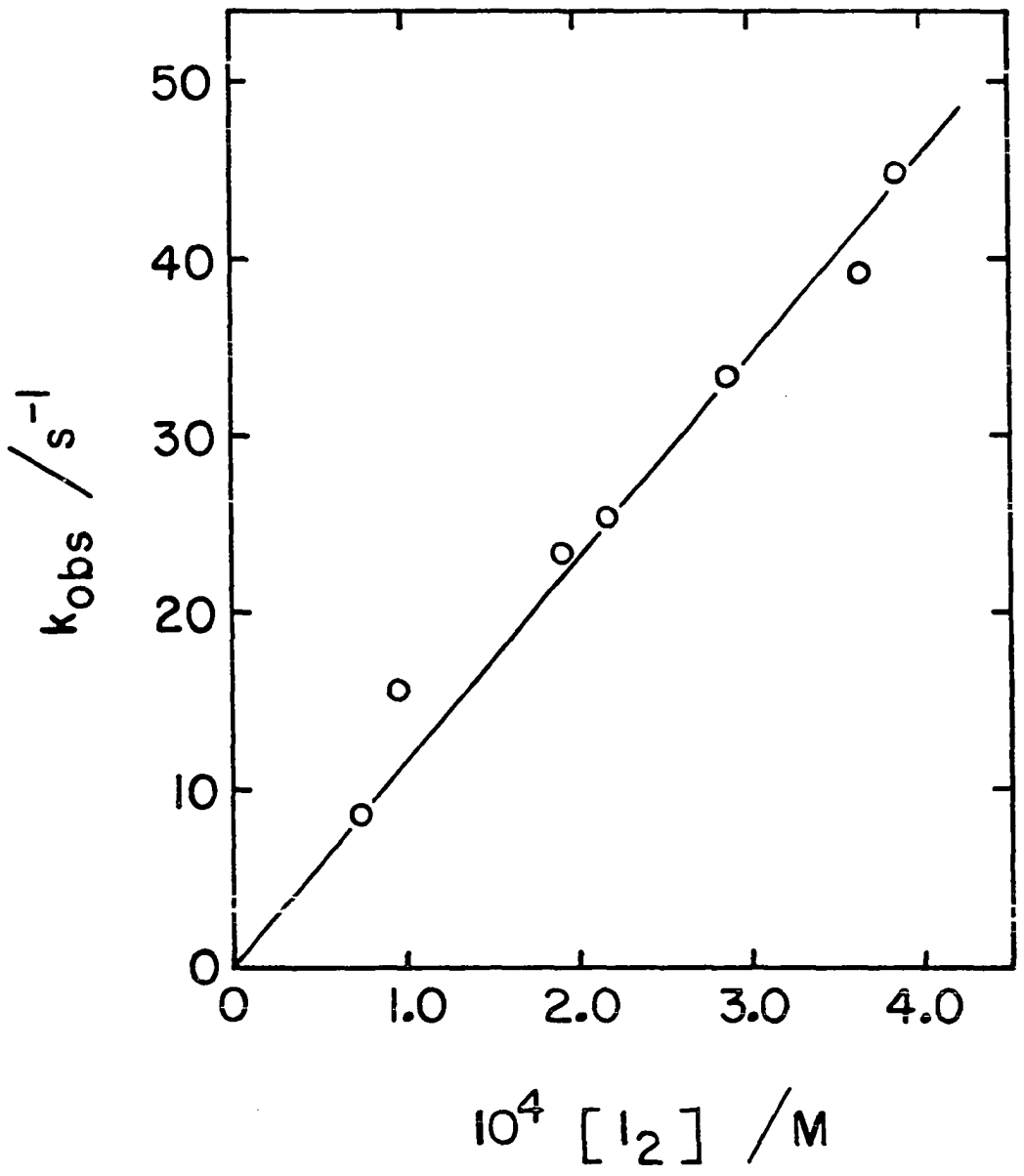

Figure I-39. The dependence of k_{obs} on [I_2] for the reaction of B_{12r} with I_2

subsequent determinations. The potential of an equimolar mixture of $Co([14]ane)(H_2O)_2^{3+}$ and $Co([14]ane)^{2+}$ of + 0.180 V was corrected by 0.020 V to give E° = + 0.200 V.

The half-wave reduction potentials of all the complexes studied except B_{12a} were determined by cyclic voltametry in aqueous acidic solution. The results are given in Table I-23 along with values obtained previously by other workers. Conditions used in the study varied somewhat due to solubility problems with some complexes as noted in the Experimental section. Where the diaquo cobalt(III) complexes were on hand, the Co(III) complex was used for the voltametric work. Such was the case for $Co([14]ane)(H_2O)_2^{3+}$, $Co(dpnH)(H_2O)_2^{2+}$, and $Co(dmgH)_2(H_2O)_2^{+}$.

The reversibility of the electrode reactions was not studied in detail, but one comment may be made. A peak separation of between 60 and 90 mV was seen for all complexes except $Co([14]ane)(H_2O)_2^{3+}$ where the separation was between 120 and 170 mV for a series of determinations. The theoretical separation for completely reversible reactions is 59 mV, so all reactions were assumed to be reversible except for that of $Co([14]ane)(H_2O)_2^{3+}$.

Table I-23. Reduction potentials for macrocyclic compounds of cobalt, Co(III)(mac) ⟶ Co(II)(mac)

Macrocycle	Reduction potential[a]	Supporting electrolyte	References
[14]ane	+ 0.20[b]	0.1 M $HClO_4$	-
meso-Me_6[14]ane	+ 0.25[c]	0.1 M $HClO_4$	-
	+ 0.351[b]	0.1 M $HClO_4$	50
Me_6-4,11-diene	+ 0.27[c]	0.1 M $HClO_4$	-
	+ 0.315[b]	0.1 M $HClO_4$	50
tim	+ 0.27[c]	0.1 M $HClO_4$	-
	+ 0.30[b,d]	0.1 M $NEt_4^+ClO_4^-$ in CH_3CN	54
$dpnH^-$	+ 0.17[c]	0.1 M $HClO_4$	-
	+ 0.16	0.2 M $NEt_4^+ClO_4^-$ in DMF	55
$(dmgH)_2^{2-}$	+ 0.12[c]	0.1 M $LiClO_4$	-
	+ 0.075	0.25 M $LiNO_3$ in 95% ethanol	56
B_{12}	- 0.06[b]	0.1 M K_2SO_4	57
	- 0.002[b]	Phosphate buffer pH 7.43	58

[a]Potential in volts versus the saturated calomel electrode.

[b]E°.

[c]$E_{1/2}$, from this work unless otherwise indicated.

[d]Corrected for estimated junction potential.

DISCUSSION

Kinetic, stoichiometric, and electrochemical results are summarized in Table I-24.

All reactions studied here have a rate law of the form of Equation I-49 with the value of n representing a stoichiometric factor of 1 or 2.

$$-\frac{d[Co(II)]}{dt} = nk[Co(II)][X_2] \qquad (I-49)$$

The rate-limiting step of all reactions is therefore a bimolecular reaction which, in accord with the numerous precedents delineated in the introductory section, would result in either atom transfer (Scheme I) or electron transfer (Scheme II). For the cobalt(II) reductions of the

Scheme I

$$Co(II) + X_2 \rightleftharpoons XCo(III) + X\cdot \qquad (I-50)$$

$$Co(II) + X\cdot \longrightarrow XCo(III) \qquad (I-51)$$

Scheme II

$$Co(II) + X_2 \rightleftharpoons Co(III) + X_2^- \qquad (I-52)$$

$$Co(II) + X_2^- \longrightarrow XCo(III) + X^- \qquad (I-53)$$

halogens the particular mechanism which is operative can be determined by the product yield. That is, Scheme I would result in two moles of the halogenated product while Scheme II would result in the production

Table I-24. Summary of electrochemical, kinetic, and stoichiometric data for the reactions of Co(II)(mac) with H_2O_2, Br_2, and I_2.

Mac	Reduction potential[b]	Rate constants[a] and stoichiometries		
		H_2O_2	Br_2	I_2
[14]ane	+ 0.20	(3.75 ± 0.53) x 10^3 2:1	> 1 x 10^7 2:1	(2.83 ± 0.08) x 10^3 2:1
meso-Me_6[14]ane	+ 0.35	(2.67 ± 0.01) x 10^2 1:1	(4.93 ± 0.24) x 10^4 -	5.0 ± 1.0 -
Me_6-4,11-diene	+ 0.32	75.4 ± 3.2 1:1	(1.70 ± 0.21) x 10^4 2:1	4.0 ± 0.2 -
tim	+ 0.27	(1.41 ± 0.03) x 10^2 1:1	(1.03 ± 0.21) x 10^6 2:1	(6.1 ± 1.3) x 10^3 2:1
$dpnH^-$	+ 0.17	(4.61 ± 0.07) x 10^2 -	3 x 10^7 -	(8.7 ± 1.4) x 10^4 -
$(dmgH)_2^{2-}$	+ 0.12	(1.88 ± 0.06) x 10^3 1:1	- -	- -
B_{12r}	- 0.06	(1.31 ± 0.01) x 10^2 1:1	5 - 8 x 10^6 -	(5.85 ± 0.60) x 10^4 2:1

[a] In M^{-1} s^{-1}.

[b] In volts versus sce for the one-electron reduction of Co(III)(mac).

of one mole of the halogenated product and one mole of diaquo product. Studies here have shown conclusively that the reaction of $Co([14]ane)^{2+}$ with I_2 produces only $ICo([14]ane)(H_2O)^{2+}$ establishing that Scheme II is inoperative. A possible alternative second step for Scheme I (Equation I-54) is also eliminated from consideration by the same argument. Also,

$$Co(II) + X\cdot \longrightarrow Co(III) + X^- \qquad (I\text{-}54)$$

two-stage reaction sequences and spectral observations were consistent with the formation of $BrCo([14]ane)(H_2O)^{2+}$, $BrCo(meso\text{-}Me_6[14]ane)(H_2O)^{2+}$, $ICo(meso\text{-}Me_6[14]ane)(H_2O)^{2+}$, $BrCo(Me_6\text{-}4,11\text{-}diene)(H_2O)^{2+}$, $ICo(Me_6\text{-}4,11\text{-}diene)(H_2O)^{2+}$, and iodocobalamin ($IB_{12}$).

Other considerations, however, show that Scheme I cannot adequately explain the results at hand. Thermodynamic data can be used to calculate a theoretical equilibrium constant and reverse rate constant k_{-1} for Equation I-50, shown by the elementary steps of the reaction of $Co([14]ane)^{2+}$ with I_2 (Equations I-55 to I-57). From this work the stan-

$$Co([14]ane)(H_2O)_2{}^{3+} + e^- \longrightarrow Co([14]ane)^{2+} \qquad (I\text{-}55)$$

$$I_2 + e^- \longrightarrow I\cdot + I^- \qquad (I\text{-}56)$$

$$Co([14]ane)(H_2O)_2{}^{3+} + I^- \rightleftharpoons ICo([14]ane)(H_2O)^{2+} + H_2O \qquad (I\text{-}57)$$

dard reduction potential of $Co([14]ane)(H_2O)_2{}^{3+}$ and the formation constant of $ICo([14]ane)(H_2O)^{2+}$ are known (+ 0.20 V versus sce and 4 ± 1 x

10^2 M^{-1}, respectively) and the one-electron reduction potential of I_2 is known from the calculations of Woodruff and Margerum (59) to be - 0.42 V versus sce. The respective standard free energy changes for Equations I-55, I-56, and I-57 are + 4.61, + 9.69 and - 3.55 kcal $mole^{-1}$ and give an overall ΔG° of + 10.75 kcal $mole^{-1}$ for Equation I-50. The corresponding equilibrium constant is then 1.4×10^{-8}. Since the experimental forward rate constant k_1 is 2.83×10^3 M^{-1} s^{-1} the calculated reverse rate constant k_{-1} is 2.1×10^{11} M^{-1} s^{-1}, an impossibly large number considering that the diffusion-controlled limit for a bimolecular reaction is on the order of 10^{10} M^{-1} s^{-1}. The situation is even worse than implied by the diffusion-controlled limit since the simple first-order kinetics observed requires that the rate constant for the second step of Scheme I be at least a factor of ten greater than the reverse rate constant of the first step.

A similar calculation for the reduction of Br_2 by $Co([14]ane)^{2+}$ cannot be done exactly because the formation constant of $BrCo([14]ane)(H_2O)^{2+}$ is not known. However, the calculation is relatively insensitive to the value of the formation constant and in any event a good estimate of its value can be made. If the formation constant is assumed to be 1×10^3,[1] using - 0.13 V versus sce for the one-electron reduction potential of Br_2 gives an equilibrium constant of 2.7×10^{-3} for

---

[1]This estimate is not unreasonable since other workers (52) have found that $ClCo([14]ane)(H_2O)^{2+}$ is aquated only to negligible extent.

Equation I-50. Since $k_1 > 1 \times 10^7\ M^{-1}\ s^{-1}$ (Table I-24) the lower limit for k_{-1} is $> 3.7 \times 10^9\ M^{-1}\ s^{-1}$.

In the study of the halogen oxidations of $Co(EDTA)^{2-}$ and $Co(CyDTA)^{2-}$ Woodruff, Burke, and Margerum pointed out that the activation energy, and consequently the rate constant, for an atom transfer mechanism (Scheme I) should be related to the homolytic bond energy of the halogen (25). Therefore, iodine oxidations (D = 36.1 kcal $mole^{-1}$) should be faster than those by bromine (D = 46.1 kcal $mole^{-1}$) (60), a trend opposite to that observed both here and previously (25). Clearly activation processes other than homolytic halogen dissociation are involved.

Since the mechanisms of the $Co(EDTA)^{2-}$ and $Co(CyDTA)^{2-}$ reactions were inner-sphere, but the rates were not substitution controlled, the authors proposed that the rate limiting step occurred subsequent to coordination of the oxidant to the metal center. They proposed that the rate limiting process (Equation I-59) involved inner-sphere electron transfer and dissociation of a halogen atom. Presumably Equation I-59 represents a composite of oxidation-reduction and subsequent atom

$$Co(II)L^{2-} + X_2 \rightleftharpoons [Co(II)LX_2]^{2-} \qquad (I\text{-}58)$$

$$[Co(II)LX_2]^{2-} \longrightarrow Co(III)LX^{2-} + X\cdot \qquad (I\text{-}59)$$

dissociation. The fate of the halogen atom was then either reaction with another $Co(II)L^{2-}$ or recombination to form X_2.

Such a mechanism is consistent with the data obtained here for the Co(II)(mac) reductions of Br_2 and I_2, with the redox process again

representing the rate limiting step of the reaction (Equation I-61).

$$Co(II) + X_2 \rightleftharpoons [Co(II) - X_2] \qquad (I\text{-}60)$$

$$[Co(II) - X_2] \longrightarrow [Co(III) - X_2^-] \qquad (I\text{-}61)$$

$$[Co(III) - X_2^-] \longrightarrow Co(III)X + X\cdot \qquad (I\text{-}62)$$

$$[Co(III) - X_2^-] + Co(II) \longrightarrow 2Co(III)X \qquad (I\text{-}63)$$

Assignment of dihalide dissociation (Equation I-62) as the rate limiting step may be rejected by the bond energy argument of Woodruff, Burke, and Margerum (25). Decomposition of the cobalt(III)—dihalide complex probably occurs by one of two routes; either by unimolecular loss of a halogen atom or direct reaction with another Co(II) species. The proposal of coordinated dihalide radical anion is unique to the macrocyclic cobalt systems, although the data could for the $Co(EDTA)^{2-}$ and $Co(CyDTA)^{2-}$ reactions be equally well accommodated.

The reaction of $B_{12}r$ with Br_2 was seriously complicated by a side reaction of $B_{12}a$ with Br_2. The only way, therefore, to study the reaction of interest was in the presence of excess $B_{12}r$. Ellis, et al. (61) have previously reported the reaction of $B_{12}a$ with Br_2 although their product analysis was inconclusive. The authors said only that the product contained more than one atom of bromine per cobalt atom.

The oxidations of the Co(II) complexes by H_2O_2 in most cases did not result in the production solely of $Co(III)(mac)(H_2O)_2^{n+}$. The $B_{12}r$—H_2O_2 reaction demonstrated this fact most clearly in terms of reaction

products, and all other reactions (except that of Co([14]ane)$^{2+}$) showed this feature in terms of stoichiometry. The simplest explanation in accord with the mechanism of Scheme I is that the very highly reactive hydroxyl radical intermediate suffers a fate other than reaction with another Co(II) complex or recombination. The most likely fate (as shown for the B_{12r}—H_2O_2 system) is reaction with the macrocycle of a Co(III) complex. For the meso-Me_6[14]ane system the methyl groups may react with •OH by hydrogen atom abstraction such as is known for tert-butanol (Equation I-64) (62). Similarly, Me_6-4,11-diene, tim, dpnH, and $(dmgH)_2$

$$\bullet OH + (CH_3)_3COH \longrightarrow H_2O + \bullet CH_2C(CH_3)_2OH \qquad \text{(I-64)}$$

have pendent methyl groups available for reaction with •OH as well as potentially reactive imine linkages. The corrin ring and benzimidazole side-chain of the B_{12} system have many potentially reactive sites. No similarly reactive sites are available in Co([14]ane)$(H_2O)_2^{3+}$.

The reaction of hydroxyl radical with a macrocyclic ring was seen by Tait, Hoffman, and Hayon (63). In particular, pulse radiolysis-generated •OH reacted with Co(II)(Me_6-4,11-diene)$^{2+}$ to give a product which was not completely characterized, but which did not exhibit the electronic spectrum of the Co(III) analogue. The oxidation of the metal center was thus ruled out. The most likely fate of •OH was concluded to be reaction with the imine function of the macrocyclic ring.

The failure of scavenging experiments to detect the hydroxyl radical with Br^- or CH_3OH implies either that •OH is not being produced or

that upon production •OH reacts immediately with the ligand without escaping from the solvent cage. A third possibility is that hydrogen peroxide reacts simultaneously with the metal center and with the ligand, effectively circumventing production of the high-energy hydroxyl radical. Such a mechanism would be in accord with the transition state required by the rate law, the stoichiometry, and the observed oxidation of the cobalt center.

The yellow product from the B_{12r}—H_2O_2 reaction can also be obtained by the reaction of B_{12r} with O_2 (37). The reactive intermediate in air oxidation giving rise to the yellow product was felt to be H_2O_2, HO_2^-, or •OH, the former two species being present as a consequence of the primary reaction of B_{12r} with O_2 in water.

For all the Co(II) complexes studied the most rapidly reacting oxidant was Br_2. Comparison of the reduction potentials for the formation of Br• (- 0.13 V versus sce) and I• (- 0.42 V) from Br_2 and I_2 indicates clearly that Br_2 is a stronger oxidant than I_2. Since direct correlations often exist between the reduction potentials of similar species and their rates of reaction with a common substrate, Br_2 is expected to react more rapidly than I_2 with each of the cobalt complexes. The reduction of H_2O_2 to H_2O and •OH, however, has a potential of + 0.47 V versus sce which should make it by far the most rapidly reacting species. The thermodynamic diagnosis gives no clue as to the kinetic sluggishness of H_2O_2 as an oxidizing agent other than to suggest that a different mechanism may be operative for the H_2O_2 redox reactions, which, as discussed above, is most likely the case.

A correlation to be derived from this study is the relative rates of reaction of the seven cobalt complexes. With the exception of B_{12r} the systems may be described as a series of 14-membered tetraaza macrocycles varying in degrees of unsaturation, charge, and substitution of the ring periphery. Two groups of complexes may be defined for purposes of discussion: $Co([14]ane)^{2+}$, $Co(meso\text{-}Me_6[14]ane)^{2+}$, $Co(Me_6\text{-}4,11\text{-}diene)^{2+}$, and $Co(tim)^{2+}$ = Group I; and $Co(tim)^{2+}$, $Co(dpnH)^{+}$, and $Co(dmgH)_2$ = Group II.

Workers have shown through strain energy and ligand field calculations (64) that 14-membered tetraaza macrocycles provide the "best fit" for Co^{3+} and that this good fit is reflected in physical properties of the complexes such as ligand field strengths and redox potentials. The Group I macrocycles therefore represent a good situation for electron transfer study in that a highly desirable environment is provided for the product Co(III). Standard reduction potentials (Table I-23) are in the order $Co(Me_6\text{-}4,11\text{-}diene)^{2+} > Co(meso\text{-}Me_6[14]ane)^{2+} > Co(tim)^{2+}$ (estimated) $>> Co([14]ane)^{2+}$. The difference in potentials between the two saturated complexes indicates that steric crowding of the axial coordination sites of cobalt must be considered, while the similarity of the Me_6-4,11-diene and meso-Me_6[14]ane complex potentials shows that the effect of unsaturation is small. The rate constants for reaction with H_2O_2[$Co([14]ane)^{2+} >> Co(meso\text{-}Me_6[14]ane)^{2+} > Co(tim)^{2+} > Co(Me_6\text{-}4,11\text{-}diene)^{2+}$] and Br_2[$Co([14]ane)^{2+} >> Co(tim)^{2+} >> Co(meso\text{-}Me_6[14]ane)^{2+} > Co(Me_6\text{-}4,11\text{-}diene)^{2+}$] show the same effects. Additional effects are

apparent in the reactions of I_2 where the reactivity order is $Co(tim)^{2+}$ > $Co([14]ane)^{2+}$ >> $Co(meso\text{-}Me_6[14]ane)^{2+}$ ≃ $Co(Me_6\text{-}4,11\text{-}diene)^{2+}$. The effects will be discussed below.

Space-filling molecular models show clearly the steric effect of the six methyl groups in $Co(meso\text{-}Me_6[14]ane)^{2+}$ (Figure I-40). The most stable conformation of the hetero-six-membered rings of the complex is expected to be the chair form with methyl groups in the 3 and 5 positions equatorial thus forcing the axial methyl in the 3 position directly over the axial coordination site of cobalt. The result of the pair of substituted six-membered rings is to effectively block close coordination at the two axial sites of the cobalt atom. The unsubstituted [14]ane system, on the other hand, shows no such blocking. The net effect of substitution is two-fold. First, the axial bonds which are elongated in the d^7 Co(II) complexes (5) (John-Teller distortion) must be shortened upon oxidation of the metal center. Crystal structures of $Co(Me_6\text{-}4,11\text{-}diene)(H_2O)_2^{2+}$ (expected to show the same steric effects as the saturated analog) and $Co([14]ane)(ClO_4)_2$ show that the steric hindrance in the Co(II) complexes is unimportant. Since no distortion is expected in the d^6 Co(III) systems the steric crowding of the methyl groups becomes important, thus destabilizing the Co(III) state in the $meso\text{-}Me_6[14]ane$ and $Me_6\text{-}4,11\text{-}diene$ complexes relative to the [14]ane complex. Second, the extreme steric crowding inhibits the inner-sphere coordination of oxidants to $Co(meso\text{-}Me_6[14]ane)^{2+}$ as shown by the very large differences in rates of reactivity for the Br_2 and I_2 reactions

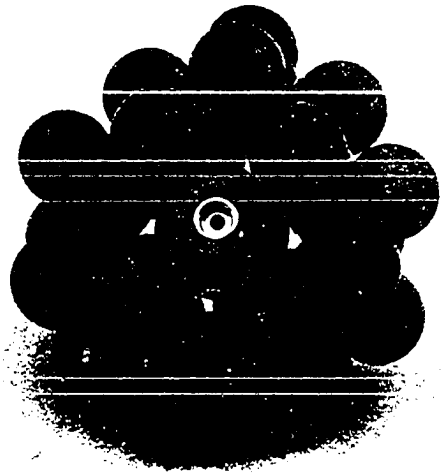

(a)

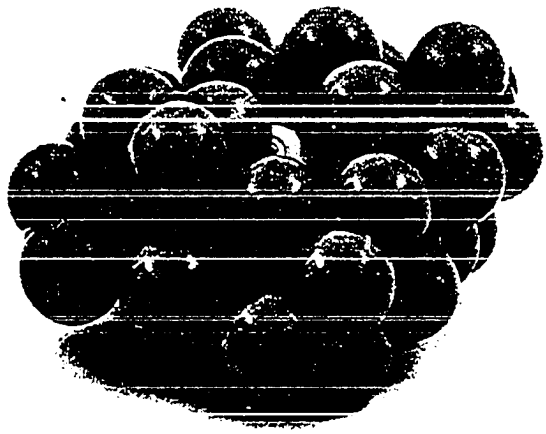

(b)

Figure I-40. Space-filling molecular models of (a) $Co([14]ane)^{2+}$ and (b) $Co(meso\text{-}Me_6[14]ane)^{2+}$. (No axial ligands are shown.)

in particular. Considerable steric crowding remains in Co(Me_6-4,11-diene)$^{2+}$ and along with partial unsaturation of the macrocycle causes additional reduction in reaction rates relative to Co([14]ane)$^{2+}$.

The effect due to unsaturation is small in the case of all three oxidants, being at most only a factor of three (comparing reaction rates of Co(meso-Me_6[14]ane)$^{2+}$ to those of Co(Me_6-4,11-diene)$^{2+}$). No steric crowding is evident in the case of Co(tim)$^{2+}$ and the reduction in reaction rates relative to Co([14]ane)$^{2+}$ is due solely to the effect of conjugated unsaturation. When steric factors are thus taken into account, the results are more in accord with the a priori estimation of Co([14]ane)$^{2+}$ > Co(Me_6-4,11-diene)$^{2+}$ > Co(tim)$^{2+}$ for the reaction rates.

The inversion of reaction rate order in the I_2 reactions with Co([14]ane)$^{2+}$ and Co(tim)$^{2+}$ deserves special comment. Steric factors are expected to be unimportant in these reactions but the reaction rates are inverted from those predicted on the basis of reduction potentials. One possibility is that the formation of the inner-sphere precursor complex [Co(tim)—$I_2$$^{2+}$] is facilitated by an affinity between the electron-rich conjugated pi system of the macrocycle and the highly electrophilic iodine molecule (65). Such a mechanism would also be operative for Co(dpnH)$^{+}$ and may account for the similarity of reaction rates there. This is, however, conjecture with no experimental basis other than the rates of reaction.

The relative rates of reaction for the Group II complexes showed no such difficulties as the Group I complexes. The rate constants for the

H_2O_2 reactions are in the same order, $Co(dmgH)_2 > Co(dpnH)^+ > Co(tim)^{2+}$, as predicted by the reduction potentials. For Br_2 and I_2 the relative rates are $Co(dpnH)^+ > Co(tim)^{2+}$.

Reductions by B_{12r} are of use only in assessing the value of macrocyclic complexes of cobalt as model compounds. Particularly as evidenced by the complicated side reactions of bromine with cobalamin, too many steric and electronic factors must be considered to achieve a simple explanation of B_{12r} reactions.

One other point arises incidentally from these studies. The fact that $Co([14]ane)(H_2O)_2^{3+}$ and I^- form a thermodynamically favored complex ($K \simeq 400\ M^{-1}$) and also, the rates of anation of $Co([14]ane)(H_2O)_2^{3+}$ by I^- and aquation of $ICo([14]ane)(H_2O)^{2+}$ are of some interest. The rate of acid hydrolysis of $Co(NH_3)_5I^{2+}$ is $8.3 \times 10^{-6}\ s^{-1}$ (66), a number similar to the hydrolysis rate seen here ($9.4 \times 10^{-6}\ s^{-1}$ at 0.45 M $HClO_4$). The typical anation rate of $Co(NH_3)_5(H_2O)^{3+}$ of $2 \times 10^{-6}\ M^{-1}\ s^{-1}$ (for any anion) differs substantially from the value of $2.35 \times 10^{-3}\ M^{-1}\ s^{-1}$ at $[H^+] = 0.49$ M determined here. The large difference in rates of anation therefore is reflected by the large difference in stability constants for the macrocyclic tetraammine versus the pentaammine system.

Assuming that the anation mechanism for $Co([14]ane)(H_2O)_2^{3+}$ is completely analogous to that of $Co(NH_3)_5(H_2O)^{3+}$ (i.e., a dissociative mechanism) then the anation rate is determined by the exchange rate for water. A value for that exchange rate has not been previously determined but the data now at hand may be used to estimate a magnitude of 10^{-3} to

10^{-2} s^{-1}. By comparison the water exchange rate for trans-$Co(en)_2(H_2O)_2^{3+}$ is 1.1 x 10^{-5} s^{-1} and that for $Co(NH_3)_5(H_2O)^{3+}$ is 6.6 x 10^{-6} s^{-1}.

PART II. THE CHROMIUM(II) REDUCTION OF SUBSTITUTED METHYLCOBALOXIMES AND DIAMMINECOBALOXIME

INTRODUCTION

The reactions of organocobaloximes (Figure II-1a) with metal ions have been extensively studied with particular emphasis on those processes resulting in cleavage of the cobalt-carbon σ bond and very often the concomitant formation of other organometallic species (67-73). The reaction with Hg^{2+} (67,68), for example, results in transfer of the organic group to the mercuric cation without change of oxidation state and subsequent decomposition of the bis(dimethylglyoximato)cobalt center, $Co(dmgH)_2B_2^+$ (Equation II-1). On the other hand, the reaction of simple

$$RCo(dmgH)_2B + Hg^{2+} \longrightarrow RHg^+ + Co(dmgH)_2B_2^+ \qquad \text{(II-1)}$$

alkyl- and benzylcobaloximes with Cr^{2+} (73) results in simultaneous transfer of the organic group to chromium and reduction of the cobaloxime center (Equation II-2), followed by the very rapid acidolysis of the cobaloxime(II)[1] (Equation II-3).

$$RCo(dmgH)_2B + Cr^{2+} \longrightarrow RCr^{2+} + Co(dmgH)_2 \qquad \text{(II-2)}$$

---

[1]The question of axial ligation in bis(dimethylglyoximato)cobalt(II) and other Co(II)(mac) systems is a matter of some controversy, irrelevant to the present problem. All such complexes discussed in this work will be written showing no axial ligands, e.g., $Co(dmgH)_2$, with the understanding that these complexes are really either five or six coordinate (4).

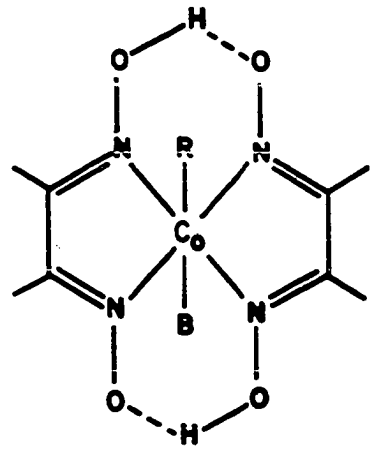

(a)

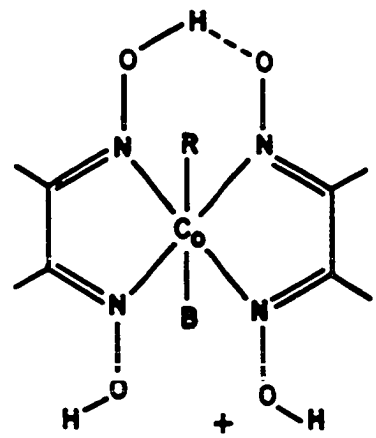

(b)

Figure II-1. The structure of (a) an alkylcobaloxime and (b) the protonated derivative.

$$Co(dmgH)_2 + 2H^+ \longrightarrow Co^{2+} + 2dmgH_2 \qquad \text{(II-3)}$$

Equation II-2 for alkylcobaloximes (at least with simple alkyl groups) was found by Espenson and Shveima (73) to follow a second-order rate law (Equation II-4) with k showing an acid dependence consistent

$$-\frac{d[RCo(dmgH)_2(H_2O)]}{dt} = k[RCo(dmgH)_2(H_2O)][Cr^{2+}] \qquad \text{(II-4)}$$

with the known incidental protonation of alkylcobaloximes (67,74) (Figure II-1b). The rate constants were found to vary greatly with the steric bulk of the alkyl group, the range being from $k = 6.1 \times 10^{-5}$ M^{-1} s^{-1} for the neopentyl group to $k = 23.0$ M^{-1} s^{-1} for the unprotonated form of methylcobaloxime. The researchers concluded that the mechanism operating involved bimolecular homolytic substitution at a saturated carbon atom; i.e., an S_H2 mechanism.

As an extension of the study of the Cr^{2+} reduction of alkylcobaloximes, an investigation of the Cr^{2+} reduction of monohalomethylcobaloximes was undertaken and is reported in this thesis. In contrast to the results of Equation II-2, the reaction of chloromethylcobaloxime with Cr^{2+} did not result in the production of chloromethylchromium ion. Instead, the initial product of the reaction was a species which had an absorption maximum at $\lambda = 460$ nm and was subsequently decomposed at a rather slow rate. Both bromo- and iodomethylcobaloximes reacted similarly, as did the cyanomethyl- and methoxycarbonylmethylcobaloximes. In

addition, Prince and Segal (75) reported that a completely inorganic cobaloxime, $Co(dmgH)_2(NH_3)_2^+$, was reduced by Cr^{2+} to produce a species which had an absorption maximum at λ = 464 nm. The authors commented that the species was susceptible to decomposition in acidic media.

Kinetic experiments and final product studies done here showed that the second-stage reaction is not nearly as simple as that depicted in Equation II-3. The sum of all these results, therefore, requires that a mechanism be invoked other than attack by Cr^{2+} at the α-carbon of the organocobaloxime as shown in Equation II-2.

EXPERIMENTAL

Materials

$ClCH_2Co(dmgH)_2py$

Chloromethylpyridinecobaloxime was prepared by slight modification of Schrauzer's method (33,76) for preparation of methylpyridinecobaloxime. Dimethylglyoxime (23.2 g, 0.2 mol) and $CoCl_2 \cdot 6H_2O$ (23.8 g, 0.1 mol) were stirred for 30 minutes under N_2 in 200 ml of methanol in a 500-ml 2-neck round-bottom flask. Sodium hydroxide (8.0 g, 0.2 mol) was then added as a 50% aqueous solution, followed immediately by 8 ml (7.9 g, 0.1 mol) pyridine and an additional 20 minutes of stirring. A further 8.0 g of NaOH (as a 50% aqueous solution) was then added along with copious amounts of $NaBH_4$ (carefully, to avoid excess foaming) until the solution became dark blue-green, at which time 10 ml (0.15 mol) $BrClCH_2$ was added. After 30 minutes, the whole reaction mixture was poured into 400 ml cold H_2O and the yellow crystals of crude product were collected by suction filtration and washed with water. The product was recrystallized by dissolution in hot methanol, filtration of the hot solution, and reprecipitation by pouring onto ice (yield - 8.2 g, 20%).

$BrCH_2Co(dmgH)_2py$

Crude bromomethylpyridinecobaloxime was prepared as in the case of the chloro derivative except that 7 ml (0.15 mol) CH_2Br_2 was used in place of the $BrClCH_2$. Recrystallization as above was found to give a product which gave poor elemental analysis and an alternative method

described by Schrauzer, et al. (77) was used. In particular, approximately 10 g of the crude product was dissolved in about 25 ml CH_2Cl_2. The addition of hexane caused precipitation of the pure product which was filtered, washed with hexane, and vacuum dried (yield - 10 g, 22%).

$ICH_2Co(dmgH)_2py$

Iodomethylpyridinecobaloxime was prepared by modification of the method of Vickrey, Katz, and Schrauzer (78) which used acetoin ($CH_3CH(OH)C(O)CH_3$) as the reducing agent instead of borohydride. Preparation was the same as for the chloro derivative through the second addition of NaOH, but then 15 ml of acetoin was added. About 15 minutes was required for the appearance of the dark blue-green cobalt(I) color at which time 8 ml (0.15 mol) CH_2I_2 was added. The crude product, isolated as above, was recrystallized from CH_2Cl_2 by addition of hexane (yield - 18 g, 35%).

$NCCH_2Co(dmgH)_2py$

Cyanomethylpyridinecobaloxime (76) was prepared analogously to the halomethylcobaloximes using $NaBH_4$ as the reducing agent and 10 ml $ClCH_2CN$ as the alkylating agent. The product was recrystallized by the addition of a hot methanolic solution of the cobaloxime to 500 ml of an ice/water slush (yield - 8 g, 20%).

$CH_3O_2CCH_2Co(dmgH)_2py$

Methoxycarbonylmethylpyridinecobaloxime was prepared by the method of Rudakova, et al. (79). A 0.60 g (1.5 mmol) sample of $ClCo(dmgH)_2py$ was stirred under N_2 in 30 ml 1:1 ethanol-water for 30 minutes at which

time 0.18 g (4.7 mmol) $NaBH_4$ in 10 ml absolute ethanol was added. When the blue-green hydride had formed (about two minutes) 2 ml (20 mmol) $ClCH_2CO_2CH_3$ was added. When the color had changed to red (about one minute) 2 ml acetone was added to destroy excess $NaBH_4$, thus preventing reduction of the ester. The solution was evaporated to dryness at 30° C and the orange crude product dissolved in CH_2Cl_2 and dried for 30 minutes over anhydrous $MgSO_4$. Upon filtration the product was precipitated with hexane, filtered, and vacuum dried. During the evaporation of the ethanol-water solvent it was noted that heating above 40° C caused extensive decomposition of the product. The pure compound was therefore stored in a refrigerator (yield - 0.3 g, 45%).

All of the substituted methylcobaloximes except the cyanomethyl derivative were found to be somewhat light sensitive although solutions stored in the dark were stable for at least eight hours. An aqueous solution of cyanomethylcobaloxime, however, was unaffected after six hours of exposure to direct sunlight if kept under a nitrogen atmosphere. Modest precautions were therefore taken to protect all solutions from direct light during preparation of the complexes and subsequent experiments. Usually, the only precaution consisted of wrapping containers in aluminum foil. The solid compounds were also stored in the dark.

The compounds were characterized by elemental analysis, NMR, and uv-vis spectrophotometry. Table II-1 contains elemental analyses for the five organocobaloximes and Table II-2 shows the respective NMR and spectrophotometric data.

Table II-1. Elemental analyses for substituted methylcobaloximes

R		% Co	% C	% H	% N	% Halogen
$ClCH_2$	(calc)	14.11	40.24	5.07	16.77	8.49
	(found)	14.1	40.43	4.77	16.49	8.22
$BrCH_2$	(calc)	12.75	36.38	4.58	15.16	17.29
	(found)	12.4	36.54	4.77	13.54	18.03
ICH_2	(calc)	11.57	33.02	4.16	13.76	24.92
	(found)	11.4	32.82	4.30	13.47	27.34
$NCCH_2$	(calc)	14.43				
	(found)	14.6				
$CH_3O_2CCH_2$	(calc)	13.35				
	(found)	13.3				

Table II-2. NMR and uv-visible spectrophotometric data for substituted methylcobaloximes

R	NMR[a]	uv-vis[b,c]
$ClCH_2$	2.17 (s, CH_3)	433 (780)
	3.75 (s, CH_2)	360 (sh) (1550)
		280 (sh) (6560)
		232 (25800)
$BrCH_2$	2.18 (s, CH_3)	436 (784)
	3.61 (s, CH_2)	365 (sh) (1340)
		280 (sh) (6762)
		237 (24700)
ICH_2	2.20 (s, CH_3)	442 (804)
	3.18 (s, CH_2)	325 (sh) (4510)
		280 (sh) (6220)
		235 (25700)
$NCCH_2$[d]	1.37 (s, CH_2)	422 (400)
	2.25 (s, CH_3)	370 (sh) (1080)
		285 (sh) (11000)
		236 (31000)
$CH_3O_2CCH_2$	1.68 (s, CH_2)	430 (397)
	2.19 (s, oxime CH_3)	370 (sh) (1150)
	3.42 (s, methoxy CH_3)	285 (sh) (11100)
		237 (29400)

[a] In $CDCl_3$, δ in p.p.m. relative to TMS.

[b] λ/nm (ε/M^{-1} cm^{-1}).

[c] In 0.01 M $HClO_4$, μ = 1.0 M.

[d] Axial base is pyridine.

$ClCH_2CO_2CH_3$

Methyl chloroacetate (the starting material for preparation of methoxycarbonylmethylcobaloxime) was synthesized by a standard literature method (80). Chloroacetic acid (52 g, 0.55 mol) was dissolved in 120 ml (3 mol) dry CH_3OH and 6 ml (0.1 mol) concentrated H_2SO_4 was carefully added. The mixture was refluxed for five hours with exclusion of moisture at which time 80 ml of the excess methanol was distilled through a 20-cm Vigreux column and the distillation residue was poured into five volumes of ice/water. The organic layer was removed and the aqueous layer was extracted with three 70-ml portions of ether. The combined organic layers were neutralized with saturated Na_2CO_3 solution, washed with three 50-ml portions of water, dried overnight on $CaCl_2$, and distilled (b.p. 130° C). The yield was 25 ml (60%). NMR of the product (neat) showed two singlets at δ 3.68 and δ 4.08 relative to TMS in the ratio of 3:2.

Other cobaloxime complexes

Chloropyridinecobaloxime and diaquocobaloxime(II) were prepared using the standard methods of Schrauzer (33). Diamminecobaloxime perchlorate was prepared by the addition of a concentrated $NaClO_4$ solution to a saturated aqueous solution of the chloride salt of the diammine complex (81).

$Cr(ClO_4)_3$ and Cr^{2+}

An acidic solution of CrO_3 was reduced with 30% H_2O_2 and crystals of chromium(III) perchlorate were collected after partial evaporation of

the solvent. Reduction to Cr^{2+} was attained by the action of zinc amalgam on deaerated Cr^{3+} solutions. Solutions of chromous ion were analyzed by injecting an aliquot into a deaerated solution of $Co(NH_3)_5Br^{2+}$. The liberated Co^{2+} was analyzed as described below.

$[Co(NH_3)_5Br]Br_2$

Bromopentamminecobalt was prepared earlier by a literature method (82).

Other materials

All compounds used in the above syntheses and compounds used in subsequent experiments not specifically mentioned above were commercially available reagent grade chemicals and were used without further purification.

Instrumental Methods

A Cary 14 recording spectrophotometer was used in all uv-visible determinations, including spectral analysis of compounds, stoichiometric determinations, kinetic experiments, and product identification and analysis. The cell compartment of the instrument contained a water bath connected via a circulating pump to a constant temperature bath for temperature control to ± 0.1° C. NMR spectra of the various cobaloximes were obtained in $CDCl_3$ solution using a Varian A-60 instrument. Elemental analyses for C, H, N, and halogen were obtained from Chemalytics, Inc. The cobalt content of the complexes was determined as described below. Fast kinetic runs were performed with a Durrum D-110 stopped-flow

spectrophotometer equipped with a constant temperature bath. Volatile organic products of the reaction were determined by mass spectral analysis with the aid of Mr. G. D. Flesch. The relative content of Cr and Co adsorbed on ion exchange resins was determined by x-ray fluorescence by Mr. Ed DeKalb.

Procedures

Co analysis

The cobalt content of the cobaloximes was determined as follows. An accurately weighed sample of the cobaloxime was digested with fuming $HClO_4$ to yield cobaltous ion, Co^{2+}. In the presence of excess NH_4SCN in 50% acetone-water the absorbance maximum of the $Co(SCN)_4^{2-}$ (λ_{max} 623 nm, ε 1842 M^{-1} cm^{-1}) produced was used to calculate the percentage of Co in the sample.

Products

The volatile products of the reactions of the halomethylcobaloximes with Cr^{2+} were determined by mass spectral analysis of the atmosphere directly over the reaction mixture. Typically, 30 ml of a 4 x 10^{-4} M solution ($[H^+]$ = 0.01 M) of $XCH_2Co(dmgH)_2py$ was placed in the bottom of a Y-tube with about 5 ml of an 0.06 M Cr^{2+} solution in the side-arm container. A background scan of the system was made before mixing the two reagents. A few minutes after mixing of the reagents another scan was made to detect the volatile products of reaction.

Non-volatile products were separated by cation exchange chromatography. Early runs used Dowex 50W-X8 resin with $NaClO_4$ as the eluting

agent, but X2 resin eluted with HCl was found later to be much more convenient. Generally, a 4 x 0.5 cm column of resin was used. The usual procedure was to deaerate 50 ml of a 0.5-1.0 x 10^{-3} M solution of the halomethylcobaloxime of the desired acidity in a 60-ml bottle stoppered with a rubber septum. Cr^{2+} was injected and the solution was allowed to react for a period of time usually dictated by the time required for complete reaction in analogous kinetic studies. After complete reaction the solution was oxidized by bubbling with air for five minutes and loaded onto the ion exchange column. The column was eluted with $NaClO_4$ or $HClO_4$ of gradually increasing ionic strength or acidity and the eluent was collected in 50-ml portions for analysis.

Unreacted starting material, dimethylglyoxime (acidic and basic forms), pyridine, and Cr(III) products (except the dimeric species) were identified by their characteristic uv-visible spectra (Table II-3). Cobaltous ion was determined quantitatively as the tetrathiocyanatocobaltate ion as described above. Very highly charged (or very tightly bound) material was not eluted but instead the resin containing that product was manually removed, washed with water, air dried, and analyzed for relative Cr/Co content by x-ray fluorescence.

Stoichiometry

The stoichiometry of the first-stage reaction was determined by spectrophotometric titration for the faster reacting cobaloximes in two ways. In the first, a 2.5-cm diameter quartz tube with a flat bottom was placed in the cell compartment of the spectrophotometer above a

Table II-3. Uv-vis spectra of some species of interest in this study

	λ/nm (ε/M^{-1} cm^{-1})
Cr^{3+}	574 (15.6)
	408 (15.6)
Dimethylglyoxime	225 (22200)
Dimethylglyoximate ion	268 (23100)
Pyridine	253

magnetic stirrer. A 25.0 ml sample of a 3.60×10^{-4} M solution of methoxycarbonylmethylcobaloxime was added along with a small stirring bar and the tube was capped with a rubber septum. The apparatus was deaerated with N_2 blowing through a 6-inch syringe needle inserted through a small hole in the Cary cell compartment cover into the solution. While stirring, aliquots of a 0.025 M Cr^{2+} solution were injected into the cobaloxime solution. The absorbance at 460 nm was monitored and when the absorbance reached a maximum, another aliquot was injected.

Alternatively, a deaerated solution of the cobaloxime in a 2-cm cell was injected with an aliquot of Cr^{2+} and the absorbance at 460 nm monitored. A fresh solution was then used for injection of a different volume of Cr^{2+}.

The overall stoichiometry with respect to Cr^{2+} was determined by similar spectrophotometric titration except the reaction was allowed to proceed to completion (i.e., both stages). Typically, a 4×10^{-4} M solution of the cobaloxime in 0.01 M H^+ was deaerated and injected with an aliquot of 0.018 M Cr^{2+} and allowed to react for four hours. At that time the absorbance at 460 nm was seen to be unchanging and was read and used in subsequent calculations.

Kinetics

Typically, for the more slowly reacting systems a 1×10^{-4} M solution of the cobaloxime ($[H^+] = 0.01$ M, $\mu = 1.0$ M, T = 25° C) was allowed to react with Cr^{2+} in a 5-cm spectrophotometric cell, capped with a rubber septum. The absorbance was monitored at 460 nm in all cases.

The second stage of the methoxycarbonylmethylcobaloxime reaction was followed similarly.

The rapid first-stage reaction of the methoxycarbonylmethyl and both stages of the cyanomethyl derivative reactions were followed at 460 nm on the stopped-flow.

Treatment of kinetic data

The cases in which the first- and second-stage pseudo-first-order rate constants were of similar magnitude required a two-stage (biphasic) treatment of the data, as described in Part I of this dissertation. For the situations in which $k^{I} >> k^{II}$ the kinetic data for both stages were treated by simple first-order plots of $\ln(D - D_{\infty})$ versus time or by Swinbourne plots (83).

RESULTS

Chloromethyl-, bromomethyl-, iodomethyl-, methoxycarbonylmethyl-, cyanomethyl-, and diamminecobaloxime[1] all react with chromous ion in weakly acidic solution to give an intermediate which has a strong absorption band at 460 nm and which is subsequently decomposed. The position of the absorption peak is invariant with the identity of the axial ligands of the starting cobaloximes. The time dependence of absorbance at 460 nm for the reaction of $ICH_2Co(dmgH)_2(H_2O)$ with Cr^{2+} is shown in Figure II-2 and is typical of all the reactions studied although the time scales varied. Figure II-3 shows the visible spectrum of $ICH_2Co(dmgH)_2(H_2O)$ and the spectrum of the solution, which approximates the intermediate, produced upon the addition of Cr^{2+}.

Stoichiometry

The stoichiometry of the first-stage reaction was determined for the methoxycarbonylmethyl and cyanomethyl derivatives since in these cases the rate of production of the intermediate was much greater than the rate of decomposition (at least in the absence of a large excess of Cr^{2+}). For the halomethyl cobaloximes such determinations were not

---

[1] The sixth ligand of all the organocobaloximes in the solid state was pyridine. In aqueous solution, however, the chloromethyl and iodomethyl (and probably the bromomethyl) complexes are rapidly converted to the aquo derivatives (84). The cyanomethyl complex is only very slowly converted ($t_{\frac{1}{2}} = 7.0 \times 10^4$ s).

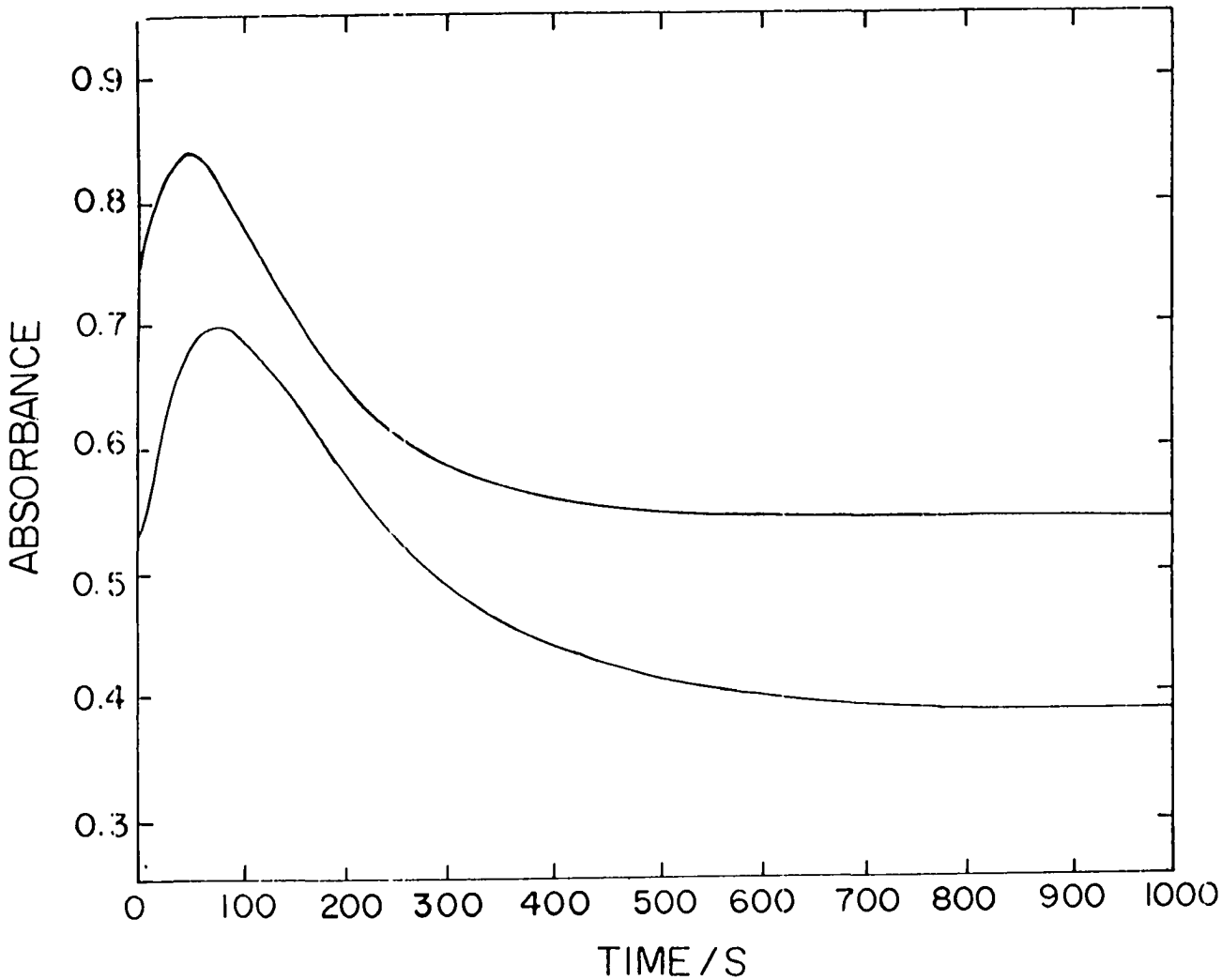

Figure II-2. The time dependence of the optical absorption at 460 nm for the reaction of $ICH_2Co(dmgH)_2(H_2O)$ with Cr^{2+}. Conditions: $[ICH_2Co(dmgH)_2(H_2O)] = 9.0 \times 10^{-5}$ M (both traces); $[Cr^{2+}] = 8.15 \times 10^{-3}$ M (upper), 4.08×10^{-3} M (lower); $[H^+] = 0.010$ M

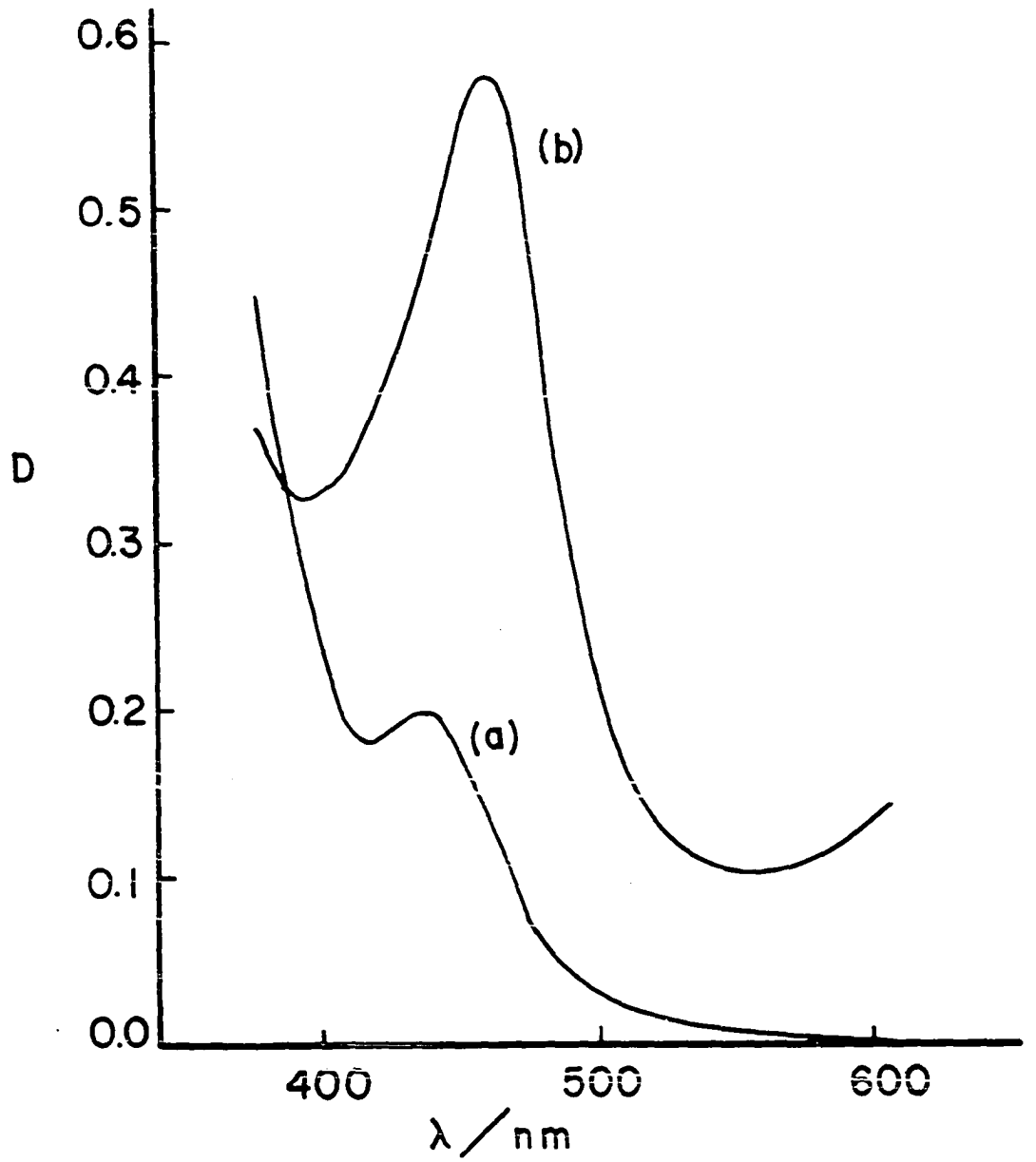

Figure II-3. The electronic spectra of (a) 2.5×10^{-4} M $ICH_2Co(dmgH)_2(H_2O)$ and (b) the product of reaction with 0.116 M Cr^{2+} 30 seconds after mixing. Conditions: $[H^+] = 0.010$ M, $\mu = 1.0$ M, $\ell = 1$ cm

possible as the rates of the first-stage reactions were considerably slower than in the above cases and the second-stage rates were therefore competitive.

The stoichiometry of the first-stage reaction of the methoxycarbonylmethylcobaloxime with chromous ion was determined by the addition of successive aliquots of Cr^{2+} to a stirred solution of the $CH_3O_2CCH_2Co(dmgH)_2(H_2O)$. Conditions were $[CH_3O_2CCH_2Co(dmgH)_2(H_2O)]_{init.} = 3.60 \times 10^{-4}$ M, $[H^+] = 0.01$ M, and 1.0 M ionic strength. The chromous injections were on the order of 0.1 ml of an 0.025 M solution containing 0.01 M $HClO_4$. A plot of $D_{460}^{corr}[CH_3O_2CCH_2Co(dmgH)_2(H_2O)]^{-1}$ versus moles Cr^{2+}/moles $CH_3O_2CCH_2Co(dmgH)_2(H_2O)$ is shown in Figure II-4 to have a break at a ratio of 1.15. D_{460}^{corr} corresponds to the observed absorbance corrected for volume differences; i.e., $D_{460}(V_1 + V_2)/V_1$, where V_1 indicates the volume of Cr^{2+} added and V_2 represents the volume of organocobalt solution added.

Since the above result was somewhat deviant from the expected value of 1, the experiment was repeated in a slightly different manner under the same conditions of acidity and ionic strength. A series of $CH_3O_2CCH_2Co(dmgH)_2(H_2O)$ solutions of concentrations varying from 6.33 to 6.85×10^{-4} M were injected with 0.05–0.50 ml aliquots of 0.0156 M Cr^{2+}. A plot like Figure II-4 resulted with a break at 0.79. One further experiment where the concentration of $CH_3O_2CCH_2Co(dmgH)_2(H_2O)$ varied from 2.79 to 10.9×10^{-4} M and aliquots of 0.0186 M Cr^{2+} were added gave a stoichiometric ratio of 1.14. Therefore, the stoichiometry of the first-stage reaction was determined to be 1:1 for this particular cobaloxime.

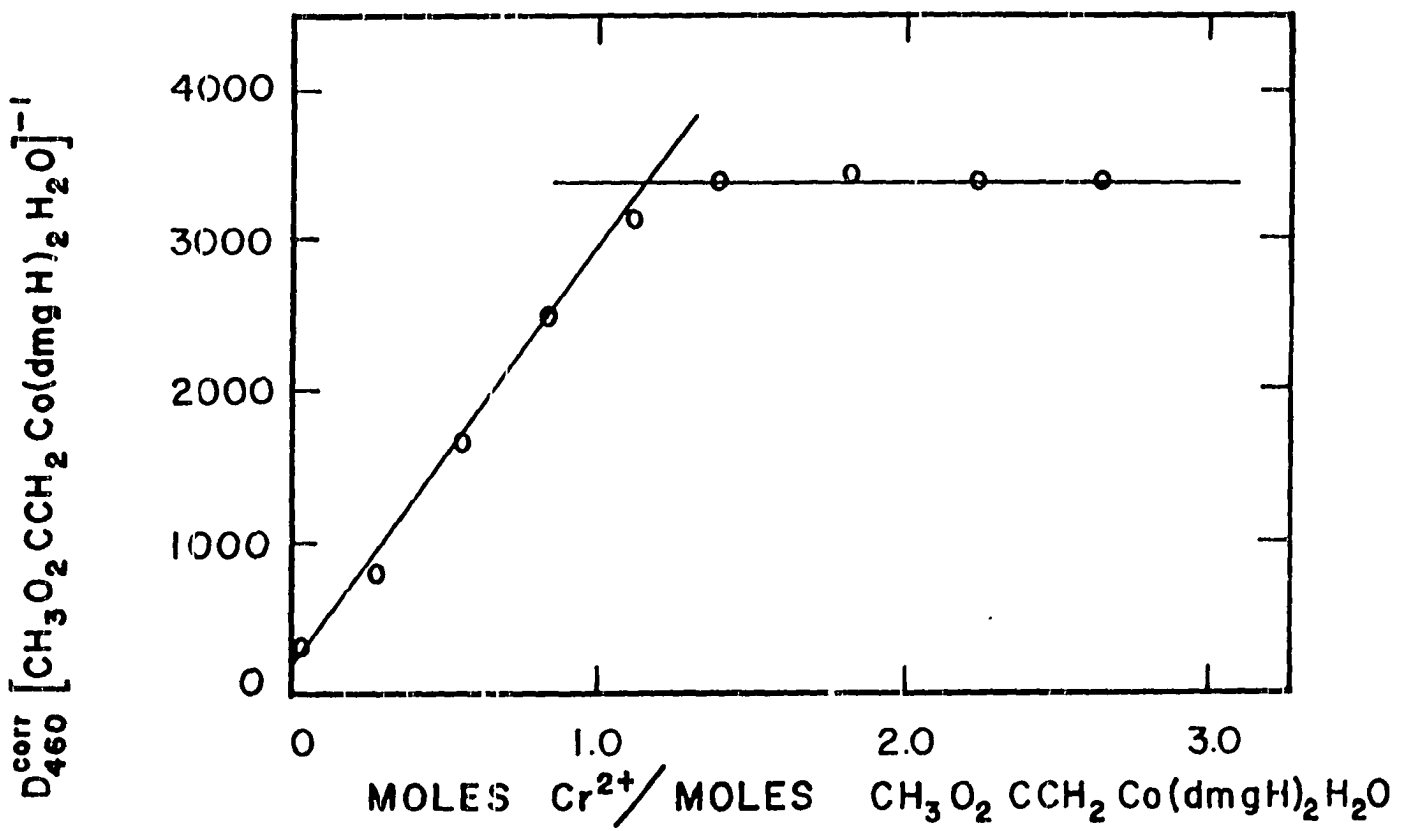

Figure II-4. Spectrophotometric titration for the first-stage reaction of $CH_3O_2CCH_2Co(dmgH)_2(H_2O)$ with Cr^{2+} (ℓ = 2 cm)

The first-stage stoichiometry for the cyanomethylcobaloxime-chromous reaction was determined using from 2.92 to 6.05 x 10^{-4} M $NCCH_2Co(dmgH)_2B$ in 0.01 M H^+, μ = 1.0 M, by adding increments of 0.0162 M Cr^{2+}. The resulting plot of $D_{460}^{corr}[NCCH_2Co(dmgH)_2B]^{-1}$ versus moles Cr^{2+}/moles $NCCH_2Co(dmgH)_2B$ (Figure II-5) gave a break at 1.22 which was felt to be within error of 1.

The intersection of the extrapolated lines in both Figures II-4 and II-5 represents the conversion of 100% of the starting cobaloxime to intermediate and thus the value of the ordinate at that point can be used to estimate a molar absorptivity for the intermediate. Since a 2-cm cell was used in the titration, a value of approximately 1700 M^{-1} cm^{-1} may be assigned. This should, however, be regarded as a lower limit since some second-stage reaction is bound to occur, giving a spuriously low value.

The stoichiometries for the overall reactions were less easily and less satisfactorily determined. There were two cases considered. The reduction of $ICH_2Co(dmgH)_2(H_2O)$ was considered typical of all cobaloximes studied except for $NCCH_2Co(dmgH)_2B$, which was found kinetically to react differently (vide infra).

Solutions of $ICH_2Co(dmgH)_2(H_2O)$ in 0.01 M $HClO_4$ and μ = 1.0 M were prepared in a series of 2-cm cells such that the cobaloxime concentrations ranged from 5.97 to 7.13 x 10^{-4} M. After deaeration an aliquot of Cr^{2+} was injected into each cell so that the ratio of $[Cr^{2+}]$ to $[ICH_2Co(dmgH)_2(H_2O)]$ varied from 0 to 4.95. The cells were then placed in the

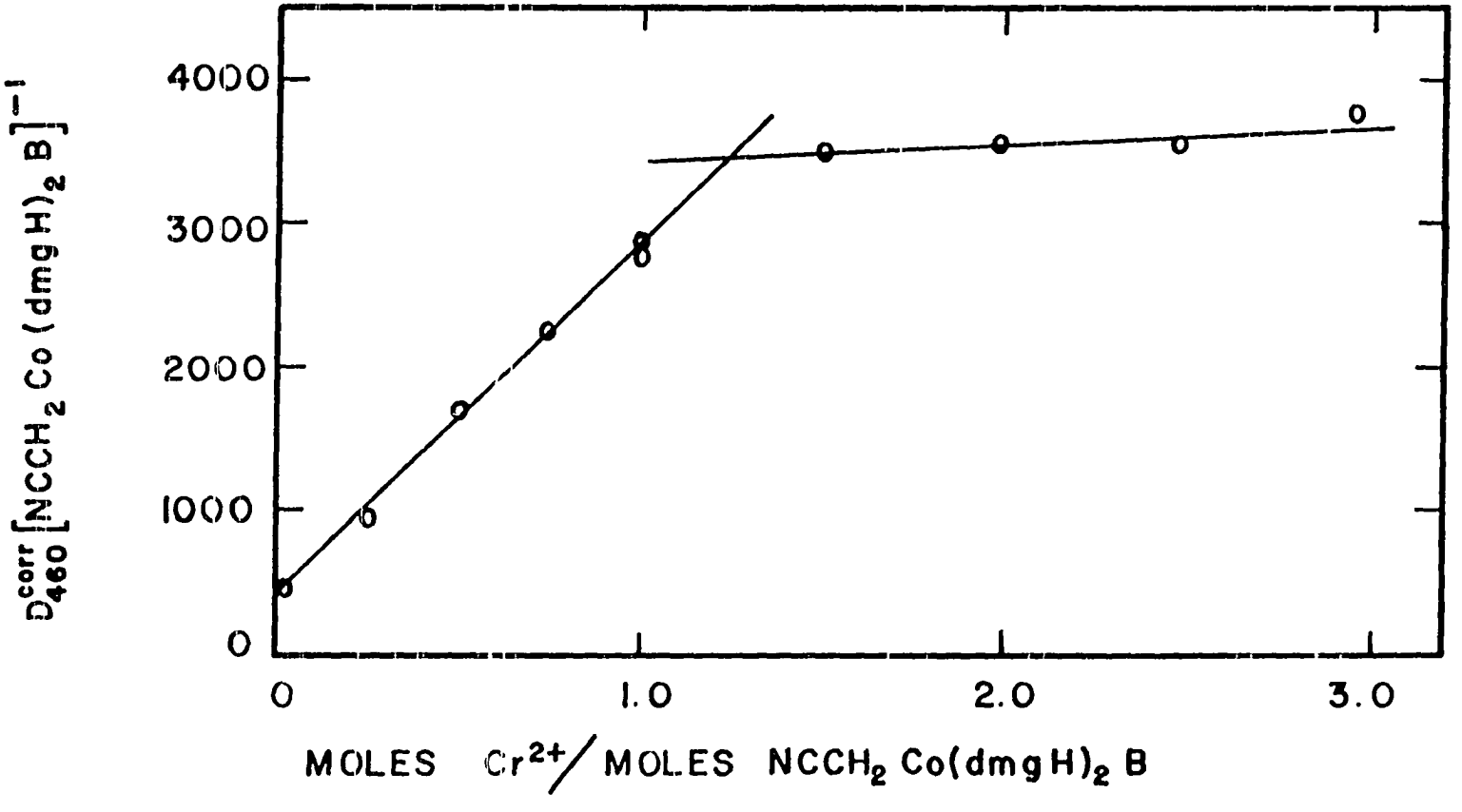

Figure II-5. Spectrophotometric titration for the first-stage reaction of $NCCH_2Co(dmgH)_2B$ with Cr^{2+} (ℓ = 2 cm)

dark for four hours (to ensure complete reaction) and then the absorbance at 460 nm was read. The usual plot for spectrophotometric titrations (Figure II-6) shows breaks at chromium/cobaloxime ratios of approximately 1 and 2. The break at 1 is easily explained by the occurrence of the first-stage reaction in the presence of a stoichiometric deficiency of Cr^{2+}.

$NCCH_2Co(dmgH)_2B$ was titrated with Cr^{2+} similarly and again allowed to react for four hours at which time the absorbance at 460 nm was seen to be unchanging. The cobaloxime concentration range was from 5.97 to 6.27×10^{-4} M in 0.01 M $HClO_4$ and μ = 1.0 M. The standard titration plot (Figure II-7) shows distinct breaks at chromous/cobaloxime ratios of 1 and 2 and a very ill-defined break at either 3 or 4. The break at 1 is explained as above.

Products

Mass spectral experiments revealed that each of the halomethylcobaloximes evolved the corresponding halomethane upon reduction with chromous ion and acidolysis. In particular, chloromethane was identified by molecular ion peaks at m/e 50 (base peak) and 52 in the ratio of 3 to 1, corresponding to $CH_3{}^{35}Cl^+$ and $CH_3{}^{37}Cl^+$, and fragment ion peaks at m/e 15, 35, 36, 37, 47, 48, 49, 51, corresponding to CH_3^+, $^{35}Cl^+$, $H^{35}Cl^+$, $^{37}Cl^+$, $C^{35}Cl^+$, $CH^{35}Cl^+$, $CH_2{}^{35}Cl^+$ and $C^{37}Cl^+$, and $CH_2{}^{37}Cl^+$. The reduction of bromomethylcobaloxime gave molecular ion peaks at m/e 94 and 96 ($CH_3{}^{79}Br^+$ and $CH_3{}^{81}Br^+$, respectively) along with peaks at m/e 15 (CH_3^+), 79 ($^{79}Br^+$), 80 ($H^{79}Br^+$), 81 ($^{81}Br^+$), 82 ($H^{81}Br^+$). Double ion peaks were

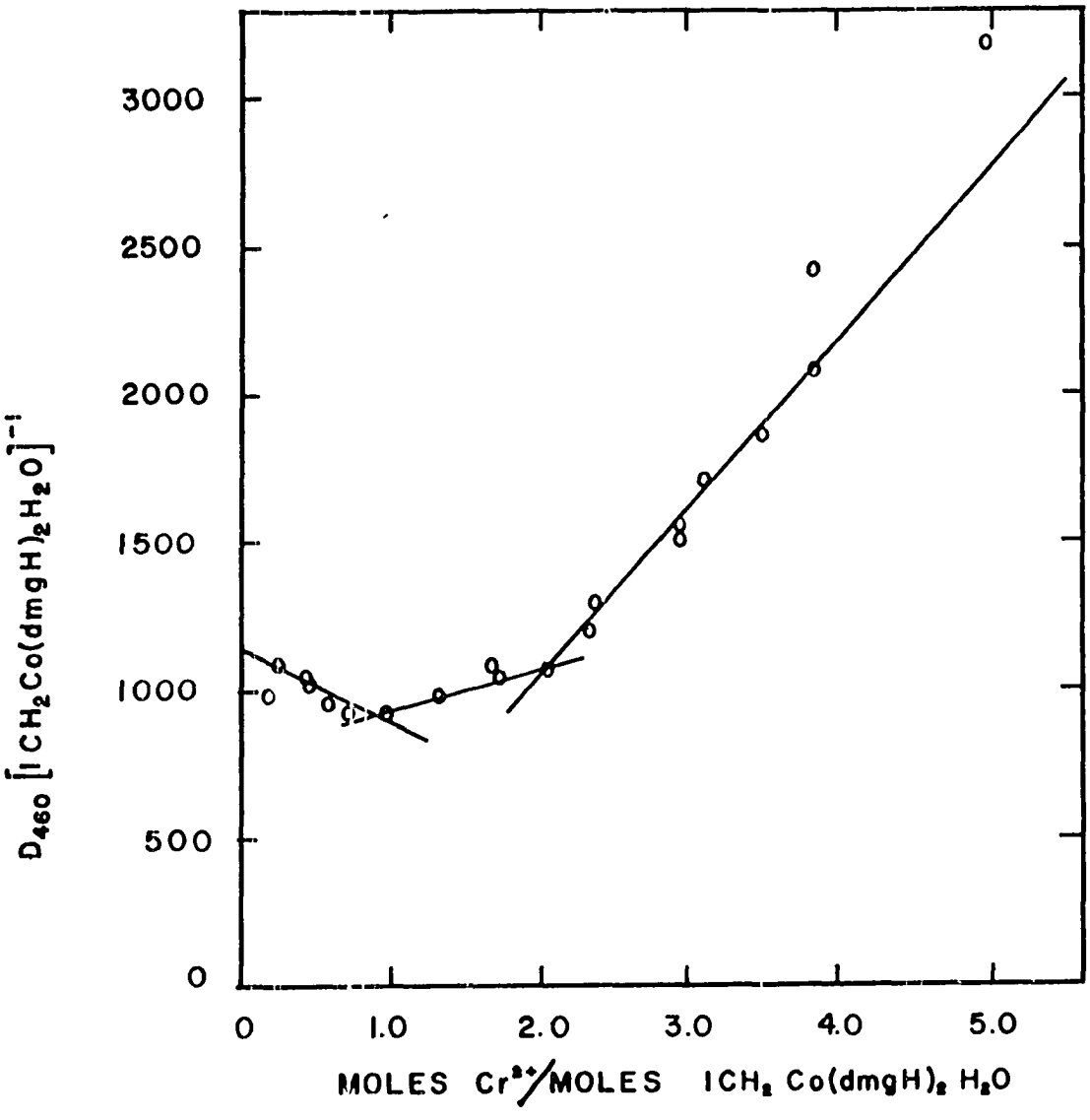

Figure II-6. Spectrophotometric titration for the overall reaction of $ICH_2Co(dmgH)_2(H_2O)$ with Cr^{2+} (ℓ = 2 cm)

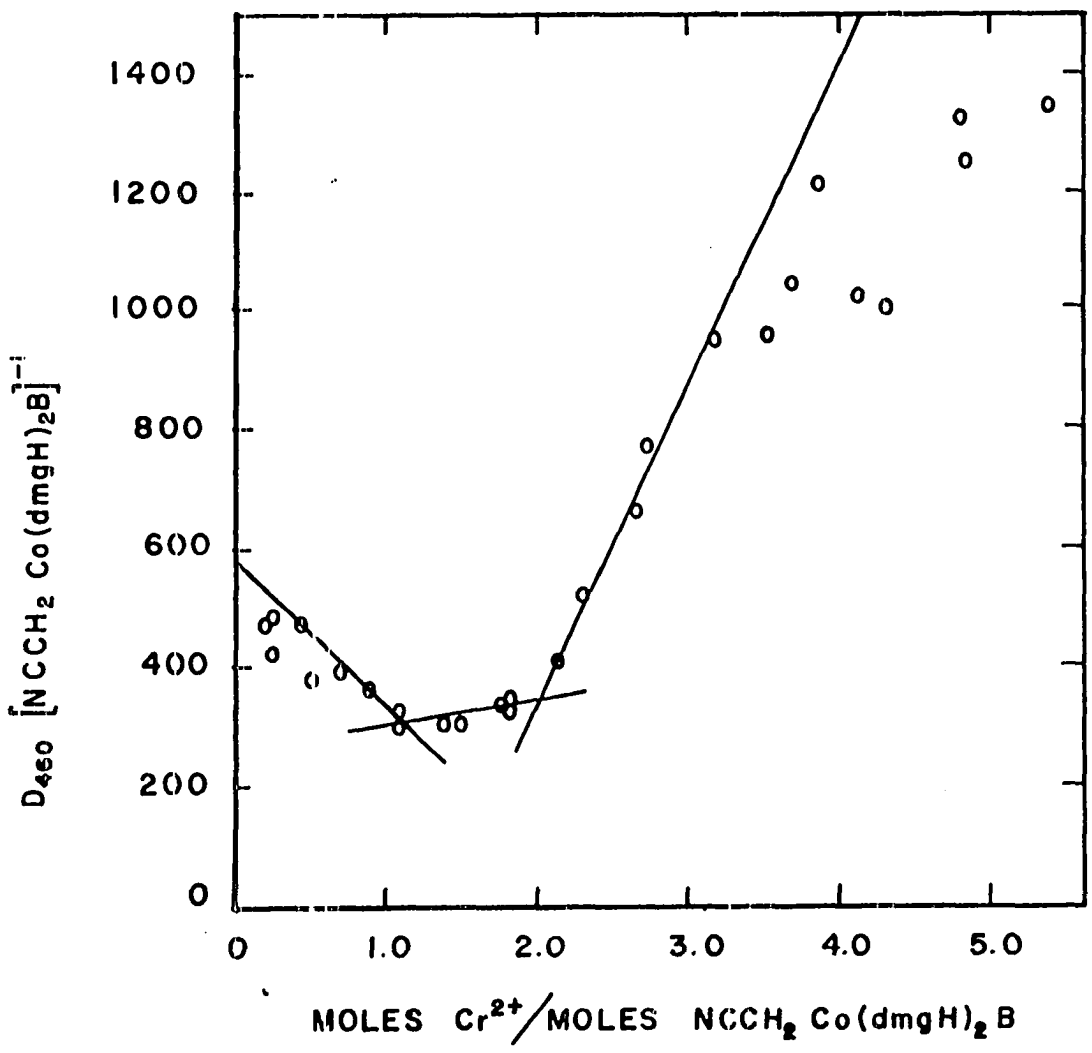

Figure II-7. Spectrophotometric titration for the overall reaction of $NCCH_2Co(dmgH)_2(H_2O)$ with Cr^{2+} (ℓ = 2 cm)

seen at m/e 46.5 and 47.5 (CH_2Br^{++}). The reaction of iodomethylcobaloxime with chromous ion gave the mass spectrum characteristic of CH_3I; i.e., peaks at m/e 127 (I^+), 128 (HI^+), 139 (CI^+), 140 (CHI^+), 141 (CH_2I^+), and 142 (base peak, CH_3I^+). Scans were run over the unreacted Cr^{2+} and cobaloxime solutions to demonstrate that the halomethane mass spectra were not due to decomposition of the cobaloxime solutions in the presence of weak acid or high vacuum. Similarly, the presence of halomethane impurity in any reagents was discounted.

Non-volatile products of the reaction of $ICH_2Co(dmgH)_2(H_2O)$ with Cr^{2+} were determined by ion exchange chromatography using the procedures described in the Experimental section. Iodomethylcobaloxime was the only complex studied thoroughly, but some cursory work was done with cyanomethylcobaloxime.

A solution of 3.9×10^{-4} M $ICH_2Co(dmgH)_2(H_2O)$ and 2.4×10^{-2} M Cr^{2+} in 50 ml of 0.01 M $HClO_4$ was allowed to react for one hour and then air oxidized. The oxidized solution was loaded onto a Dowex 50W-X8 column, Na^+ form. The solution which passed directly through the column contained 0.9×10^{-6} moles of dimethylglyoxime, or about 5% of the theoretical yield of $dmgH_2$. No unreacted starting material was found. Elution with 0.5 M $NaClO_4$ removed the absorbed cobaltous ion (1.3×10^{-5} moles, 65% yield) and the pyridine (as the protonated form) which was present in the starting cobaloxime. Elution with 1.0 M $NaClO_4$ yielded a green solution whose visible spectrum showed a peak at 575 nm, a shoulder at about 400 nm, and intense absorption in the uv range with shoulders at

250 and 220 nm. The visible absorptions are consistent with a Cr(III) product and the 250 and 220 nm absorptions imply the presence of dimethylglyoxime also. No pure $Cr(H_2O)_6^{3+}$ was apparent on the column without the concurrent presence of dimethylglyoxime. Dimeric Cr(III) produced by the air oxidation was eluted with 3 M $NaClO_4$. Even with 3 M $NaClO_4$, however, a brown material remained fixed at the top of the column. Another experiment under similar conditions was not air oxidized and did not give Cr(III) dimer, but a brown material was again produced and the yield of Co^{2+} was not increased.

A nearly identical mixture ($[ICH_2Co(dmgH)_2(H_2O)] = 3.4 \times 10^{-4}$ M, $[Cr^{2+}] = 2 \times 10^{-2}$ M, $[H^+] = 0.01$ M) was allowed to react for one hour, air oxidized, and loaded onto a column of Dowex 50W-X2 resin, H^+ form. A solution of 0.5 M HCl was sufficient to elute Co^{2+} (1.09×10^{-5} moles, 63%) and 1.5 M HCl separated the dimeric Cr(III) from the brown, tightly-bound material. Other products were determined qualitatively in the expected order of elution. The resin containing brown material was removed from the column, washed with H_2O, air dried, and qualitatively analyzed for heavy-element content by x-ray fluorescence. Cr and Co were the only elements detected, in a ratio of Cr/Co = 3.83. A second determination of the same sample gave Cr/Co = 3.92. A sample of clean, dry resin was used as a blank in the x-ray fluorescence analysis.

Several experiments were done to determine if the amount of Cr^{2+} influenced the yield of Co^{2+}. In particular, a reaction mixture was allowed to react for one hour and then oxidized, loaded onto an X2 column,

and eluted with 0.5 M HCl. The yield of Co^{2+} was then determined and the results are shown in Table II-4. The range of Cr^{2+} concentrations is limited, but still covers a portion of the range covered in kinetics experiments. The scatter is rather large but the yield of Co^{2+} is generally in the range of 60-70%.

Two experiments were done with the reduction of cyanomethylcobaloxime. A 50-ml reaction mixture was prepared of $[NCCH_2Co(dmgH)_2B]$ = 5.0×10^{-4} M, $[Cr^{2+}] = 2 \times 10^{-2}$ M, $[H^+]$ = 0.01 M and was allowed to react for 10 minutes, air oxidized, and products separated by ion exchange using HCl as eluting agent. The yield of Co^{2+} was only 11%. A brown material was eluted with 1 M HCl ahead of the dimeric Cr(III) (contrary to the results for R = ICH_2) and contained a metal atom ratio of Cr/Co = 2.53. When an identical reaction mixture was allowed to react for one hour the yield of Co^{2+} was still only 12%, but the metal atom ratio of the brown material (on the resin) was Cr/Co = 4.48.

In summary, the stoichiometric ratio of metal ion reactants in the first-stage reaction is 1, with at least one additional chromous ion being consumed in the second-stage reaction. The ultimate products of the reaction are then RH, Co^{2+}, a Cr(III)-dimethylglyoxime complex, and a highly-charged complex containing about four Cr atoms to one Co atom. The first-stage stoichiometry is also 1:1 for the cyanomethylcobaloxime reaction, although the second-stage stoichiometry requires either two or three Cr^{2+} ions. A low yield of Co^{2+} is obtained and a highly-charged product with a high ratio of Cr to Co is again produced.

Table II-4. Yield of Co^{2+} as a function of $[Cr^{2+}]$ for the reaction of iodomethylcobaloxime with Cr^{2+}. Conditions: $[H^+]$ = 0.010 M, T = 25° C, reaction time = 1 hour

$10^4[ICH_2Co(dmgH)_2(H_2O)]/M$	$10^2[Cr^{2+}]/M$	Yield Co^{2+}/%
2.45	0.305	72
2.39	0.595	68
2.90	0.595	59
2.33	0.872	64
2.28	1.14	64
2.90	1.14	59
3.9	2.4	63

Kinetics

All kinetic experiments were followed at λ = 460 nm. In most cases both the formation and decomposition of the intermediate were followed in a single run and the data were treated biphasically. Where the first- and second-stage rates were sufficiently different the two stages were treated independently and rate constants were determined from plots of $\log(D - D_\infty)$ versus time or from Swinbourne plots. Exceptions are noted below. All reactions were done at μ = 1.0 M and T = 25° C.

The most extensive kinetic study was that of the chromous reduction of iodomethylcobaloxime. All rate constants were obtained from a biphasic treatment of the data and Table II-5 lists the conditions and pseudo-first-order rate constants of each experiment. Figure II-8 shows that a plot of k^I_{obs} (the pseudo-first-order rate constant for the first-stage reaction) versus $[Cr^{2+}]$ is linear except at the lowest Cr^{2+} concentrations. The reaction therefore follows a second order rate law (Equation II-5) with $k^I = 3.88 \pm 0.19\ M^{-1}\ s^{-1}$. No effort was made to

$$\frac{d[Int]}{dt} = k^I[RCo(dmgH)_2(H_2O)][Cr^{2+}] \qquad \text{(II-5)}$$

define any possible acid dependence of k^I.

The kinetics of reduction of bromomethylcobaloxime were also analyzed by a biphasic treatment of data and the results are shown in Table II-6. As with the iodomethylcobaloxime a plot of k^I_{obs} versus Cr^{2+} is linear (Figure II-9) implying a rate law for the first-stage reaction

Table II-5. Kinetic data for the reaction of $ICH_2Co(dmgH)_2(H_2O)$ with Cr^{2+}. Conditions: μ = 1.0 M, T = 25° C, λ = 460 nm

$10^4[ICH_2Co(dmgH)_2(H_2O)]/M$	$10^2[Cr^{2+}]/M$	$10^2 k^I_{obs}/s^{-1}$	$k^I/M^{-1}\ s^{-1}$ [a]	$10^2 k^{II}_{obs}/s^{-1}$
		$[H^+]$ = 0.010 M		
0.975	0.122	1.06	8.7	0.219
1.29	0.316	1.81	5.7	0.402
0.960	0.360	1.68	4.7	0.472
0.878	0.376	1.69	4.5	0.506
1.27	0.517	-	-	0.677
0.945	0.592	2.33	3.9	0.651
0.864	0.616	2.32	3.76	0.711
1.27	0.619	2.54	4.10	0.676
0.924	0.926	3.87	4.18	0.728
0.843	0.963	3.62	3.76	0.870
1.24	1.02	-	-	0.887
1.24	1.02	-	-	0.955
0.630	1.18	4.57	3.87	0.917
0.646	1.23	4.74	3.85	0.829
0.983	1.23	4.92	4.00	0.915

[a] $k^I = k^I_{obs}[Cr^{2+}]^{-1}$.

Table II-5. (Continued)

$10^4[ICH_2Co(dmgH)_2(H_2O)]$/M	$10^2[Cr^{2+}]$/M	$10^2k^I_{obs}/s^{-1}$	$k^I/M^{-1}\ s^{-1}$	$10^2k^{II}_{obs}/s^{-1}$
1.27	1.55	-	-	1.14
1.24	2.03	-	-	1.28
1.27	2.58	-	-	1.60
1.24	3.04	-	-	1.64
1.27	3.62	-	-	1.79
1.24	4.06	-	-	1.95
1.33	5.30	-	-	2.16
1.33	7.94	-	-	2.95
	$[H^+]$ = 0.018 M			
1.33	5.30	-	-	3.08
1.35	7.94	-	-	4.21
	$[H^+]$ = 0.020 M			
1.15	0.218	-	-	0.230
1.14	0.540	-	-	0.572
1.13	0.750	-	-	0.922
1.12	1.06	-	-	1.07

Table II-5. (Continued)

$10^4[ICH_2Co(dmgH)_2(H_2O)]$/M	$10^2[Cr^{2+}]$/M	$10^2k^I_{obs}/s^{-1}$	$k^I/M^{-1}\ s^{-1}$	$10^2k^{II}_{obs}/s^{-1}$
1.12	1.06	-	-	1.16
1.14	1.62	-	-	1.66
1.12	2.12	-	-	1.93
1.12	2.12	-	-	2.03
1.14	2.70	-	-	2.10
1.12	3.18	-	-	2.15
1.18	3.93	-	-	2.78
1.12	4.24	-	-	2.63
	$[H^+]$ = 0.041 M			
1.33	5.30	-	-	4.06
1.33	7.94	-	-	4.52

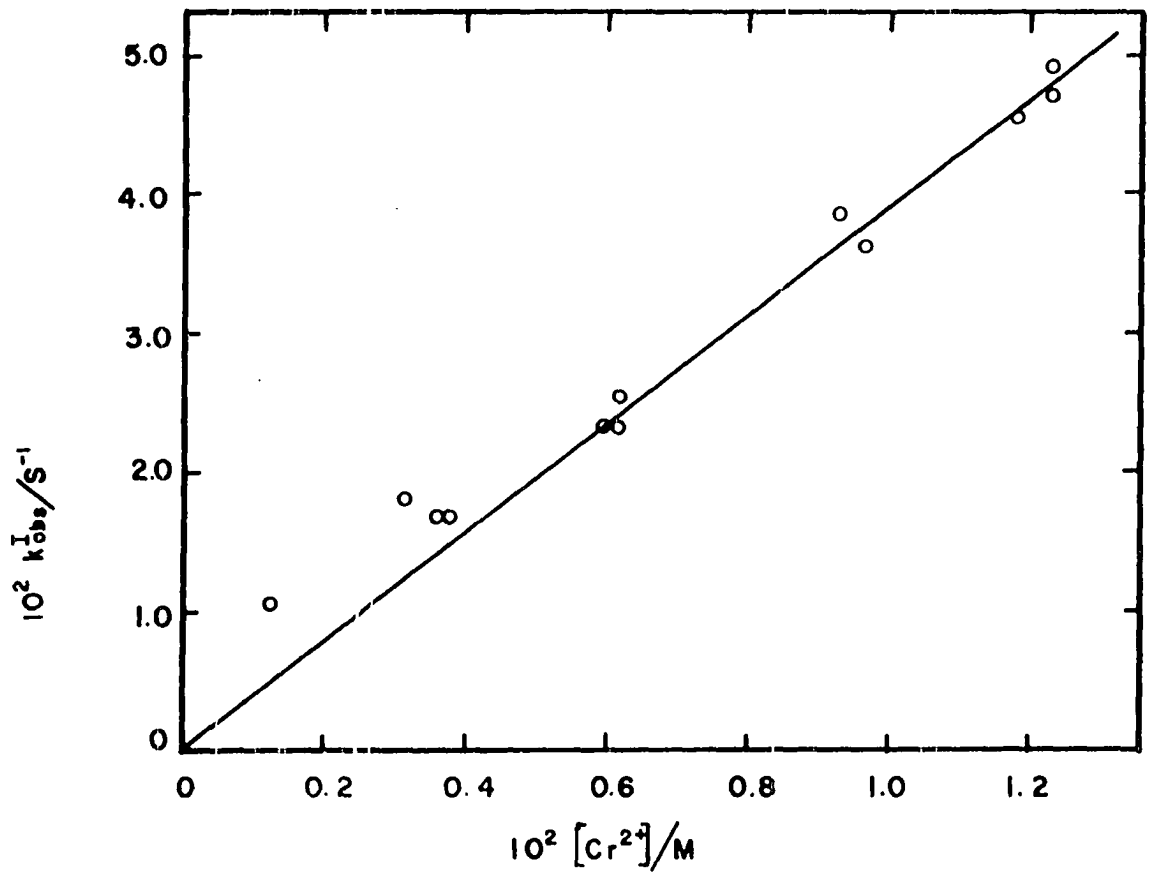

Figure II-8. The dependence of k^I_{obs} on $[Cr^{2+}]$ for the reaction of $ICH_2Co(dmgH)_2(H_2O)$ with Cr^{2+}

Table II-6. Kinetic data for the reaction of $BrCH_2Co(dmgH)_2(H_2O)$ with Cr^{2+}. Conditions: $[H^+]$ = 0.010 M, μ = 1.0 M, T = 25° C, λ = 460 nm

$10^4[BrCH_2Co(dmgH)_2(H_2O)]$/M	$10^2[Cr^{2+}]$/M	$10^2 k^I_{obs}/s^{-1}$	$k^I/M^{-1}\ s^{-1}$ [a]	$10^3 k^{II}_{obs}/s^{-1}$
1.35	0.570	1.06	1.86	2.96
1.35	1.14	1.64	1.44	4.63
1.40	1.72	2.20	1.28	6.11
1.35	3.31	3.81	1.15	8.40
1.35	6.63	7.48	1.13	9.16

[a] $k^I = k^I_{obs}[Cr^{2+}]^{-1}$.

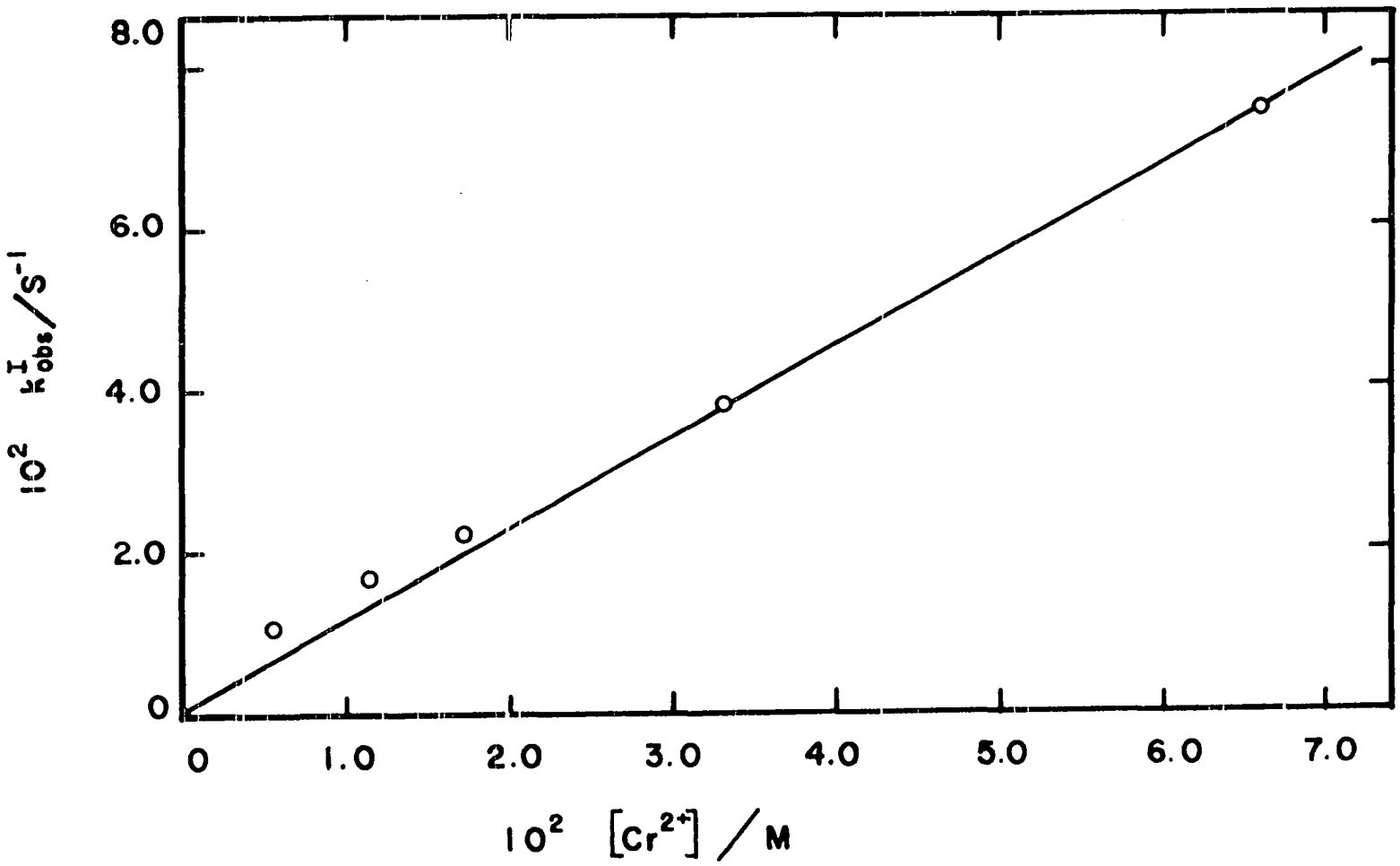

Figure II-9. The dependence of k^I_{obs} on $[Cr^{2+}]$ for the reaction of $BrCH_2Co(dmgH)_2(H_2O)$ with Cr^{2+}

which is first order in the cobaloxime and the chromous ion concentrations (Equation II-5). The value of k^I is 1.13 ± 0.02 M^{-1} s^{-1}.

The Cr^{2+} reduction of chloromethylcobaloxime presented a considerable problem with respect to the treatment of kinetic data. As with all other cobaloximes studied here, both first- and second-stage reactions could be followed but the rates of both reactions were of similar slow magnitude. Such a situation gives rise to the difficult problem of separation of rate constants of a biphasic reaction which are of similar magnitude (85). The net result of these problems was to make the reaction too slow to be studied kinetically by spectrophotometric methods.

Table II-7 gives data obtained for the first-stage rate by following the absorbance at 460 nm until the maximum absorbance was attained. The data were then treated by the method of Swinbourne (83) to obtain pseudo-first-order rate constants. The value of the second-order rate constant was determined by Equation II-6. The average value thus calculated is 0.94 ± 0.096 M^{-1} s^{-1}.[1]

---

[1]The value of k^I should, however, be viewed with suspicion. If Equation I-37 is used to compute artificial kinetic traces, the values of k^I_{obs} computed from Swinbourne plots of that data are invariably higher than the values of k^I_{obs} used in calculating the artificial traces. The problem becomes progressively worse as values of k^I_{obs} and k^{II}_{obs} become more and more similar.

Table II-7. Kinetic data for the reaction of $ClCH_2Co(dmgH)_2(H_2O)$ with Cr^{2+} as determined by Swinbourne plots. Conditions: $[H^+]$ = 0.010 M, μ = 1.0 M, T = 25° C, λ = 460 nm

$10^4[ClCH_2Co(dmgH)_2(H_2O)]$/M	$10^2[Cr^{2+}]$/M	$10^2[H^+]$/M	$10^3 k^I_{obs}/s^{-1}$	$k^I/M^{-1}\ s^{-1}$ [a]
1.20	0.135	0.1	1.37	1.01
1.20	0.308	0.1	2.19	0.711
1.20	0.615	0.1	5.89	0.958
1.20	1.23	0.1	11.0	0.895
1.20	1.23	0.1	11.0	0.895
1.05	2.50	1.0	24.2	0.968
1.05	5.00	1.0	44.5	0.890

[a] $k^I = k^I_{obs}[Cr^{2+}]^{-1}$.

$$k^I = k^I_{obs}[Cr^{2+}]^{-1} \qquad \text{(II-6)}$$

For methoxycarbonylmethylcobaloxime the first-stage reaction with chromous ion was of sufficiently greater rate than the second-stage reaction rate that each stage could be studied independently without interference by the other stage. Table II-8 shows the kinetic results for the study of the first-stage reaction. A plot of k^I_{obs} versus $[Cr^{2+}]$ (Figure II-10) is linear with a slope of $k^I = 1500 \pm 40\ M^{-1}\ s^{-1}$.

The chromous ion reduction of cyanomethylcobaloxime was found also to form a λ 460 intermediate, but this intermediate decomposed by a different mechanism. In particular, the first-stage reaction was still of stopped-flow speed and the second-stage reaction was too fast for slower-speed techniques. Therefore, both stages were followed on the stopped-flow instrument and the data were analyzed by a two-stage treatment.

Table II-9 shows pseudo-first-order rate constants obtained for the reaction at two different acid concentrations. Figure II-11 is a plot of k^I_{obs} as a function of $[Cr^{2+}]$. The linearity of the plot indicates that the first-stage reaction follows the same rate law as all other first-stage reactions studied here (Equation II-5). The value of k^I is $153 \pm 10\ M^{-1}\ s^{-1}$. Included in the table and plot are data taken from the reduction of aged cyanomethylcobaloxime solutions. According to the data of Brown, et al. (84), fresh solutions (with pyridine as the axial base) aquate only slowly. The data show that the identity of the axial base has no effect on the rate of reduction.

Table II-8. Kinetic data for the first-stage reaction of $CH_3O_2CCH_2Co(dmgH)_2(H_2O)$ with Cr^{2+}. Conditions: $[H^+] = 0.010$ M, $\mu = 1.0$ M, T = 25° C, $\lambda = 460$ nm

$10^4[CH_3O_2CCH_2Co(dmgH)_2(H_2O)]/M$	$10^2[Cr^{2+}]/M$	k^I_{obs}/s^{-1}	$10^{-3}k^I/M^{-1}\ s^{-1}$ [a]
1.31	0.565	9.7	1.72
1.31	1.13	16.1	1.42
0.99	2.09	29.1	1.39
1.31	2.32	30.8	1.33
0.99	3.01	42.4	1.41
0.99	5.12	73.2	1.43
1.31	7.06	107.2	1.52

[a] $k^I = k^I_{obs}[Cr^{2+}]^{-1}$.

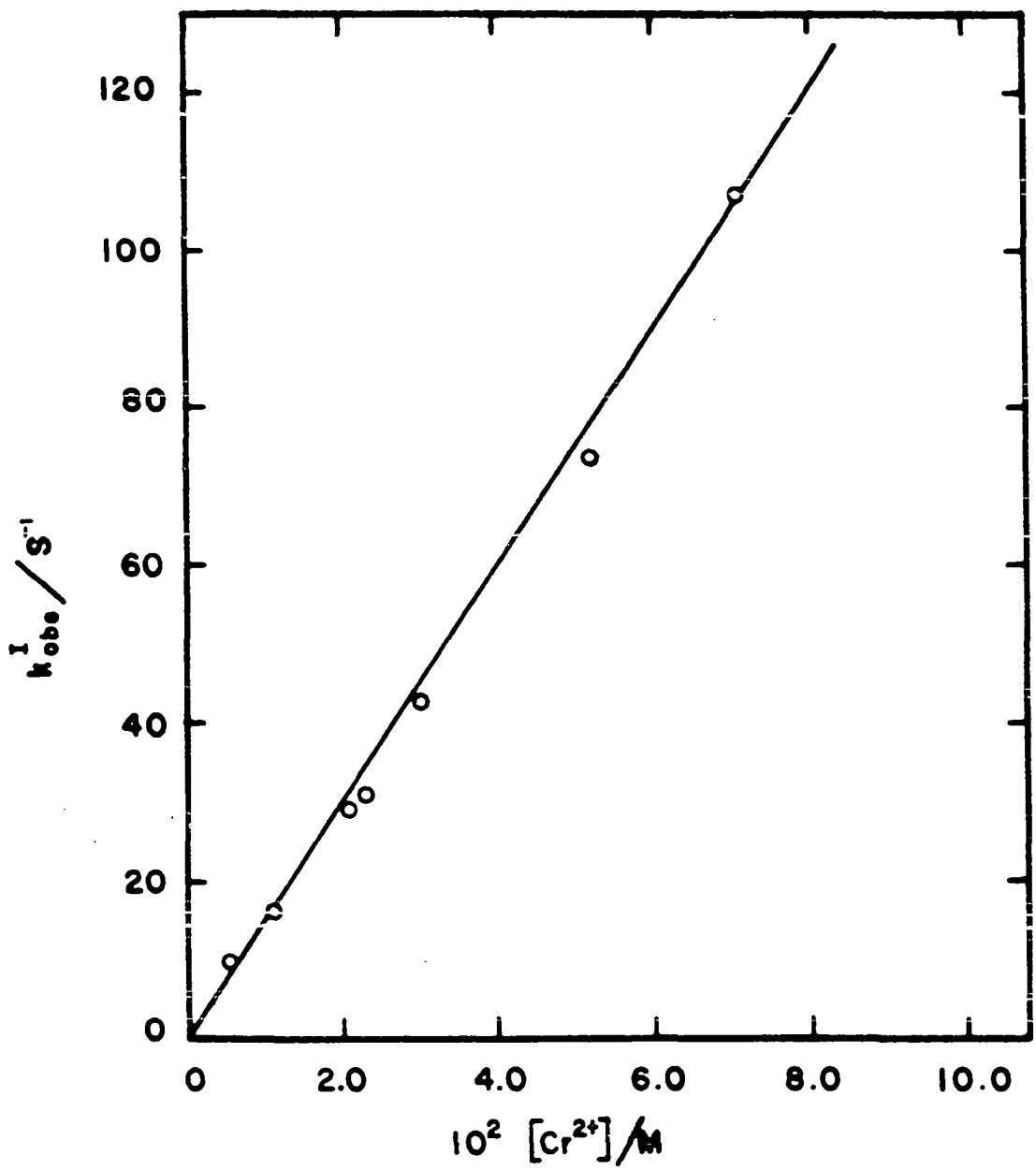

Figure II-10. The dependence of the k^I_{obs} on [Cr^{2+}] for the reaction of $CH_3O_2CCH_2Co(dmgH)_2(H_2O)$ with Cr^{2+}

Table II-9. Kinetic data for the reaction of $NCCH_2Co(dmgH)_2B$ with Cr^{2+}. Conditions: μ = 1.0 M, T = 25° C, λ = 460 nm

$10^4[NCCH_2Co(dmgH)_2B]$/M	$10^2[Cr^{2+}]$/M	k^I_{obs}/s^{-1}	$10^{-2}k^I/M^{-1}\ s^{-1}$ [a]	k^{II}_{obs}/s^{-1}
	$[H^+]$ = 0.01 M (fresh solution)			
0.865	0.360	0.637	1.77	0.120
0.865	0.770	1.08	1.40	0.266
0.865	1.50	2.59	1.73	0.817
0.865	2.00	2.75	1.38	1.02
0.865	3.67	6.22	1.69	1.18
0.865	5.43	9.11	1.68	1.99
	$[H^+]$ = 0.02 M (fresh solution)			
1.12	0.51	0.774	1.52	0.089
1.12	1.14	1.72	1.51	0.208
1.12	2.71	3.17	1.17	0.489
1.12	4.08	5.69	1.39	0.633
1.12	5.35	6.44	1.20	0.755
1.12	6.02	9.51	1.58	0.964

[a] $k^I = k^I_{obs}[Cr^{2+}]^{-1}$.

Table II-9. (Continued)

$10^4[NCCH_2Co(dmgH)_2B]$/M	$10^2[Cr^{2+}]$/M	k^I_{obs}/s^{-1}	$10^{-2}k^I/M^{-1}\ s^{-1}$	k^{II}_{obs}/s^{-1}
	$[H^+]$ = 0.02 M (aged solution)			
1.12	0.51	1.03	2.02	0.112
1.12	1.14	2.76	2.42	0.246
1.12	2.71	3.94	1.45	0.609
1.12	4.08	7.08	1.74	0.873
1.12	5.35	7.29	1.36	1.10
1.12	6.02	10.90	1.81	1.16

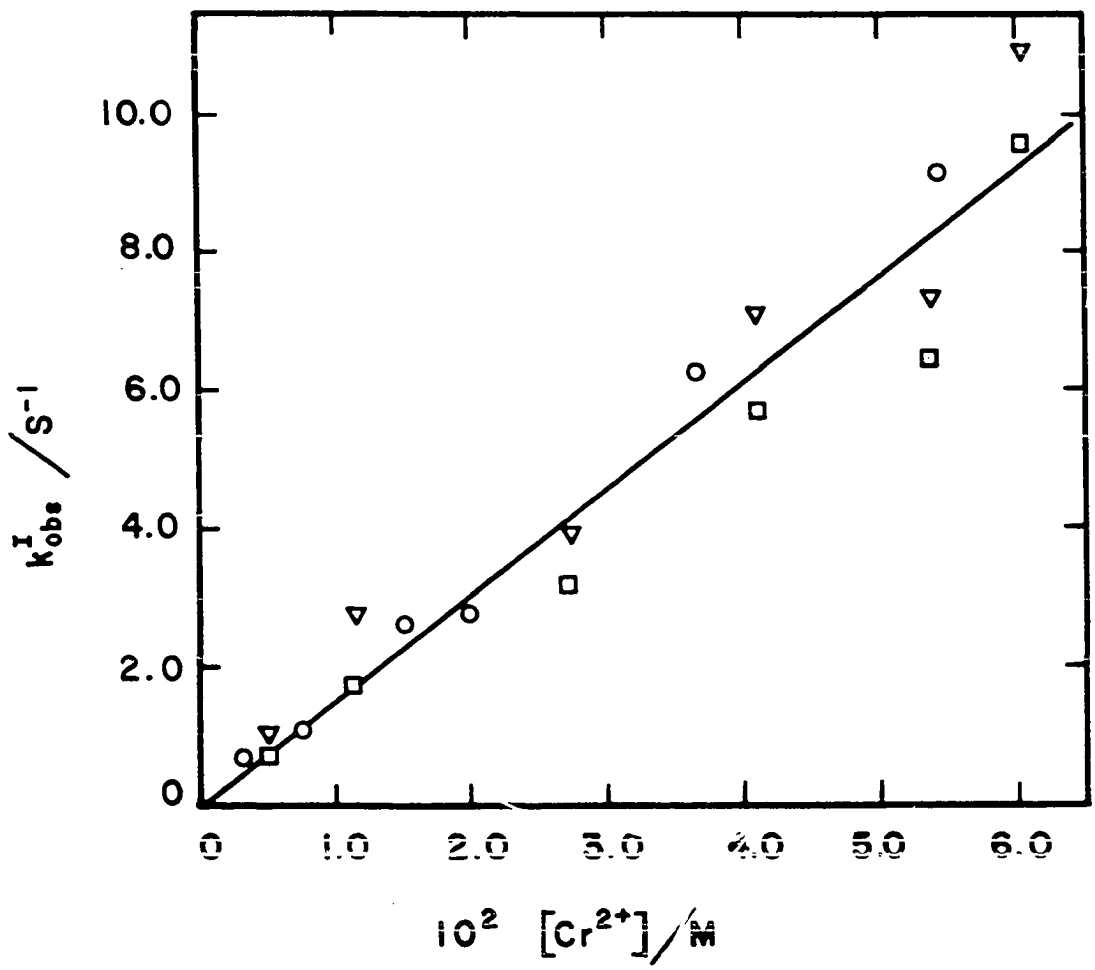

Figure II-11. The dependence of k^I_{obs} on $[Cr^{2+}]$ for the reaction of $NCCH_2Co(dmgH)_2B$ with Cr^{2+}. o, $[H^+]$ = 0.010 M, freshly prepared solution; □, $[H^+]$ = 0.020 M, freshly prepared solution; ∇, $[H^+]$ = 0.020 M, aged solution

The kinetics of decay of the intermediate were not so simply explained as were the data for the first-stage reactions. A plot of $k_{obs}^{II}[H^+]^{-1}$ versus $[Cr^{2+}]$ for the reduction of $ICH_2Co(dmgH)_2(H_2O)$ gave a curved line for each acid concentration (Figure II-12). Thus the rate law was neither first-order in $[H^+]$ nor zero-order in $[Cr^{2+}]$. The single-term rate law containing only Cr^{2+} and H^+ concentration dependencies in k_{obs}^{II} which best fits the data at hand was of the form of Equation II-7 with k_{obs}^{II} being defined as shown. A plot of $[Cr^{2+}](k_{obs}^{II})^{-1}$

$$-\frac{d[Int]}{dt} = k_{obs}^{II}[Int] \qquad \text{(II-7)}$$

$$k_{obs}^{II} = \frac{[Cr^{2+}][H^+]}{\alpha[Cr^{2+}] + \beta[H^+]} \qquad \text{(II-8)}$$

versus $[Cr^{2+}][H^+]^{-1}$ would give a straight line of slope = α and intercept = β if this were the correct rate law. Figure II-13 shows that such an assignment was not unreasonable although the scatter is very great. The values of the slope and intercept are $\alpha = 0.267 \pm 0.024$ M s and $\beta = 0.828 \pm 0.068$ M s, respectively. (Other two-parameter expressions for k_{obs}^{II} were tried and found to fit the data very poorly. More complicated expressions were not tried because such attempts soon become an exercise in mathematics with little or no meaningful physical interpretation.)

The observed first-order rate constants (Table II-6) for the second-stage reaction of bromomethylcobaloxime were again found not to be a

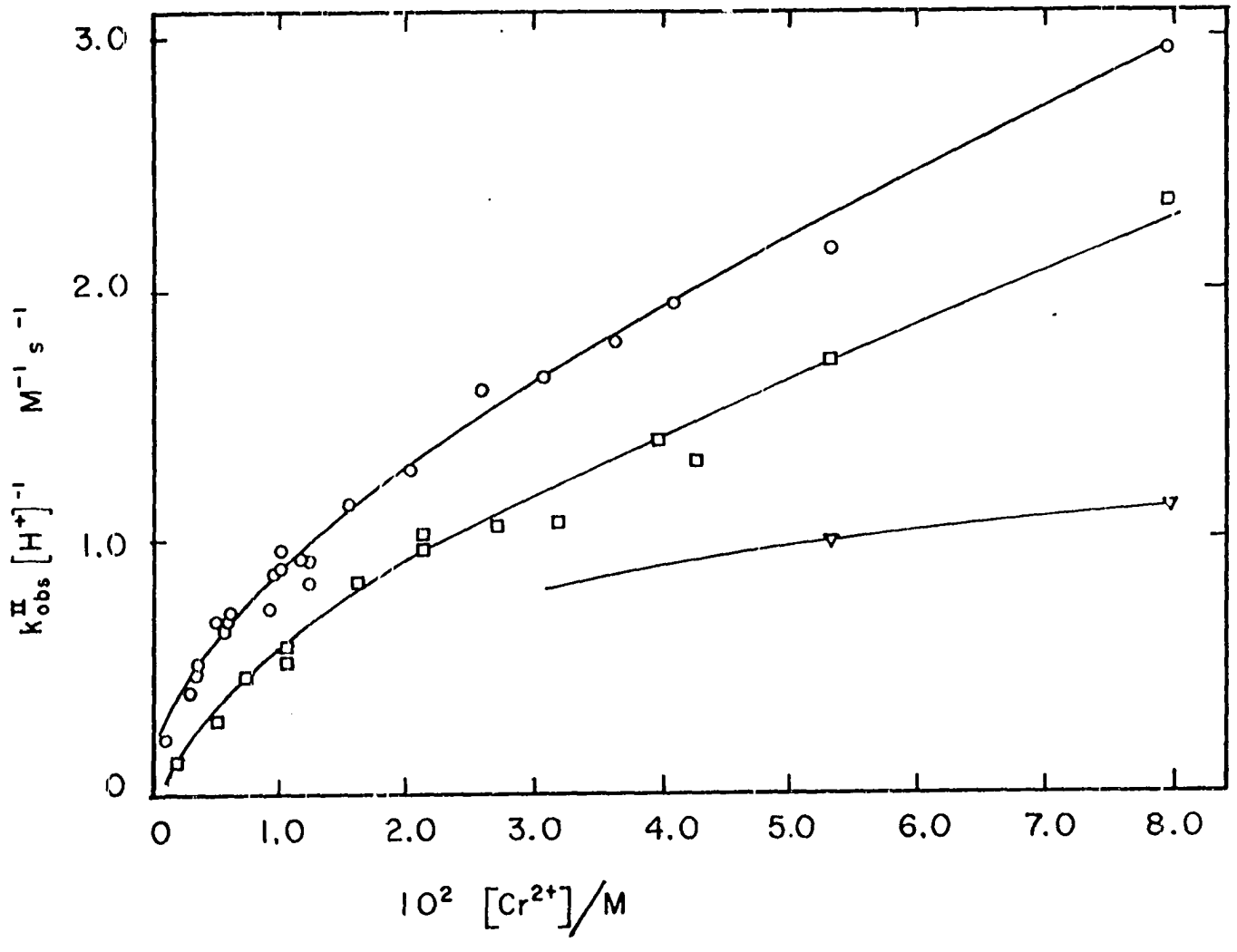

Figure II-12. The dependence of k^{II}_{obs} on $[Cr^{2+}]$ and $[H^+]$ for the reaction of $ICH_2Co(dmgH)_2(H_2O)$ with Cr^{2+}. o, $[H^+]$ = 0.010 M; □, $[H^+]$ = 0.020 M; ∇, $[H^+]$ = 0.040 M

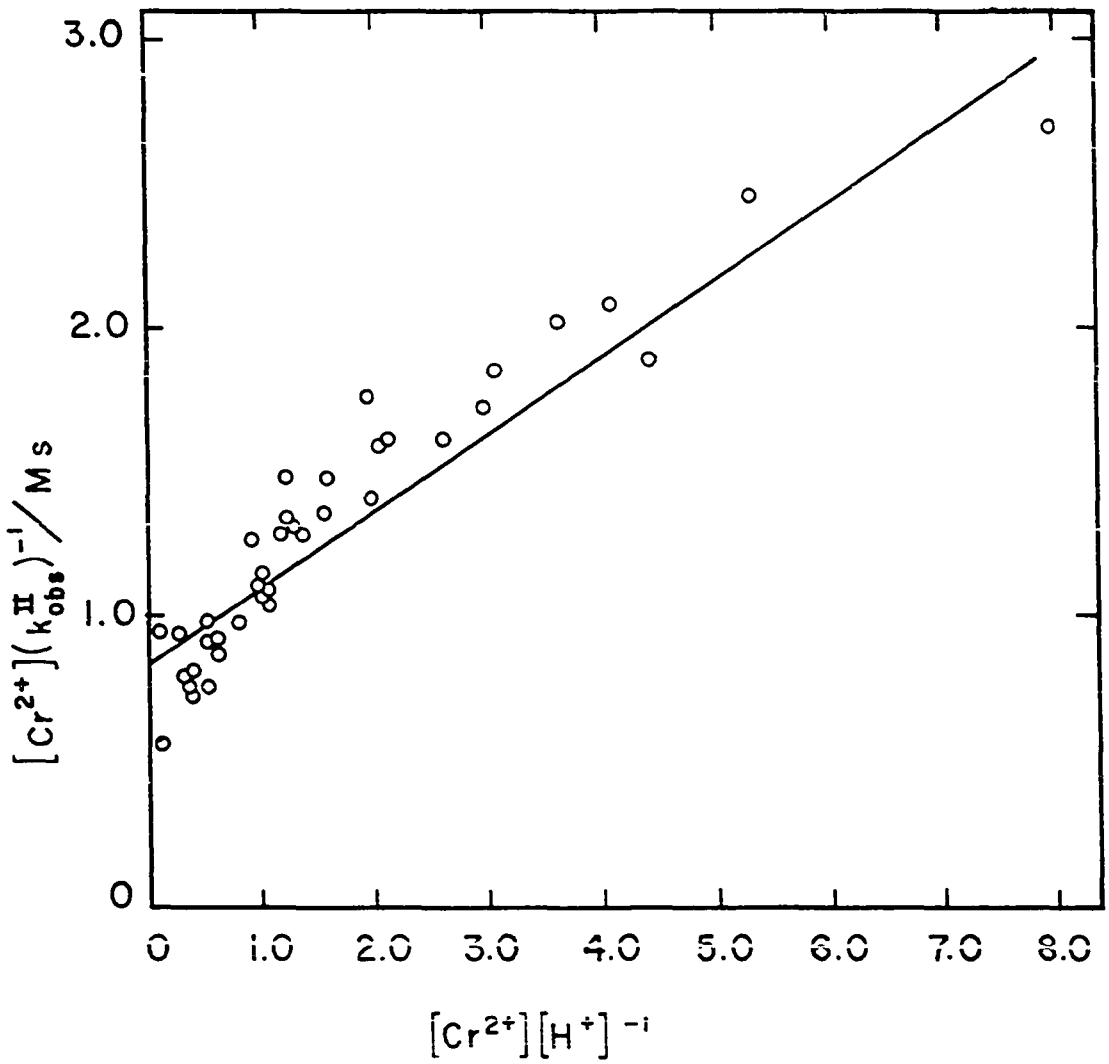

Figure II-13. Plot according to Equation II-8 for the reaction of $ICH_2Co(dmgH)_2(H_2O)$ with Cr^{2+}

simple linear function of chromous concentration (Figure II-14). Although the data were limited, a plot of $[Cr^{2+}](k^{II}_{obs})^{-1}$ versus $[Cr^{2+}][H^+]^{-1}$ (Figure II-15) was linear as in the case of iodomethylcobaloxime. The values of the slope and intercept are $\alpha = 0.869 \pm 0.041$ M s and $\beta = 1.36 \pm 0.14$ M s, respectively.

Pseudo-first-order rate constants for the second-stage reaction of methoxycarbonylmethylcobaloxime at two slightly different H^+ concentrations are given in Table II-10. A plot of k^{II}_{obs} versus $[Cr^{2+}]$ (Figure II-16) again gave a different curved line for each acid concentration. A plot of $[Cr^{2+}](k^{II}_{obs})^{-1}$ versus $[Cr^{2+}][H^+]^{-1}$ (Figure II-17), however, gave a very good straight line with slope = $\alpha = 0.934 \pm 0.020$ M s and intercept = $\beta = 0.0266 \pm 0.0106$ M s.

The kinetic data for the second-stage reaction of cyanomethylcobaloxime (Table II-9) showed that the mechanism of intermediate reaction was distinct from all other systems studied here. A plot of $k^{II}_{obs}[H^+]$ versus $[Cr^{2+}]$ (Figure II-18) was linear, demonstrating that the second-stage rate law was of the form of Equation II-9. The slope was k^{II} =

$$-\frac{d[Int]}{dt} = k^{II}\frac{[Int][Cr^{2+}]}{[H^+]} \qquad \text{(II-9)}$$

$0.346 \pm 0.020\ s^{-1}$ and the intercept was zero. The plot also shows that the second-stage reaction is also independent of the nature of the axial ligand.

Prince and Segal (75) previously studied the reaction of diamminecobaloxime with Cr^{2+} to give a species absorbing intensely at 464 nm.

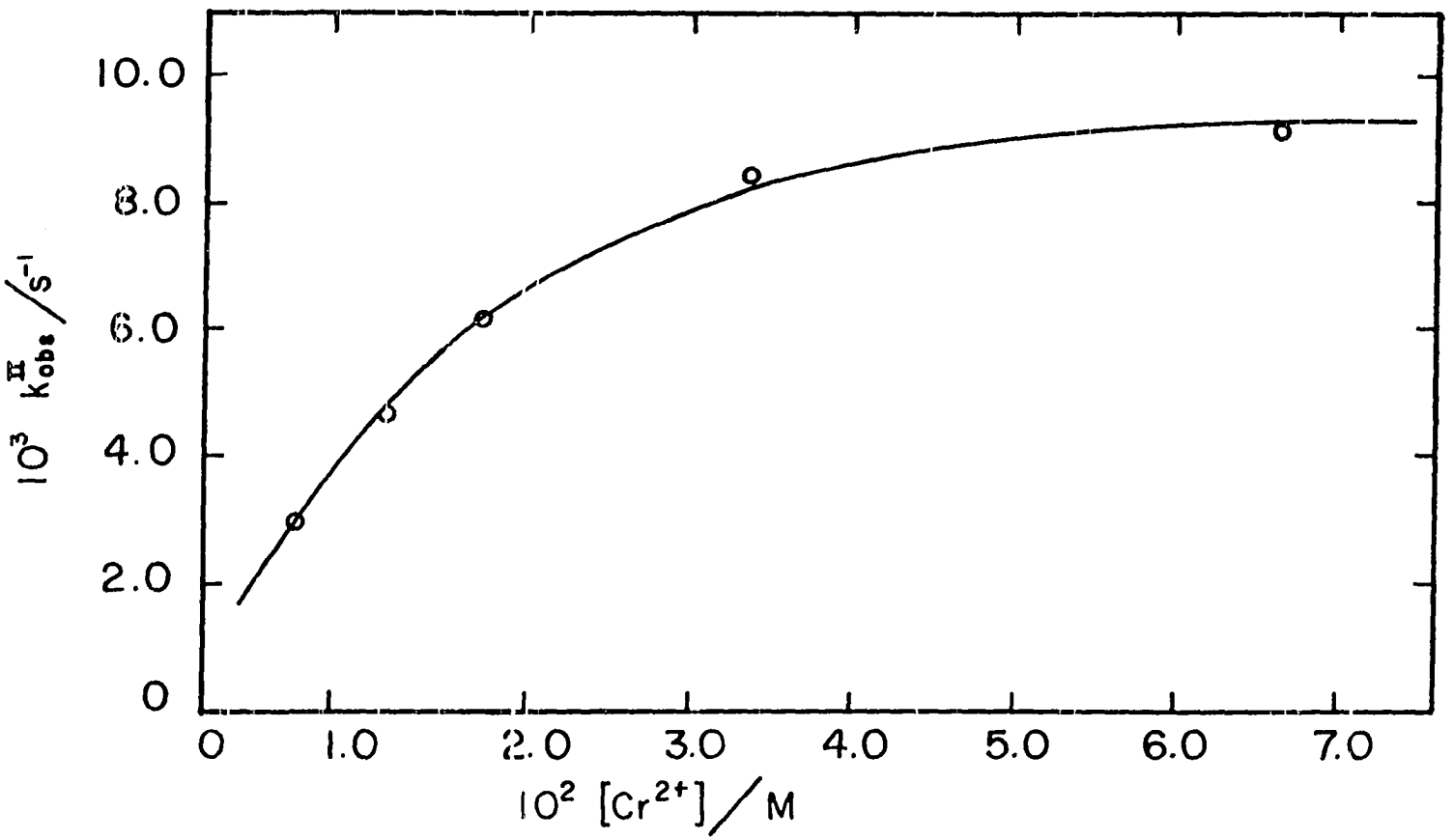

Figure II-14. The dependence of k^{II}_{obs} on $[Cr^{2+}]$ for the reaction of $BrCH_2Co(dmgH)_2(H_2O)$ with Cr^{2+}

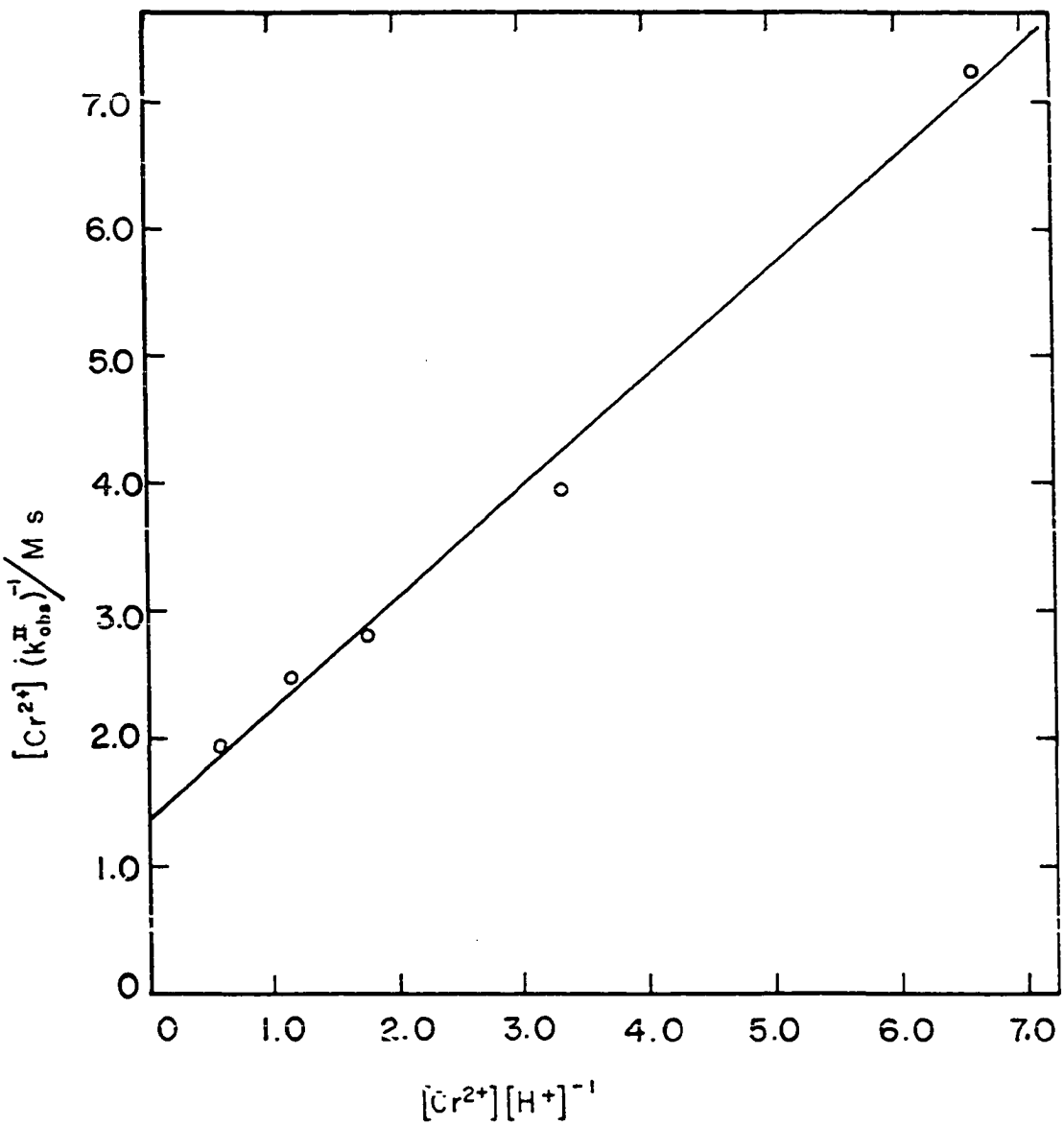

Figure II-15. Plot according to Equation II-8 for the reaction of $BrCH_2Co(dmgH)_2(H_2O)$ with Cr^{2+}

Table II-10. Kinetic data for the second-stage reaction of $CH_3O_2CCH_2Co(dmgH)_2(H_2O)$ with Cr^{2+}. Conditions: μ = 1.0 M, T = 25° C, λ = 460 nm

$10^4[CH_3O_2CCH_2Co(dmgH)_2(H_2O)]$/M	$10^2[Cr^{2+}]$/M	$10^2 k^{II}_{obs}/s^{-1}$
$[H^+]$ = 0.005 M		
0.65	0.077	0.228
0.65	0.231	0.324
0.65	0.384	0.417
0.65	0.537	0.390
0.65	0.768	0.416
0.65	1.152	0.363
$[H^+]$ = 0.010 M		
0.71	0.126	0.789
0.73	0.320	0.933
0.76	0.615	1.00
0.70	1.23	1.42
$[H^+]$ = 0.015 M		
0.683	0.0985	1.41
0.455	0.295	1.44
0.683	0.492	1.51
0.683	0.689	1.46
0.683	0.985	1.55
0.683	0.985	1.62
0.683	1.477	1.55

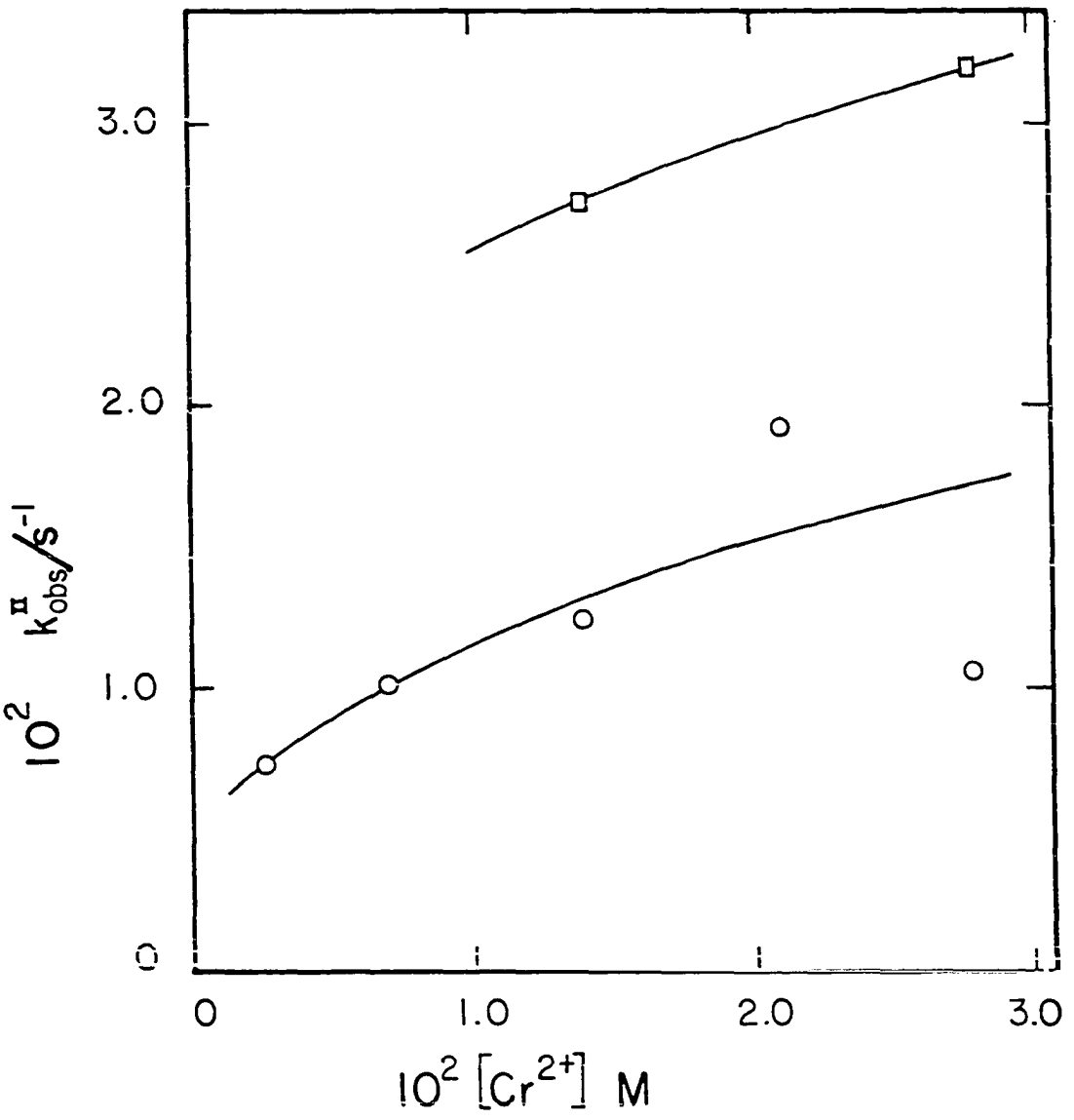

Figure II-16. The dependence of k^{II}_{obs} on [Cr^{2+}] and [H^+] for the reaction of $CH_3O_2CCH_2Co(dmgH)_2(H_2O)$ with Cr^{2+}. ○, [H^+] = 0.010 M; □, [H^+] = 0.015 M

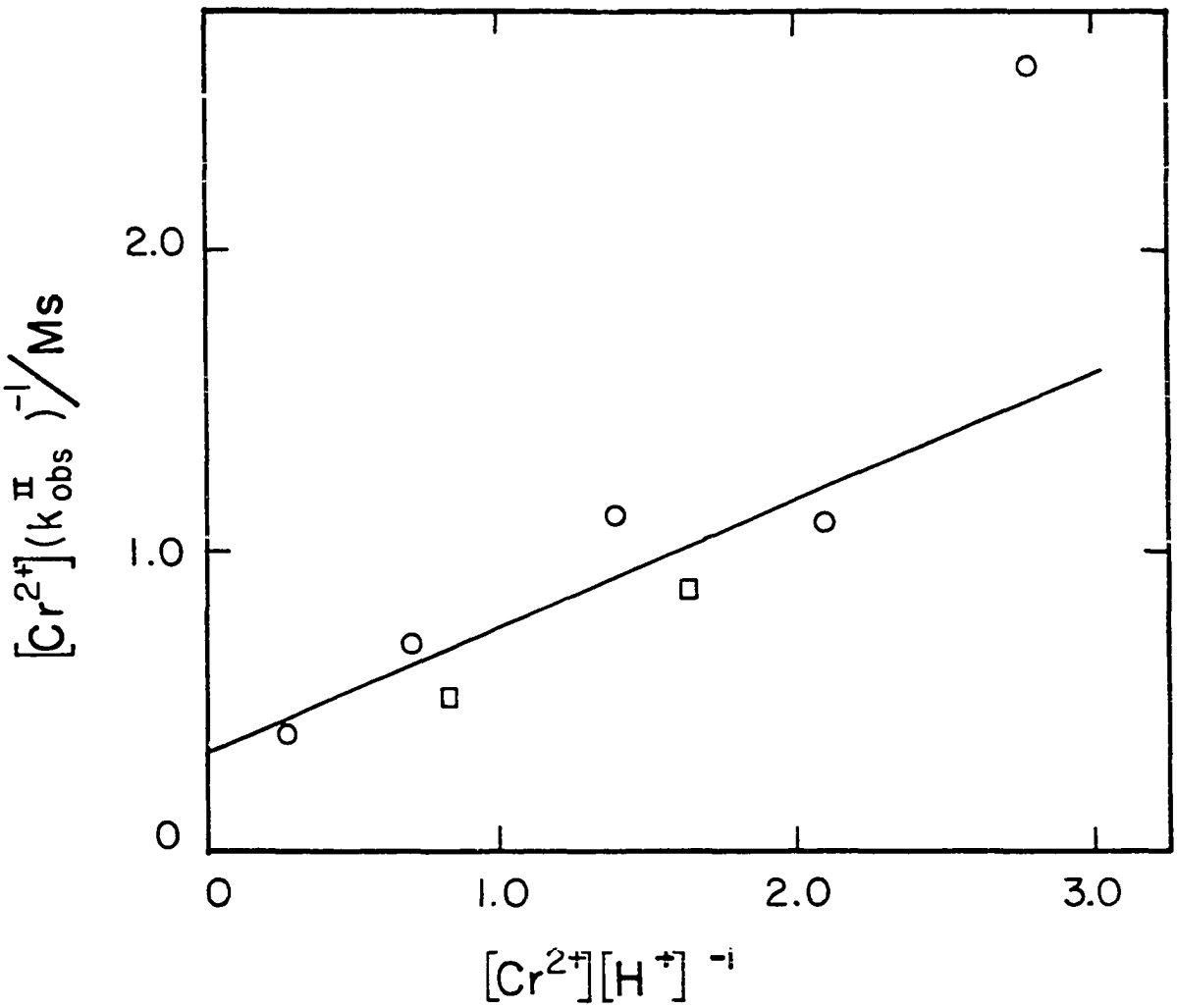

Figure II-17. Plot according to Equation II-8 for the reaction of $CH_3O_2CCH_2Co(dmgH)_2(H_2O)$ with Cr^{2+}. ○, $[H^+]$ = 0.010 M; □, $[H^+]$ = 0.015 M

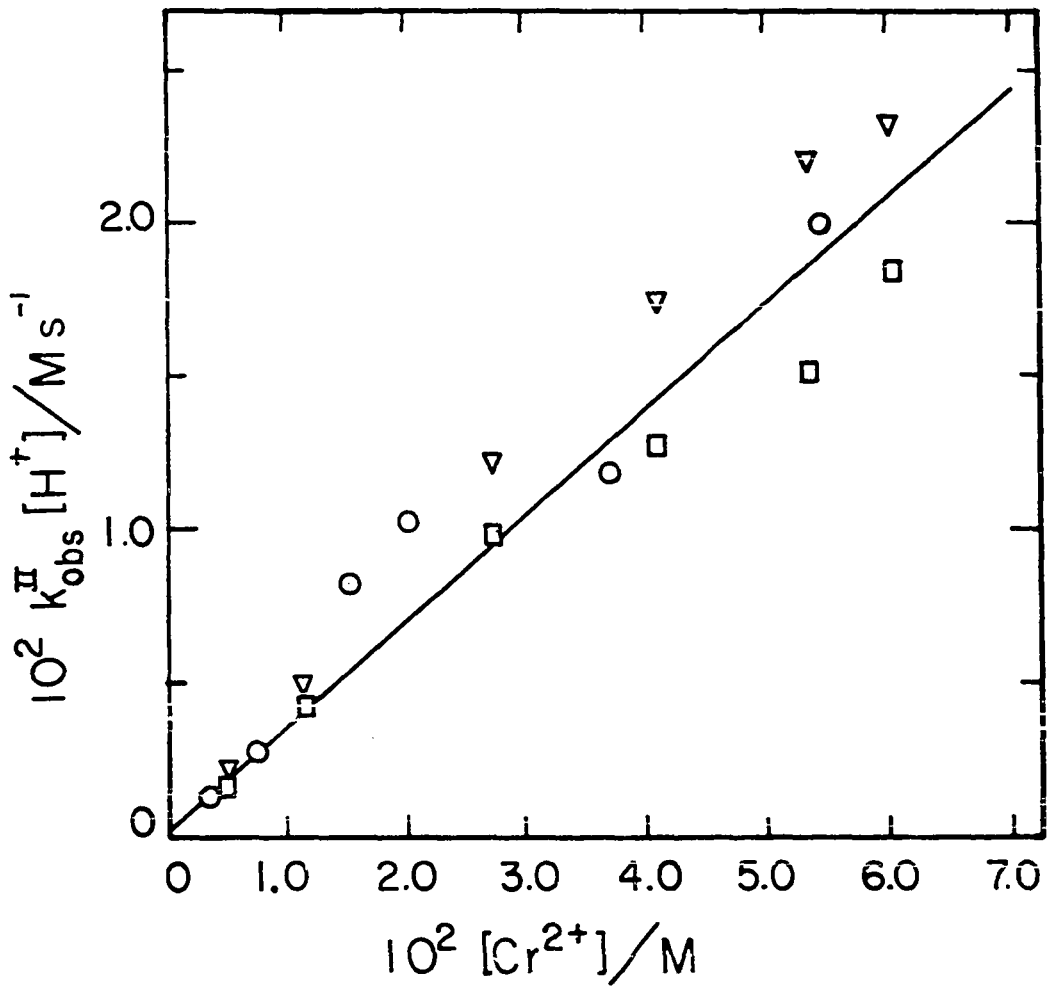

Figure II-18. The dependence of k^{II}_{obs} on $[Cr^{2+}]$ and $[H^+]$ for the reaction of $NCCH_2Co(dmgH)_2B$ with Cr^{2+}. o, $[H^+]$ = 0.010 M, fresh solution; □, $[H^+]$ = 0.020 M, fresh solution; ▽, $[H^+]$ = 0.020 M, aged solution

The rate law was of the form of Equation II-5 where $k^{I} = 40 + 780\ [H^{+}]$. Although experimental details in the report are very limited, the experiments were not repeated here. Prince states that the 464 nm species rapidly decomposes in acid solution, and that decomposition was studied in this work.

The particular feature of the second-stage reaction of the diammine complex is that k_{obs}^{II} (Table II-11) is again not a simple linear function of chromous ion concentration (Figure II-19). The functional dependence of k_{obs}^{II} as described in Equation II-8 was found to adequately represent the data as shown in Figure II-20. The slope of the least squares line is $\alpha = 0.396 \pm 0.107$ M s and the intercept is $\beta = 0.320 \pm 0.140$ M s.

All kinetic data are summarized in Table II-12.

Table II-11. Kinetic data for the second-stage reaction of $Co(dmgH)_2(NH_3)_2^+$ with Cr^{2+}. Conditions: $[H^+]$ = 0.010 M, μ = 1.0 M, T = 25° C, λ = 460 nm

$10^4[Co(dmgH)_2(NH_3)_2^+]$/M	$[H^+]$/M	$10^2[Cr^{2+}]$/M	$10^2 k_{obs}^{II}$/s^{-1}
1.29	0.010	0.274	0.729
1.29	0.010	0.696	1.01
1.29	0.010	1.39	1.24
1.29	0.010	2.09	1.92
1.29	0.010	2.78	1.06
1.29	0.017	1.39	2.72
1.29	0.017	2.78	3.19

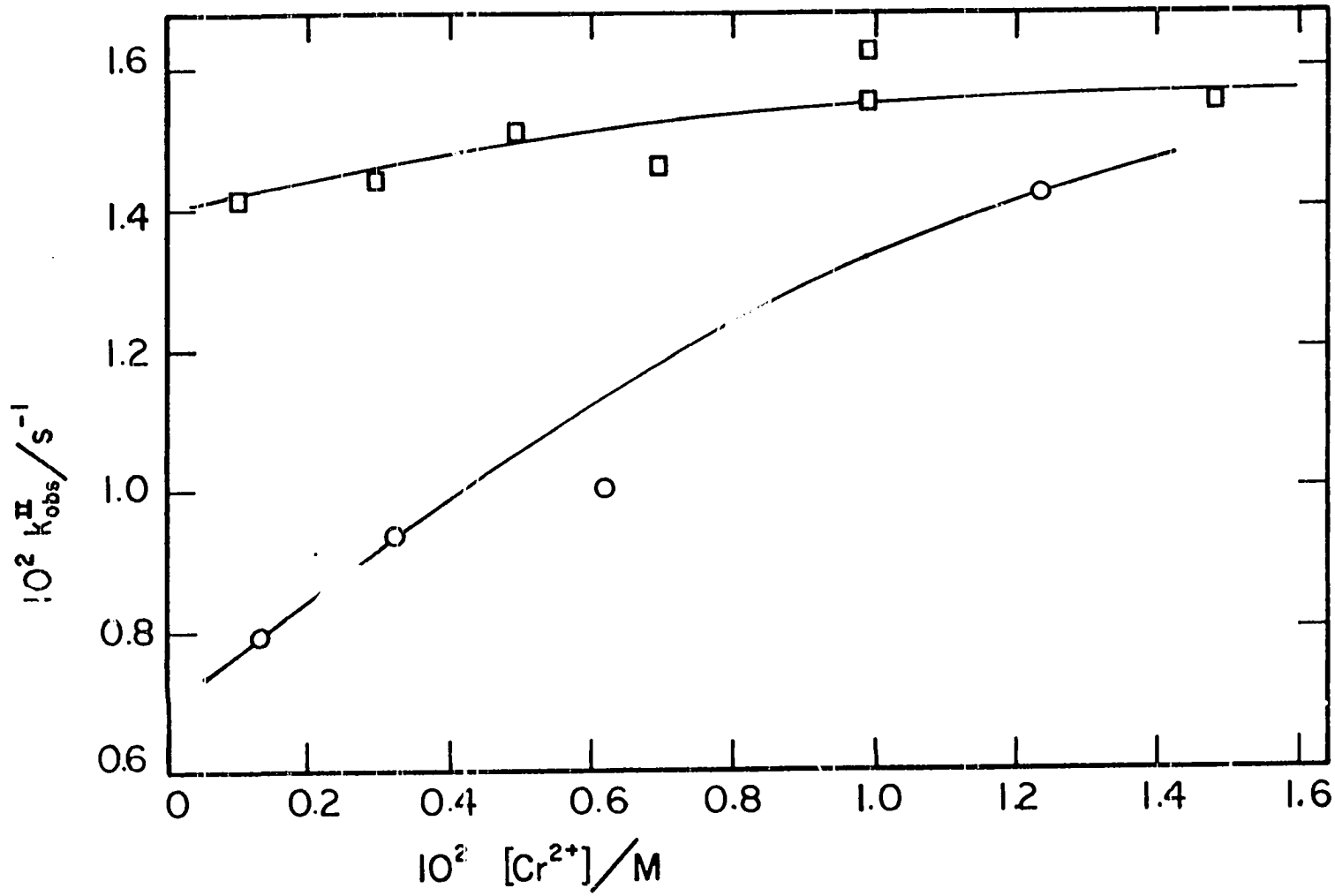

Figure II-19. The dependence of k^{II}_{obs} on $[Cr^{2+}]$ and $[H^+]$ for the reaction of $Co(dmgH)_2(NH_3)_2^+$ with Cr^{2+}. o, $[H^+]$ = 0.010 M; □, $[H^+]$ = 0.017 M

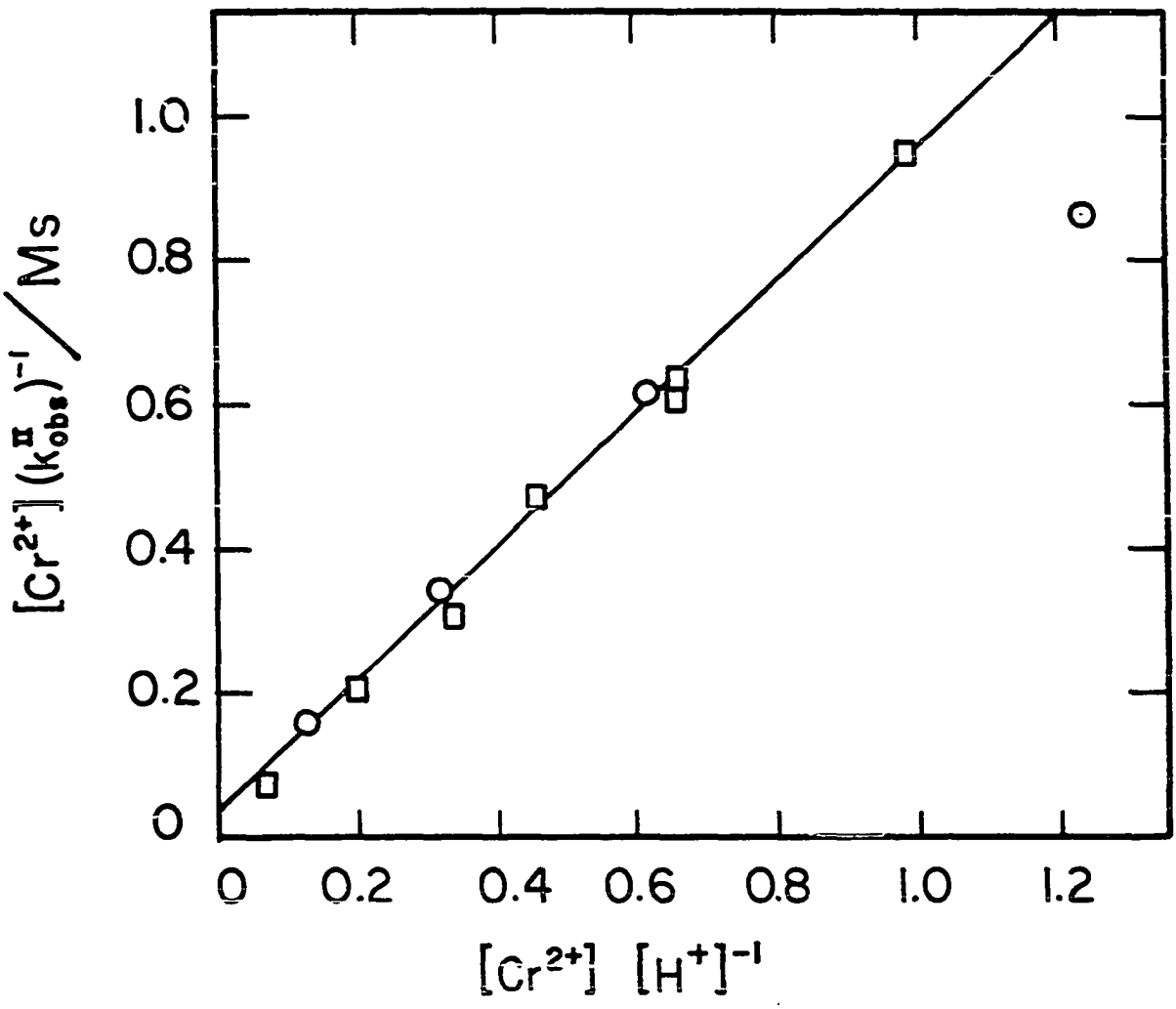

Figure II-20. Plot according to Equation II-8 for the reaction of $Co(dmgH)_2(NH_3)_2^+$ with Cr^{2+}. o, $[H^+]$ = 0.010 M; □, $[H^+]$ = 0.017 M

Table II-12 Summary of kinetic data for the reactions of substituted methylcobaloximes and $Co(dmgH)_2(NH_3)_2^+$ with Cr^{2+}. Conditions: μ = 1.0 M, T = 25° C

Compound	$k^I/M^{-1}\ s^{-1}$	$\alpha/M\ s^a$	$\beta/M\ s^a$
$ClCH_2Co(dmgH)_2(H_2O)$	0.904 ± 0.1	--	-
$BrCH_2Co(dmgH)_2(H_2O)$	1.13 ± 0.02	0.869 ± 0.041	1.36 ± 0.14
$ICH_2Co(dmgH)_2(H_2O)$	3.88 ± 0.19	0.267 ± 0.024	0.828 ± 0.068
$CH_3O_2CCH_2Co(dmgH)_2(H_2O)$	1500 ± 40	0.934 ± 0.020	0.0266 ± 0.0106
$Co(dmgH)_2(NH_3)_2^+$	$40 + 780[H^+]^b$	0.396 ± 0.107	0.320 ± 0.140
$NCCH_2Co(dmgH)_2py^c$	153 ± 10	--	-

[a] Parameters α and β defined according to Equation II-8.

[b] From Reference 75.

[c] $k^{II} = 0.346 \pm 0.020\ s^{-1}$ as defined in Equation II-9.

DISCUSSION

The salient features of the reactions which require explanation are these:

(1) The reactions of substituted methylcobaloximes with Cr^{2+} do not produce the corresponding substituted methylchromium compounds.

(2) The volatile products of reaction are halomethanes.

(3) Each reaction produces an intermediate whose electronic absorption maximum is at 460 nm.

(4) The second-stage reaction, i.e., loss of intermediate, proceeds at a slow rate in all but one case with a complicated functional dependence upon $[Cr^{2+}]$ and $[H^{+}]$.

(5) Some products are obtained which have a high ratio of Cr to Co.

The mechanism of Espenson and Shveima (73) (Equation II-2) results in a transfer of the organic group from cobalt to chromium. The monohalomethylchromium compounds which would result from an S_N2 mechanism have been known for several years (86) and their stability and spectra are documented. In particular, chloromethylchromium is stable to hydrolysis (87) and to reaction with Cr^{2+}. If Equation II-2 were the reaction operative here then ion exchange should have easily separated $CrCH_2Cl^{+}$ for spectrophotometric identification (λ_{max} = 517, 391, and 262 nm; ε = 20, 204, and 3470 M^{-1} cm^{-1}, respectively). Complex added prior to reaction was, in fact, easily recovered and identified by this method, verifying not only the above assumption but also ruling out some

unexpected process leading during this reaction to the destruction of the otherwise stable $CrCH_2Cl^{2+}$.

The volatile product of the reaction of iodomethylcobaloxime with Cr^{2+} is CH_3I. Nohr and Spreer (87) studied the reaction of $CrCH_2I^{2+}$ with Cr^{2+} and showed the inorganic products to be Cr^{3+} and CrI^{2+} with CH_4 being the only volatile organic product. Since the excess of Cr^{2+} in the reactions studied here was always large, any $CrCH_2I^{2+}$ produced should be decomposed by Cr^{2+} as in Equation II-10. Therefore, the production of $CrCH_2I^{2+}$ in the cobaloxime reaction must be ruled out. Based on these two examples $CrCH_2X^{2+}$ is assumed absent in other instances as well.

$$2Cr^{2+} + 2H^{+} + CrCH_2I^{2+} \longrightarrow CrI^{2+} + 2Cr^{3+} + CH_4 \qquad \text{(II-10)}$$

Furthermore, an S_H2 mechanism like Equation II-2 results in the simple cobalt(II) cobaloxime $Co(dmgH)_2$ which has been shown by Adin and Espenson (88) to undergo extremely rapid acidolysis ($t_{1/2}$ = 2.9 s at pH 4.9) (see Equation II-3). At the acid concentrations of the studies reported here, 0.010 M, the reaction is virtually instantaneous. Since the absorbance maxima for the intermediates are all identical to that reported by Adin and Espenson for cobaloxime(II) (460 nm), the implication is that the intermediates may well be different species of cobalt(II) cobaloxime, suggested also by its formation from reaction of RCo(III) with a one-electron reducing agent. However, since the intermediates are relatively slow to decompose, the intermediate species must be additionally stabilized to decomposition in some manner.

The Cr^{2+} reduction of $Co(dmgH)_2(NH_3)_2^+$ as investigated by Prince and Segal (75) showed an intermediate with an absorbance maximum at 464 nm. In the course of this study, we have observed that the intermediate from the same reaction has λ_{max} = 460 nm. Since electron transfer mediated by an amino group is an unlikely occurrence in acidic solution, the authors concluded that the reaction mechanism was either outer-sphere or inner-sphere through one or two of the N-O bonds of the oxime linkages of the cobaloxime. The reduction of other dimethylglyoxime complexes (89,90) by V^{2+} was shown by comparison of activation parameters to be inner-sphere with electron transfer through the N-O bonds. The authors therefore concluded that the Cr^{2+} ion reductions were of a similar nature. They also mentioned isolation by ion exchange of a Cr(III)-dimethylglyoxime complex formed in the above reaction whose stoichiometry was uncertain.

An additional piece of evidence is available to support such speculation. Bertrand, Smith, and Eller (91) have prepared a dimeric Cu(II) complex in which the two metal atoms are bridged by the N-O groups of two oxime compounds. The complex is virtually diamagnetic at room temperature, indicating a pathway for exchange of electrons or at least electronic information. The suggestion that oxime linkages can serve as electron transfer bridges is, therefore, not unreasonable.

Espenson and Bakac (92) have also noted an oxime bridged bimetallic species as an indirect result of their studies of the Br_2 oxidation of $CH_3Co(dmgH)_2(H_2O)$. The tetravalent cobaloxime produced by the oxidation

is reduced by Fe^{2+} to give a yellow complex which subsequently decomposes at a rate dependent on acid. A mixture of Fe^{3+} and $CH_3Co(dmgH)_2(H_2O)$ also gives a yellow complex which decomposes in acid solution at a rate identical to the decomposition subsequent to the Fe^{2+}—Co(IV) redox reaction. The conclusion is that both processes involve iron coordination to the oxime oxygen atoms and (for the redox process) electron transfer through the N-O bond.

The first-stage reaction of the substituted methylcobaloximes with chromous ion therefore most likely involves binding of the Cr atom to the cobaloxime through one or two of the oxygen atoms of the oxime linkages (Equation II-11) to give a heterobinuclear species; i.e., the

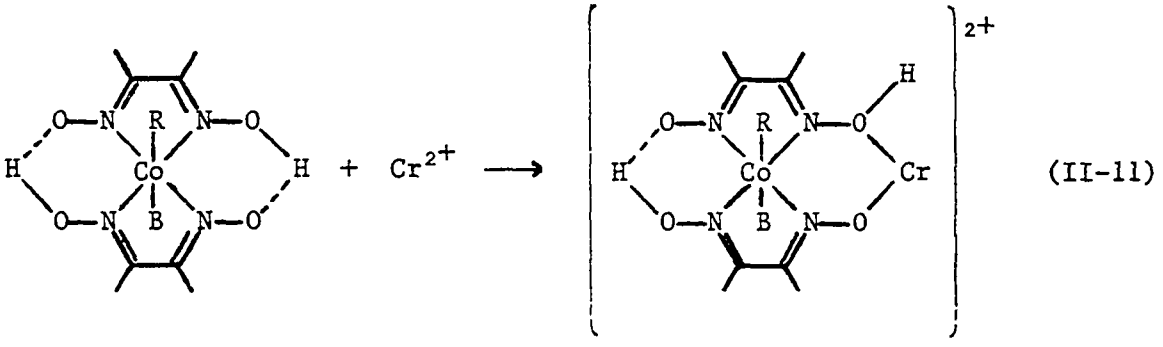

(II-11)

intermediate which absorbs light at 460 nm. The intermediate, I, has been drawn showing the R group and the base still attached to the Co atom. The presence of the different R groups for each starting material should seemingly alter the position of the absorbance maximum by at least ± 10 nm as in the $RCo(dmgH)_2(H_2O)$ starting materials. In fact, this is not observed. However, different rates of reaction in the

second-stage indicate that a distinction must exist between the various species of intermediate. The simplest explanation of that distinction is the presence of different R groups. The interaction of the R group with the Co atom must in some way be lessened so as to result in the congruence of the absorption maxima of I.

As mentioned before, the intermediate is probably a complex of Co(II) on the basis of the position of the absorption maxima, and the structure shown in Equation II-11 may possibly account for the metastability of the complex. The stability of Co(II) macrocyclic compounds toward hydrolysis is known to increase as weakly bonded portions of the macrocycle are fused and/or the charge of the complex is increased. In particular, Co(II)$(dmgH)_2$ very rapidly hydrolyzes even in weak acid, Co(II)$(dpnH)^+$ hydrolyzes much less rapidly, and Co(II)$(tim)^{2+}$ is quite stable in acidic solution (see Figure I-2). In the intermediate the O-Cr-O bridge may be acting analogously to the trimethylene bridge of Co(II)$(dpnH)^+$ to fuse the two dimethylglyoximate moities and thus stabilize the system.

The mechanism of the second-stage reaction is significantly less well-defined. The rate law as shown in Equations II-7 and II-8 is of the form of a two-step mechanism with competition between H^+ and Cr^{2+} for reaction with the steady-state intermediate. Two mechanisms, related by microscopic reversibility, are therefore possible, although the data are insufficient to delineate the intimate details of the second-stage reaction. Features of the mechanism are these:

(1) At least one additional Cr^{2+} ion must be consumed and possibly incorporated into the Co—Cr—dimethylglyoxime complex to account for the stoichiometry (2:1 overall), the high charge of the brown material tightly held on cation exchange resin, and the high Cr:Co ratio of the brown material.

(2) Two different paths must be followed to account for the two fates of cobalt; i.e., the highly-charged brown cobalt-containing complex and Co^{2+} ion.

Little more can be said of the second-stage reaction.

The reaction of cyanomethylcobaloxime has a different second-stage rate law and therefore follows a mechanism that is unique among the systems studied. There is no indication that the first-stage reaction is any different than that proposed above, but the second-stage rate law (Equation II-9) is of the same form as, for example, the Cr^{2+}-catalyzed aquation of $CrCl^{2+}$ (93). A clue to the mechanism may lie in the fact that the R group ($-CH_2CN$) contains the most strongly electron-withdrawing group of all the complexes studied here.

BIBLIOGRAPHY

1. D. H. Busch, D. G. Pillsbury, F. V. Lovecchio, A. M. Tait, Y. Hung, S. Jackels, M. C. Rakowski, W. P. Schammel, and L. Y. Martin, ACS Symp. Ser., 38, 32 (1977).

2. A. M. Tait, F. V. Lovecchio, and D. H. Busch, Inorg. Chem., 16, 2206 (1977).

3. C. K. Poon, Coord. Chem. Rev., 10, 1 (1973).

4. P. W. Schneider, P. F. Phelan, and J. Halpern, J. Am. Chem. Soc., 91, 77 (1969).

5. J. F. Endicott, J. Lilie, J. M. Kuszaj, B. S. Ramaswamy, W. G. Schmonsees, M. G. Simic, M. D. Glick, and D. P. Rillema, J. Am. Chem. Soc., 99, 429 (1977).

6. H. J. H. Fenton, J. Chem. Soc., 65, 899 (1894).

7. F. Haber and J. Weiss, Proc. Roy. Soc., A147, 332 (1934).

8. W. G. Barb, J. H. Baxendale, P. George, and K. R. Hargrave, Trans. Faraday Soc., 47, 462 (1951).

9. P. R. Carter and N. Davidson, J. Phys. Chem., 56, 877 (1952).

10. F. A. L. Anet and E. LeBlanc, J. Am. Chem. Soc., 79, 2649 (1957).

11. J. K. Kochi and D. D. Davis, J. Am. Chem. Soc., 86, 5264 (1964).

12. M. R. Hyde and J. H. Espenson, J. Am. Chem. Soc., 98, 4463 (1976).

13. H. Taube and H. Myers, J. Am. Chem. Soc., 76, 2103 (1954).

14. G. H. Kramer, Ph.D. Thesis, University of Sussex (1974).

15. G. Davies, N. Sutin, and K. O. Watkins, J. Am. Chem. Soc., 92, 1892 (1970).

16. M. Ardon and R. A. Plane, J. Am. Chem. Soc., 81, 3197 (1959).

17. J. M. Malin and J. H. Swinehart, Inorg. Chem., 8, 1407 (1969).

18. A. Adegite, H. Egboh, J. F. Ojo, and R. Olieh, J. Chem. Soc., Dalton Trans., 833 (1977).

19. A. W. Adamson, J. Am. Chem. Soc., 78, 4260 (1956).

20. A. Haim and W. K. Wilmarth, J. Am. Chem. Soc., 83, 509 (1961).

21. P. B. Chock, R. B. K. Dewar, J. Halpern, and L.-Y. Wong, J. Am. Chem. Soc., 91, 82 (1969).

22. P. B. Chock and J. Halpern, J. Am. Chem. Soc., 91, 582 (1969).

23. J. K. Thomas, Trans. Faraday Soc., 61, 702 (1965).

24. W. H. Woodruff, D. C. Weatherburn, and D. W. Margerum, Inorg. Chem., 10, 2102 (1971).

25. W. H. Woodruff, B. A. Burke, and D. W. Margerum, Inorg. Chem., 13, 2573 (1974).

26. W. H. Woodruff and D. W. Margerum, Inorg. Chem., 13, 2578 (1974).

27. J. Halpern and P. F. Phelan, J. Am. Chem. Soc., 94, 1881 (1972).

28. L. G. Marzilli, P. A. Marzilli, and J. Halpern, J. Am. Chem. Soc., 93, 1374 (1971).

29. L. G. Marzilli, P. A. Marzilli, and J. Halpern, J. Am. Chem. Soc., 92, 5752 (1970).

30. A. Adin and J. H. Espenson, Inorg. Chem., 11, 686 (1972).

31. J. H. Espenson and A. H. Martin, J. Am. Chem. Soc., 99, 5953 (1977).

32. T. S. Roche and J. F. Endicott, Inorg. Chem., 13, 1575 (1974).

33. G. N. Schrauzer, Inorg. Synth., 11, 61 (1968).

34. J. M. Brierly, J. L. Ellingboe, and H. Diehl, Iowa State Coll. J. Sci., 27, 425 (1953).

35. J. Halpern, Ann. N. Y. Acad. Sci., 239, 2 (1974).

36. J. M. Pratt and R. J. P. Williams, Disc. Faraday Soc., 46, 187 (1968).

37. E. W. Abel, J. M. Pratt, R. Whelan, and P. J. Wilkinson, S. Afr. J. Chem., 30, 1 (1977).

38. C. K. Poon and M. L. Tobe, J. Chem. Soc. A, 1549 (1968).

39. D. P. Rillema, J. F. Endicott, and E. Papaconstantinou, Inorg. Chem., 10, 1739 (1971).

40. S. C. Jackels, K. Farmery, E. K. Barefield, N. J. Rose, and D. H. Busch, Inorg. Chem., 11, 2893 (1972).

41. G. Costa, G. Mestroni, and E. deSavorgnani, Inorg. Chim. Acta, 3, 323 (1969).

42. A. V. Ablov and N. M. Samus, Russ. J. Inorg. Chem., 5, 410 (1960).

43. B. Bosnich, C. K. Poon, and M. L. Tobe, Inorg. Chem., 5, 1514 (1966).

44. J. M. Pratt and R. G. Thorp, J. Chem. Soc. A, 187 (1966).

45. I. M. Kolthoff and E. B. Sandell, "Textbook of Quantitative Inorganic Analysis," 3rd ed., Macmillan, New York, N.Y., 1952, p 600.

46. R. G. Hughes, J. F. Endicott, M. Z. Hoffman, and D. A. House, J. Chem. Educ., 46, 440 (1969).

47. J. H. Espenson, Inorg. Chem., 3, 968 (1964).

48. S. W. Benson, "The Foundations of Chemical Kinetics," McGraw-Hill, New York, N.Y., 1960, pp 18-20.

49. J. H. Espenson and T.-H. Chao, Inorg. Chem., 16, 2553 (1977).

50. M. P. Liteplo and J. F. Endicott, Inorg. Chem., 10, 1420 (1971).

51. H. Elroi and D. Meyerstein, J. Am. Chem. Soc., submitted for publication.

52. C. K. Poon and M. L. Tobe, J. Chem. Soc. A, 2069 (1967).

53. D. Thusius, J. Am. Chem. Soc., 93, 2629 (1971).

54. D. P. Rillema, J. F. Endicott, and R. C. Patel, J. Am. Chem. Soc., 94, 394 (1972).

55. G. Costa, A. Puxeddu, and E. Reisenhofer, Experientia Suppl., 18, 235 (1971).

56. G. Costa, A. Puxeddu, and G. Tauzher, Inorg. Nucl. Chem. Lett., 4, 319 (1968).

57. B. Jaselskis and H. Diehl, J. Am. Chem. Soc., 76, 4345 (1954).

58. R. L. Birke, G. A. Brydon, and M. F. Boyle, J. Electroanal. Chem., 52, 237 (1974).

59. W. H. Woodruff and D. W. Margerum, Inorg. Chem., 12, 962 (1973).

60. L. Pauling, "The Nature of the Chemical Bond," 3rd ed., Cornell University Press, Ithaca, N.Y., 1960, p 85.

61. B. Ellis, V. Petrow, G. H. Beaven, and E. R. Holiday, J. Pharm. Pharmacol., 5, 60 (1953).

62. M. Simic, P. Neta, and E. Hayon, J. Phys. Chem., 73, 3794 (1969).

63. A. M. Tait, M. Z. Hoffman, and E. Hayon, Int. J. Radiat. Phys. Chem., 8, 691 (1976).

64. Y. Hung, L. Y. Martin, S. C. Jackels, A. M. Tait, and D. H. Busch, J. Am. Chem. Soc., 99, 4029 (1977).

65. H. A. Bent, Chem. Rev., 68, 587 (1968).

66. R. G. Yalman, J. Am. Chem. Soc., 75, 1842 (1953).

67. A. Adin and J. H. Espenson, Chem. Commun., 653 (1971).

68. G. N. Schrauzer, J. H. Weber, T. M. Beckham, and R. K. Y. Ho, Tetrahedron Lett., 275 (1971).

69. J. Halpern, M. S. Chan, J. Hanson, T. S. Roche, and J. A. Topich, J. Am. Chem. Soc., 97, 1606 (1975).

70. M. E. Volpin, L. G. Volkova, I. Ya. Levitin, N. N. Boronina, and A. M. Yurkevich, Chem. Commun., 849 (1971).

71. D. Dodd and M. D. Johnson, Chem. Commun., 1371 (1971).

72. A. Van den Bergen and B. O. West, J. Organomet. Chem., 64, 125 (1974).

73. J. H. Espenson and J. S. Shveima, J. Am. Chem. Soc., 95, 4468 (1973).

74. A. L. Crumbliss and P. L. Gaus, Inorg. Chem., 14, 486 (1975).

75. R. H. Prince and M. G. Segal, Nature, 249, 246 (1974).

76. G. N. Schrauzer and R. J. Windgassen, J. Am. Chem. Soc., 89, 1999 (1967).

77. G. N. Schrauzer, A. Ribeiro, L. P. Lee, and R. K. Y. Ho, Angew. Chem. Int. Ed. Engl., 10, 807 (1971).

78. T. M. Vickrey, R. N. Katz, and G. N. Schrauzer, J. Am. Chem. Soc., 97, 7248 (1975).

79. I. P. Rudakova, V. I. Sheichenko, T. A. Postelova, and A. M. Yurkevich, J. Gen. Chem. USSR, 37, 1666 (1967).

80. B. J. Hazzard, "Organicum," Addison-Wesley, Reading, Mass., 1973, p 421.

81. Gmelins Handbuch der Anorganischen Chemie, B58, 729 (1964).

82. H. Diehl, H. Clark, and H. H. Willard, Inorg. Synth., 1, 186 (1939).

83. E. S. Swinbourne, J. Chem. Soc., 2371 (1960).

84. K. L. Brown, D. Lyles, M. Pencovici, and R. G. Kallen, J. Am. Chem. Soc., 97, 7338 (1975).

85. R. G. Wilkins, "The Study of Kinetics and Mechanism of Reactions of Transition Metal Complexes," Allyn and Bacon, Inc., Boston, Mass., 1974, pp 20-25.

86. D. Dodd and M. D. Johnson, J. Chem. Soc. A, 34 (1968).

87. R. S. Nohr and L. O. Spreer, Inorg. Chem., 13, 1239 (1974).

88. A. Adin and J. H. Espenson, Inorg. Chem., 11, 686 (1972).

89. R. H. Prince and M. G. Segal, J. Chem. Soc., Dalton Trans., 330 (1975).

90. R. H. Prince and M. G. Segal, J. Chem. Soc., Dalton Trans., 1245 (1975).

91. J. A. Bertrand, J. H. Smith, and P. G. Eller, J. Chem. Soc., Chem. Commun, 95 (1974).

92. J. H. Espenson and A. Bakac, Iowa State University, unpublished observations.

93. A. Adin and A. G. Sykes, J. Chem. Soc. A, 1518 (1966).

ACKNOWLEDGMENTS

I would like to acknowledge the patience, guidance, and encouragement of Professor James H. Espenson in my quest for the degree of Ph.D. Also, I give my deepest thanks to my loving wife and typist, Nancy, without whose companionship and support these four years would have been an eternity.